ERDC/CRREL TR-19-4

Cold Regions Research and Engineering Laboratory

US Army Corps of Engineers®
Engineer Research and Development Center

ERDC
ENGINEER RESEARCH & DEVELOPMENT CENTER

Engineering for Polar Operations, Logistics, and Research (EPOLAR)

A Snow Runway for Supporting Wheeled Aircraft

Phoenix Airfield, McMurdo, Antarctica

Robert B. Haehnel, George L. Blaisdell, Terry Melendy, Sally Shoop, and Zoe Courville

May 2019

The U.S. Army Engineer Research and Development Center (ERDC) solves the nation's toughest engineering and environmental challenges. ERDC develops innovative solutions in civil and military engineering, geospatial sciences, water resources, and environmental sciences for the Army, the Department of Defense, civilian agencies, and our nation's public good. Find out more at www.erdc.usace.army.mil.

To search for other technical reports published by ERDC, visit the ERDC online library at http://acwc.sdp.sirsi.net/client/default.

ERDC/CRREL TR-19-4
May 2019

A Snow Runway for Supporting Wheeled Aircraft

Phoenix Airfield, McMurdo, Antarctica

Robert B. Haehnel, George L. Blaisdell, Terry Melendy,
Sally Shoop, and Zoe Courville

U.S. Army Engineer Research and Development Center (ERDC)
Cold Regions Research and Engineering Laboratory (CRREL)
72 Lyme Road
Hanover, NH 03755-1290

Final Report

Prepared for National Science Foundation, Office of Polar Programs
2415 Eisenhower Avenue
Alexandria, VA 22314

Under Engineering for Polar Operations, Logistics, and Research (EPOLAR)
EP-ANT-15-01, “CRREL Support to Alpha Site Runway”

Abstract

Historically, there has been a system of as many as three airfields operated at McMurdo, Antarctica, to transport cargo and personnel to and from the continent via ski-equipped and wheeled aircraft. Owing to the runways' being founded on snow and ice, there is a constant need to adapt the airfield system to accommodate changing environmental conditions while still meeting program needs. This report provides an overview of the implementation of a new airfield to support landing wheeled aircraft that replaces the Pegasus Airfield that was founded on the superimposed glacial ice layer on the McMurdo Ice Shelf in the McMurdo Sound.

The new airfield is located approximately 5 km (3 miles) east and up shelf from the former Pegasus Airfield and is the first runway constructed on compacted snow that supports a wheeled aircraft as large as a C-17. Herein we document the design, construction, and commissioning of the new airfield. Also provided in this report are recommendations for maintenance and monitoring to prolong the life of the airfield and to determine when operations need to be suspended due to warm weather.

Contents

Figures and Tables

Figures

Tables

Preface

This study was conducted for the National Science Foundation, Office of Polar Programs (NSF-OPP) under Engineering for Polar Operations, Logistics, and Research (EPOLAR) EP-ANT-15-01, "CRREL Support to Alpha Site Runway." The technical monitor was Ms. Margaret Knuth, Program Manager, NSF-OPP, U.S. Antarctic Program.

The work was performed by the Terrestrial and Cryospheric Sciences Branch (CEERD-RRG) and the Force Projection and Sustainment Branch (CEERD-RRH) of the Research and Engineering Division (CEERD-RR), U.S. Army Engineer Research and Development Center, Cold Regions Research and Engineering Laboratory (ERDC-CRREL). At the time of publication, Dr. John Weatherly was Chief, CEERD-RRG; Dr. Harley Cudney was Acting Chief, CEERD-RRH; Mr. Jared Oren was Acting Chief, CEERD-RR; and Dr. Rosa Affleck was the program manager for EPOLAR. The Deputy Director of ERDC-CRREL was Mr. David B. Ringelberg, and the Director was Dr. Joseph L. Corriveau.

The PCASE (Pavement-Transportation Computer Aided Structural Engineering) analysis was performed by Ms. Lynette Barna, one of the CRREL representatives on the PCASE committee. Ms. Ariana Sopher, CRREL, assisted with the BAKFAA (Federal Aviation Administration Backcalculation software) analysis. Their contributions and discussions were critical to the results of this study. A field team of dedicated workers employed by Antarctic Support Contract (ASC, a Leidos company) was vital to the success of this project. That team was led superbly by Mr. Jack Green. The field data used for the analysis presented in section 4.2 was collected with the assistance of Mr. Jack Green, ASC.

COL Ivan P. Beckman was Commander of ERDC, and Dr. David W. Pittman was the Director.

Acronyms and Abbreviations

ADD	Australian Antarctic Division
AFCESA	Air Force Civil Engineer Support Agency
AMPS	Antarctic Mesoscale Prediction System
ASC	Antarctic Support Contract
AWS	Automated Weather Stations
BAKFAA	FAA Backcalculation software
CBR	California Bearing Ratio
CES	Civil Engineering Support Directorate
CL	Centerline
CRREL	U.S. Army Cold Regions Research and Engineering Laboratory
DCP	Dynamic Cone Penetrometer
DOD	Department of Defense
EPOLAR	Engineering for Polar Operations, Logistics, and Research
ERDC	Engineer Research and Development Center
FAA	Federal Aviation Administration
FEA	Finite Element Analysis
FS	Factor of Safety
IFR	Instrumental Flight Rules
LEAF	Layered Elastic Analysis Formulation
LEDFAA	FAA Layered Elastic Design
LIMA	Landsat Image Mosaic of Antarctica
LTER	Long-Term Ecological Research
MIS	McMurdo Ice Shelf

MODIS	Moderate Resolution Imaging Spectroradiomete
NA	Not Applicable
NAVAIDS	Navigational Aids
NCAR	National Center for Atmospheric Research
NOTAM	Notice to Airmen
NSF	National Science Foundation
NYANG	New York Air National Guard
NZFX	International Airfield Designation for the Phoenix Airfield
NZPG	International Airfield Designation for the Pegasus Airfield
O&M	Operations and Maintenance
OPP	Office of Polar Programs
PCASE	Pavement-Transportation Computer Aided Structural Engineering
PGC	Polar Geospatial Center
RAM	Rammsonde
RSP	Russian Snow Penetrometer
SPAWAR	Space and Naval Warfare Systems Command
SW	Southwest
TERPS	Terminal Instrument Procedures
UFC	Unified Facilities Criteria
UNESCO	United Nations Educational, Scientific and Cultural Organization
USACE	U.S. Army Corps of Engineers
USAF	U.S. Air Force
USAP	U.S. Antarctic Program
UUCS	Unconfined Uniaxial Compressive Strength
VFR	Visual Flight Rules

Unit Conversion Factors

Multiply	By	To Obtain
cubic feet	0.02831685	cubic meters
degrees (angle)	0.01745329	radians
feet	0.3048	meters
inches	0.0254	meters
kips	0.4536	tonnes
miles (nautical)	1,852	meters
miles (U.S. statute)	1,609.347	meters
miles per hour	0.44704	meters per second
pounds (force) per square inch	6.894757	kilopascals
pounds (mass)	0.45359237	kilograms
pounds (mass) per cubic foot	16.01846	kilograms per cubic meter
square feet	0.09290304	square meters
square inches	6.4516 E-04	square meters

Executive Summary

Since 1993, the United States Antarctic Program (USAP) has successfully operated the Pegasus glacial ice airstrip on the McMurdo Ice Shelf (MIS) to support the operation of wheeled aircraft into and out of McMurdo, Antarctica. It was founded on a layer of superimposed ice that is about 4.7 m (15 ft) thick and is underlain by firn (Daly et al. 2015). A thin, compacted snowcap (up to 125 mm [5 in.] thick) was constructed on the ice surface of the airstrip to increase the surface albedo and to reduce melting of the superimposed ice layer, the structural component of the airstrip.

The National Science Foundation (NSF) relies heavily on wheeled-aircraft access to McMurdo for the months when the sea-ice airstrip is no longer operable (early December through September). Starting in 2012, the Pegasus airstrip began to require more maintenance while providing fewer days of full operability, signaling that the USAP may need to construct a replacement facility if it intended to sustain air operations in the fashion it had since 1993 when Pegasus opened.

Following a review of potential sites to locate a new airfield to replace the failing Pegasus Airfield, the project team (the authors, NSF, and Antarctic Support Contract) determined that the best compromise was to place the airfield at approximately Mile Post 11 along the Pegasus access road. Unlike Pegasus, which was founded on glacial ice, this new location would require construction of a runway on snow. Capitalizing on the experience of other countries' building snow runways and recent success of the USAP building high-strength snow foundations, construction of the new Phoenix Airfield commenced in October of 2015. Using a combination of numerical computation methods and field experience, we propose in this work feasible design and construction methods for building a runway out of snow that would support a wheeled aircraft as heavy as a C-17 Globemaster III, the main aircraft that would be using this new runway.

Following compaction of the existing snow cover with a sheepsfoot roller and rubber-tired weight carts, the construction proceeded in lifts with the objective to provide final compacted lifts that were about 75 mm (3 in.) thick. The first of these lifts was constructed by pushing snow adjacent to the runway onto the compacted base layer and again compacting with a sheepsfoot roller and rubber-tired weight cart. The load in the weight cart was progressively increased as the runway was able to support the load

without rutting of the runway. Following completion of the first lift, subsequent "lifts" took advantage of naturally falling snow, which was compacted as soon as it was deposited on the runway, to continue to build up the slab thickness to at least a meter (3 ft). Though this initial 1 m (3 ft) slab of compacted strong snow is needed to support the weight of a C-17, the runway is for practical purposes constantly under construction as every snowfall is compacted and incorporated into the surface to provide a hard top layer of the runway for supporting wheeled operations. The compaction process for an additional layer of snow is considered complete when the surface can support a fully loaded weight cart (73,000 kg, or 160,000 lb) without rutting the runway. Also, the compaction process needs to occur immediately after a snowfall to prevent the fresh snow from becoming too deep before it can be uniformly compacted, thus preventing a hard compacted surface over a softer, poorly compacted snow layer; such an "egg shell" condition would not support the weight of a C-17 and would promote hoar formation that would further weaken the pavement structure.

Following construction, the runway was proofed with a fully loaded weight cart to confirm that there were no weak spots in the runway. Then the runway strength was verified by landing a fully loaded C-17 on the runway. In addition to landing, several maneuvers were carried out on the runway to test the integrity of the runway under normal and extreme loading conditions (e.g., 180° turns in the runway and a short-field takeoff) to confirm that the runway would stand up to the rigors of flight operations. After successful completion of these validation test in November of 2016, the Phoenix Airfield was certified for operations.

Owing to the warming weather, the runway was not operated from mid-November 2016 until the end of January 2017. During this time, runway maintenance continued with the weight cart being used twice a week to compact the runway. As the runway warmed during the summer, the load in the weight cart was reduced to a level that the runway would support without rutting. As the runway began to cool, the load in the weight cart was progressively increased until the runway could again support the fully loaded weight cart without producing ruts in the runway. Once the runway was able to support the fully loaded (73,000 kg, or 160,000 lb) weight cart, the runway was cleared to resume operations.

The first operational flight on the Phoenix Airfield occurred on 27 January 2017. The mission was carried out successfully with minor rutting that was

well within the operations limits for the C-17. Flight operations continued for another month on the airfield to support transport of personnel and cargo prior to station close.

To maintain runway health going forward, a key issue that needs to be managed is working new snow accumulations into the pavement structure as quickly as possible by compaction to ensure that weak layers do not have a chance to form in the pavement structure. Furthermore, management of foreign and natural surface contaminants is crucial to keep the albedo of the surface high to prevent melting and weakening of the pavement structure.

To improve runway reliability and streamline operations at the Phoenix runway, we recommend that future efforts address the following items:

1. Design and construct a new proof cart that can be tailored for each aircraft that will be operated on the runway, not just the C-17.
2. Vet and apply new strength assessment methods that can be easily related to the engineering properties of the snow and computational stress analysis methods such as BAKFAA (Federal Aviation Administration Backcalculation software). This will allow operators to directly relate runway stress analysis for new aircraft to the measured runway strength and determine when the runway can support operations for specific aircraft.
3. Identify parameters to monitor (e.g., temperature, strength, and albedo) and develop monitoring plans to assess runway health. Use this data to determine criteria for opening and closing the airfield for specific aircraft types. Along with this, for tactical mission-planning purposes, develop a forecast model to predict when operational windows are closing and opening.
4. Develop methods to understand how and when hoar-like layers can form in the runway and methods to predict, detect, and mitigate any hoar-like layer formation before it can evolve to a point that can compromise runway operation.
5. Determine the limits of runway life expectancy to better manage potential threats and determine, for long term planning, when a replacement runway will need to be reestablished at a new location.

Addressing these issues will allow better management of the existing airfield infrastructure and facilitate strategic planning for runway replacement as this new facility nears the end of its life span.

1 Introduction

1.1 Background

Since 1993, the United States Antarctic Program (USAP) has successfully operated the Pegasus glacial ice airstrip on the McMurdo Ice Shelf (MIS) to support the operation of wheeled aircraft into and out of McMurdo, Antarctica. It was founded on a layer of superimposed ice that is about 4.7 m (15 ft) thick and is underlain by firn (Daly et al. 2015). Owing to the relatively low albedo, α, of this ice layer ($\alpha \approx 0.5$), a significant amount of solar radiation can be absorbed by the ice during the summer and cause weakening and melting of the ice-pavement structure of the airstrip. Starting in the summer of 1999–2000, a thin, compacted snowcap (up to 125 mm [5 in.] thick) was constructed on the ice surface of the airstrip to increase the surface albedo and to reduce melting of the superimposed ice layer, the structural component of the airstrip. The measured albedo of the snowcap is typically 0.7 to 0.85 (Daly et al. 2015), and regular maintenance efforts were conducted to keep the albedo of this protective layer as high as possible to preserve the strength of the airstrip. Though it was desirable that the strength of the snowcap be sufficient to support the weight of the aircraft, rutting of the snowcap down to the full depth of the cap (125 m [5 in.]) can occur and not jeopardize the aircraft since the strong glacial ice is the main structural component for the airstrip. Still, extensive rutting of the cap was repaired whenever it occurred to prevent melt damage to the underlying ice layer because of a compromised snowcap.

Starting in 2012, Pegasus airstrip began to require more maintenance while providing fewer days of full operability. This was a sign that the USAP may need to construct a replacement facility if it intended to sustain air operations in the fashion it had since 1993 when Pegasus opened. The National Science Foundation (NSF) had come to rely heavily on wheeled-aircraft accessibility to McMurdo for the months when the sea-ice airstrip was no longer operable (early December through September). The USAP research and operations program as currently configured was strained; and during the last few years Pegasus operated, it could not be used from December through early March. This necessitated using the smaller and aging ski-equipped LC-130 aircraft for both on-continent and intercontinental missions as soon as Pegasus or the sea-ice airstrip could no longer sustain flight operations (typically starting in early December of each year

as of 2012; prior to December of 2012, Pegasus could maintain operations year-round). In addition to having to provide intercontinental transportation of passengers and cargo, the need to complete summer field-season missions (interior Antarctica), including topping off South Pole Station fuel reserves for the winter, and move hundreds of passengers off continent during late January and February put huge pressure on the limited number of LC-130 aircraft and their flight crews.

By the end of the 2014–2015 summer field season, it was clear to NSF that the deterioration of the Pegasus airstrip site was part of an anticipated end-of-life progression and not a temporary response to any seasonal environmental cycles. A replacement for the Pegasus airstrip was necessary.

Through discussion between NSF Polar Programs science and operations sections, it was quickly clear that the research and facilities sustainment goals for the immediate and longer-term timeframes demanded near-continuous wheeled aircraft between late August and late February each year and that the recent addition of monthly austral winter flights (April through July) could be vital to the McMurdo Master Plan initiative (NSF 2015b). Additionally, at a minimum, a new airstrip would need to support a robust schedule of 40 or more U.S. Air Force (USAF) C-17 Globemaster III missions spread over the season but most concentrated in October and in February.

Though the main objective of this effort was to provide an airstrip that supports operation of the USAF C-17 flights, it is essential that the airstrip support the Federal Aviation Administration's (FAA) Bombardier Challenger, which is used to certify USAP navigational aids (NAVAIDS). Also, usability for other colleague-country wheeled aircraft was also strongly desired: New Zealand's C-130 Hercules and Boeing 757, Australia's Airbus A-319 and C-17, and Italy's Lockheed L-100 Hercules. These aircraft each have unique landing-gear loading (individual tire load and tire pressure) and geometry (spacing of wheels). This required an airstrip pavement system to support the unique stresses imparted by each aircraft type.

The USAP operates a "production style" campaign in the Antarctic each and every year. That is, after intense and sophisticated preplanning, NSF commits to a robust research and operation and maintenance (O&M) program annually. NSF expects that, except for events that are totally unforeseen and unpredictable, well over 95% of the planned achievements will be

accomplished. With heavy reliance on intercontinental airlift to meet this expectation, any new airstrip would be required to meet or exceed the availability and reliability of the Pegasus airstrip.

The design requirements for the replacement airstrip for Pegasus is as follows: It must support flight operations for a USAF C-17 with a maximum gross weight of 227,000 kg (500,000 lb), which is 2% higher than the maximum anticipated McMurdo-area operating weight of 222,000 kg (490,000 lb). The main landing gear must carry approximately 95% of the aircraft weight, and the tire pressure is 1 MPa (144 psi). The nose gear must carry approximately 5% of the aircraft weight and have a tire pressure of 1.1 MPa (160 psi). The new airstrip must support this load with a minimum factor of safety, FS = 1.25, to account for uncertainties in the system, such as the load that the aircraft exerts on the airstrip, airstrip material strength, etc. This is in line with USAF (2015a), which recommends a minimum FS for Pegasus airstrip of 1.3* and 1.3 to 1.4 for the sea-ice airstrip. Also, the airstrip needs to meet the dimensional standards and approach and departure restrictions for safe C-17 operations as outlined in sections 2.2 and 2.3.

While not the highest priority, NSF also strongly desired that a new wheeled airstrip facility involve no more maintenance than the Pegasus airstrip and not involve any new, costly equipment acquisitions. Further, nearly everyone who traveled to and from the Pegasus airstrip wished for any new airstrip complex to be closer to McMurdo (Figure 1) so as to reduce transportation time (trips between McMurdo and Pegasus averaged 1 hour each way but could be 1.5 hours with poor snow-road conditions) and fuel use.

After a thorough review of possible locations to site the new airstrip (section 2 provides detailed discussion on site selection), NSF and the U.S. Army Cold Regions Research and Engineering Laboratory (CRREL) determined that the best location would be to found the airstrip on snow. Though snow skiways are used in McMurdo and South Pole and at Antarctic camps, the USAP has not previously attempted to construct a snow airstrip for wheeled aircraft. Even with the presence of a snowcap on the Peg-

* We note that USAF (2015a) indicates that for Pegasus the recommended FS = 3.0. However, after review of the supporting materials for USAF (2015), the present authors are certain that this is a typo in the USAF (2015a) document and that the correct FS = 1.3.

asus airstrip, it was not a snow airstrip but was fundamentally an ice airstrip as the ice provided the structural support. Though landing of aircraft with skis on snow is common, there are very few instances of building and operating airstrips for wheeled aircraft on deep snow. Most notably, the Soviets operated an airstrip at Molodezhnaya, Antarctica, for 10 years (section 3 provides more detail on this). The Australian Antarctic Division (AAD) began constructing a compressed snow airstrip in Antarctica near Casey Station in the late 1980s (Russell-Head and Budd 1989; M. Filipowski, ADD, pers. comm., 5 January 2016). AAD had constructed a proof cart with C-130H landing gear (590 kPa [85 psi] tire pressure) for testing the airstrip. However, the temperatures were too warm, and the airstrip did not hold up during proof-cart tests. Limited formal documentation is available (i.e., Appendixes in Russell-Head and Budd 1989) for the effort, and AAD made no further attempts to construct an airstrip on deep snow (M. Filipowski, pers. comm., 5 January 2016).

Figure 1. Location of the planned Phoenix Airfield on the McMurdo Ice Shelf (drawing by R. Eshelman, Antarctic Support Contract, Centennial, CO).

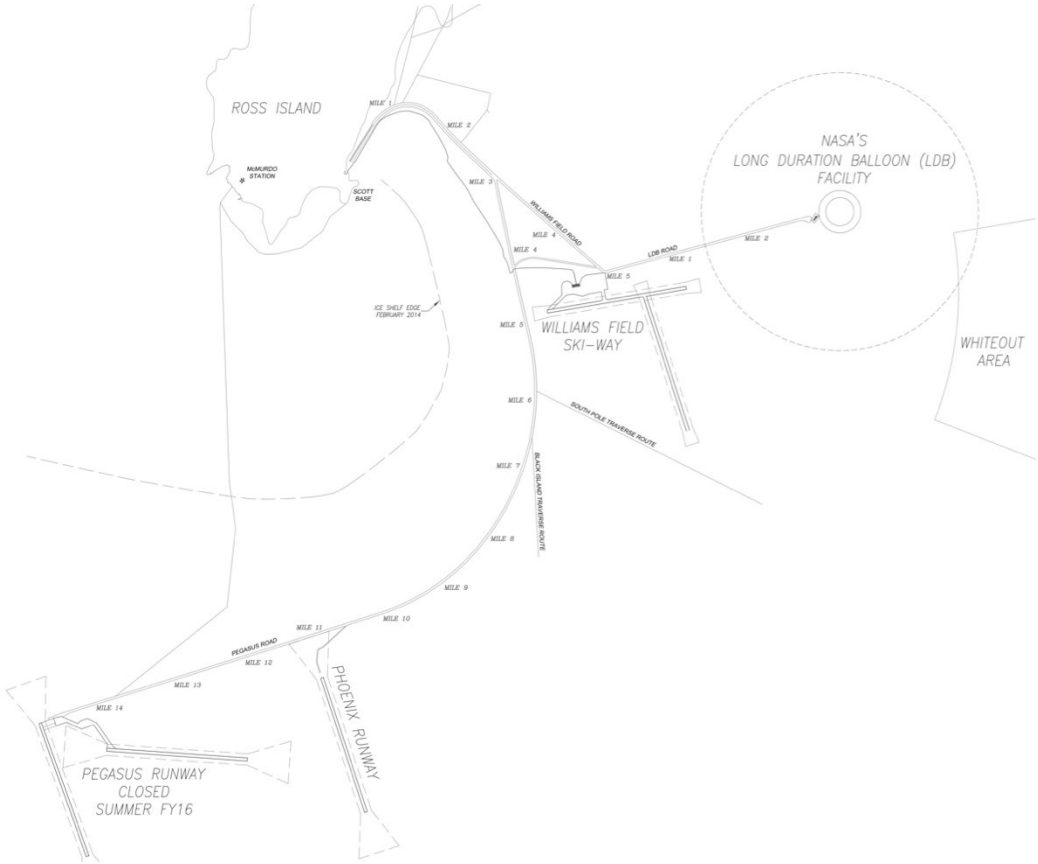

Building on what was learned by the Soviets from the experience at Molodezhnaya and experience with building snow foundations at South Pole, the USAP felt confident that construction and maintenance of a snow airstrip was feasible in McMurdo. In 2015, USAP began constructing a snow airstrip on the MIS about 5 km (3 miles) east of the Pegasus airstrip to support wheeled flights into McMurdo. The location of the new airstrip was chosen to put it to the east of the dirt plume that was plaguing the Pegasus site yet not so far east that the annual snow accumulation is more than can be managed. The siting for the new airstrip is approximately at Mile Post 11 on the Pegasus road (Figure 1); the annual snow accumulation at this site is 30–45 cm (12–18 in.) (Haehnel et al. 2014). The name of this new site is officially designated the Phoenix airstrip (section 2.10) to honor "early workhorse [C-121] aircraft but also echoes the mythological tradition of a new entity arising from the ashes of the old" (NSF 2016).

1.2 Objectives

The objective of this report is to provide a detailed record of our efforts, under the direction of the NSF, to oversee the design, construction and commissioning of a snow runway that replaces the glacial ice runway at McMurdo, Antarctica. Since this is a first-of-its-kind runway—a snow runway capable of supporting a wheeled aircraft as heavy as a C-17—the design and construction methods are documented here to provide guidance for future snow-pavement construction efforts. This effort builds on prior works (e.g., Abele 1990) yet provides more-robust design methods based on advances in the state of the art of computer modeling and on improved understanding of snow science.

1.3 Approach

In this report we provide background information on selecting the site for the Phoenix airstrip (section 2) and analysis to determine the minimum strength requirements for the new snow airstrip (section 3). The analysis is based on the observed snow conditions at the Phoenix site and the designed airstrip layering (i.e., target snow density as a function of depth). The results of this analysis are compared against the design for the snow airstrip at Molodezhnaya and USAF specifications for airstrip design at soil-based contingency landing zones. From this analysis, we provide the required strength profile needed to support C-17 operations. Methods for assessing the airstrip strength are discussed in section 4, and section 5 outlines a procedure for certifying that the airstrip strength is sufficient to

support C-17 operations on snow. Validation procedures for verifying airstrip strength are provided in section 6; and in section 7, we provide a summary of the airstrip construction methods and observations made during construction. The observations during airstrip commissioning (validation and first flights) are discussed in section 8. Considerations for maintaining airstrip health are provided in section 9, with final conclusions and recommendations provided in section 10.

2 Site Selection

There are many factors to consider when determining a suitable location for an airstrip for servicing McMurdo Station. In this section, we review these factors and provide the analysis used to determine the best balance between competing requirements to identify the final location for the new airstrip to replace the Pegasus Airfield.

2.1 Glaciological considerations

The first necessity for a satisfactory wheeled airstrip in Antarctica is the strength of the material on which the airstrip will reside. In most of the world, airstrips rely on manufactured materials (e.g., concrete or asphalt) over carefully processed granular base materials or, when this is not possible or necessary, on prepared gravel or other soils.

Antarctica has less than 5% of its non-snow/ice mass exposed. In the McMurdo area, while there is exposed rock and gravel, it is nearly entirely

1. on grades that are too steep for an airstrip;
2. in areas that are far too small for even a tiny airstrip; or
3. in internationally designated, specially protected areas.

However, in preparation for the International Geophysical Year (1957–1958), a gravel airstrip was proposed on a level area across McMurdo Sound from McMurdo Station at Marble Point (Figure 2; Mellor 1988). Rough grading was performed to discover if the site could be made to support the wheeled aircraft used at the time—small, ship-delivered propeller planes—but only crude development was accomplished and only de Havilland Otter aircraft used the site for a limited time between 1957 and 1959.

Since about the early 1980s, the requirements for aircraft operators and modern aircraft make the Marble Point site totally unacceptable because of nearby terrain elevations and available length and clear zone requirements. Further, with Marble Point being located 90 km (50 miles) from McMurdo with ephemeral sea ice spanning much of that distance, the logistics associated with this site being a primary air logistics hub are prohibitive.

Figure 2. U.S. Geological Survey (1970) map of the McMurdo Sound Area. Marble Point is in the *upper left* quadrant indicated by the *red ellipse*.

Pegasus was founded on thick (~30 m, 100 ft), floating glacial ice in a glaciologically unique feature referred to as a "zone of superimposed ice" indicted in Figure 3 (Klokov and Diemand 1995; Blaisdell et. al. 1995). In such a setting, there is no net loss or gain of mass. In practice, this means that whatever volume of snow is deposited at the site over the course of a year is matched by an equal amount of melting and ablation. This condition was considered critical at the time of siting of the Pegasus airstrip, owing to the need for strong material (thick glacial ice) to support the

mass and contact pressure of heavy wheeled aircraft and the nature-provided high albedo (reflectivity) of fresh snow in modest quantities to protect the low-albedo glacial ice from intense solar warming.

Figure 3. Glaciological regions on the McMurdo Ice Shelf (*red lines* after Klokov and Diemand 1995). (Map data: Google, NASA.)

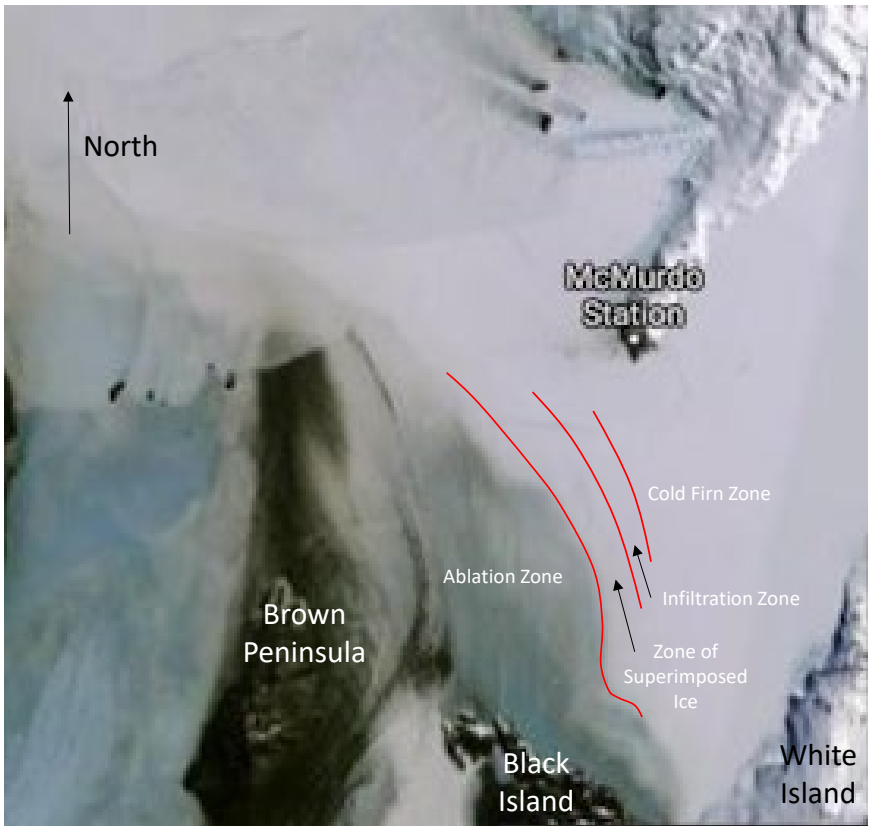

Ideally, a replacement facility for Pegasus would have been able to capitalize on the same set of glaciological conditions. Searches from surface vehicles, low-altitude aircraft, and satellite imagery concluded that no site with similar enough conditions to the Pegasus site exists in the McMurdo area, thus, requiring a new design along with an entirely new site.

In addition to strength, any site for a new airstrip would need to be appropriately distant from ice edges, crevasses, or rifts in glacial ice. At its closest point (the north end of the runway, or the north runway threshold) the Pegasus airstrip was about 7 km (4 miles) true south from the glacial ice edge (Figure 4) where it meets sea ice that can and has in any given year broken free and floated off before reforming during the austral winter. A well-known rift exists near the glacial ice edge and is only about 6 km (3.5 miles) distant from the Pegasus airstrip (circled in red in Figure 4) in

a northwest direction. At the time of siting and construction of the Pegasus airstrip, this rift and the glacial ice edge in this portion of McMurdo Sound was believed to be stable and not prone to calving for many years, which proved to be true.

Figure 4. McMurdo Ice Shelf bound by the Ross Ice Shelf (*1*), White Island (*2*), Black Island (*3*), Brown Peninsula (*4*), Ross Island (*5*), and McMurdo Sound sea ice. Note the transition from zone of accumulation to zone of ablation when traveling from east-northeast to west-southwest. Arrows identify the edge of the McMurdo Ice Shelf where, in this image, it abuts McMurdo Sound sea ice. In some years, the sea ice breaks out; and some or all of the MIS edge abuts open water for several months before a new ice forms. (LIMA [Landsat Image Mosaic of Antarctica] satellite image from December 2007; contrast adjusted to enhance ice-shelf-edge visibility.)

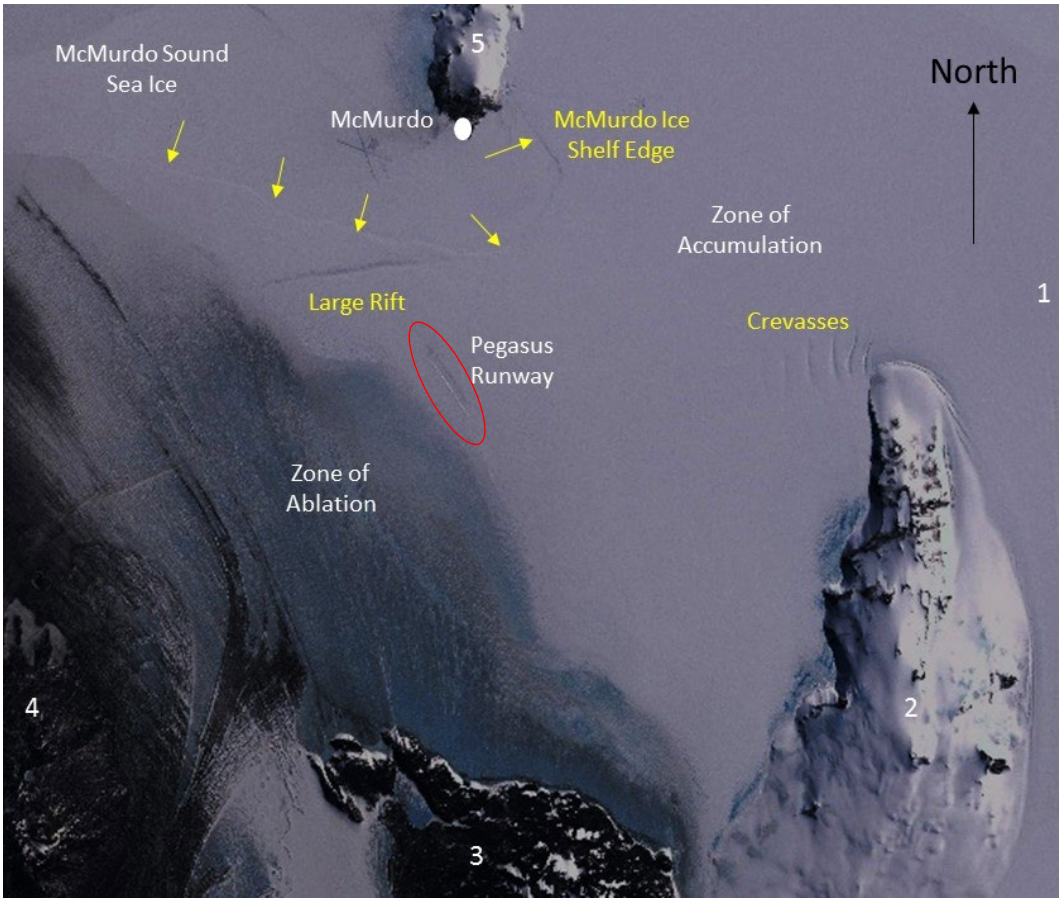

Other portions of the MIS glacial ice edge are known to calve on a frequency measured in several-year intervals. Because of the geometry and flow pattern of the MIS and currents and tidal effects in McMurdo Sound, the roughly north–south trending arcuate portion of the MIS edge breaks off routinely when the sea ice breaks out. The position of Williams Field (off the right edge of Figure 4) to the east of this ice edge and the flow pattern of the MIS—in an approximate east to west direction—has caused

William's Field to continually become closer to the ice edge, and therefore this airfield has been reestablished "upstream" or "up shelf" on several occasions, most recently in 2016.

A good understanding of ice movement, visible or hidden crevassing or rifts, and the flow direction relative to downstream hazards is essential to selecting the location for a new airstrip.

2.2 Dimensions

The planned location for the airstrip replacing Pegasus needed to be large enough to accommodate the minimum dimensional requirements for the airstrip and located such that there are no vertical obstructions that impede normal flight operations (i.e., approach, landing, takeoff, etc.). The vast majority of sorties and volume of cargo and passengers associated with McMurdo's intercontinental connection are performed with the USAF-operated C-17. Thus, the geometric requirements for any new USAP airstrip need to meet USAF standards. For routine operations (i.e., not an emergency or combat situation), these standards are the same as for Pegasus (USAF 2015a) and dictate a primary landing surface that is 3050 m (10,000 ft) long, with a 305 m (1000 ft) overrun at the typical upwind end, by 46 m (150 ft) wide with a 8 m (25 ft) shoulder on each side that is of equal strength to the main landing surface.

While the C-17 is capable of operating on shorter and narrower primary landing surfaces, a full length and width airstrip was mandatory because the airstrip would always exhibit a very low surface-friction coefficient.

Dimensional guidelines exist for the parking and embark/disembark area where aircraft operations take place (USAF 2015a). These ensure safe maneuvering space between multiple aircraft, between aircraft and buildings or flammable sources, and for cargo handling operations.

Additional dimensional requirements are levied on the terrain surrounding the primary landing surface. These are aimed at ensuring that no obstacles exist that could interfere with normal flight maneuvers when an aircraft is close to the airstrip during landing, taxiing, and takeoff. These requirements take the form of defined airfield imaginary surfaces in the space above the surrounding terrain that no surface feature can penetrate (e.g., telephone poles or buildings). The planes, or surfaces, are different for the ends and sides of the airstrip as illustrated in Figure 5.

Figure 5. Imaginary surfaces associated with typical airfields, establishing required clear areas for safe aircraft operations with approaching and departing airfields (USAF 2015a).

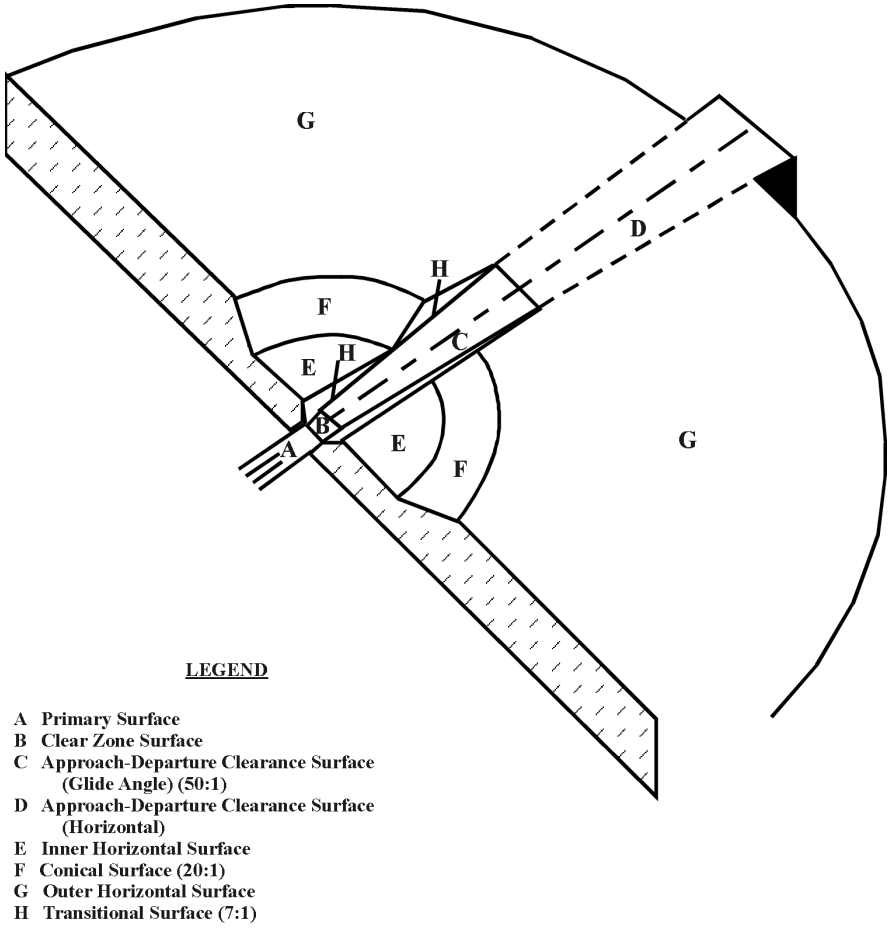

Non-USAF aircraft operators and aircraft types that have in the past and are expected in the future to access the new McMurdo-area airstrip have airfield dimensional requirements that are equal to or less demanding than for the C-17. Thus, the design team used USAF guidelines for the C-17 in laying out the new airstrip.

2.3 Airspace design

The dimensional requirements discussed above impact the geometry of real estate prepared for the airstrip, apron, and various infrastructure necessary for supporting an operational airfield. Departing and arriving aircraft execute a prescribed pattern of three-dimensional movements associated with safe operating procedures. During visual flight rules (VFR)—flight operations in good visibility—flight crews may use individual discretion in selecting how they approach or depart a runway. However, when visibility or other conditions are more restricting, or when it is required,

instrument flight rules (IFR) govern. Under IFR operations, a strict established prescription of aircraft routing is levied on flight crews that can be altered only with approval from certified flight controllers. These IFR routes in and out of airports are called instrument approach procedures, or approach plates. Although all USAP flying in Antarctica is performed in a VFR environment, all primary USAP runways operate instruments (NAVAIDS) that assist in guiding flight crews in executing IFR-specific approaches and departures during low-visibility situations, often allowing them get under low-lying clouds or snow squalls to a point where they can visually complete the actual landing.

Typically, multiple "approach" and "departure" procedures are generated for each end of each airstrip at every airport (e.g., Figure 6) and are publically available (e.g., at the Jeppesen site at http://ww1.jeppesen.com/index.jsp). These Terminal Instrument Procedures, or TERPS, take into account many factors that do not affect ground vehicles, such as terrain elevations and their geographic relationship to the runway, other potential air traffic, desired and possible climb-out (takeoff) and glide-slope (landing) angles (for both normal and lost-engine scenarios), prevailing and strong wind directions, and runway azimuth compared to the direction of most common destinations (arrival from and departure to). Procedures are generally prepared for each end of the airstrip, considered two runways by air traffic managers, each runway labeled by the heading the aircraft flies (or taxis/rolls-out) when using the runway, divided by ten. For example, a runway with a heading of 130° would be designated as runway 13. The opposite end of the runway would have a heading 180° greater (210°) and would be designated as runway 21. USAP runways are labeled using true azimuth headings, not magnetic headings as are typical in most of the world.

Siting of the new airstrip must be such that surrounding terrain (e.g., hills and mountains), weather, and runway alignment will allow these approach and departure procedures within safe operating limits of the aircraft that will use the runway.

Figure 6. Example approach procedure for runway 01 (aligned parallel to a magnetic heading of 10°) at Las Vegas International Airport (FlightAware 2019).

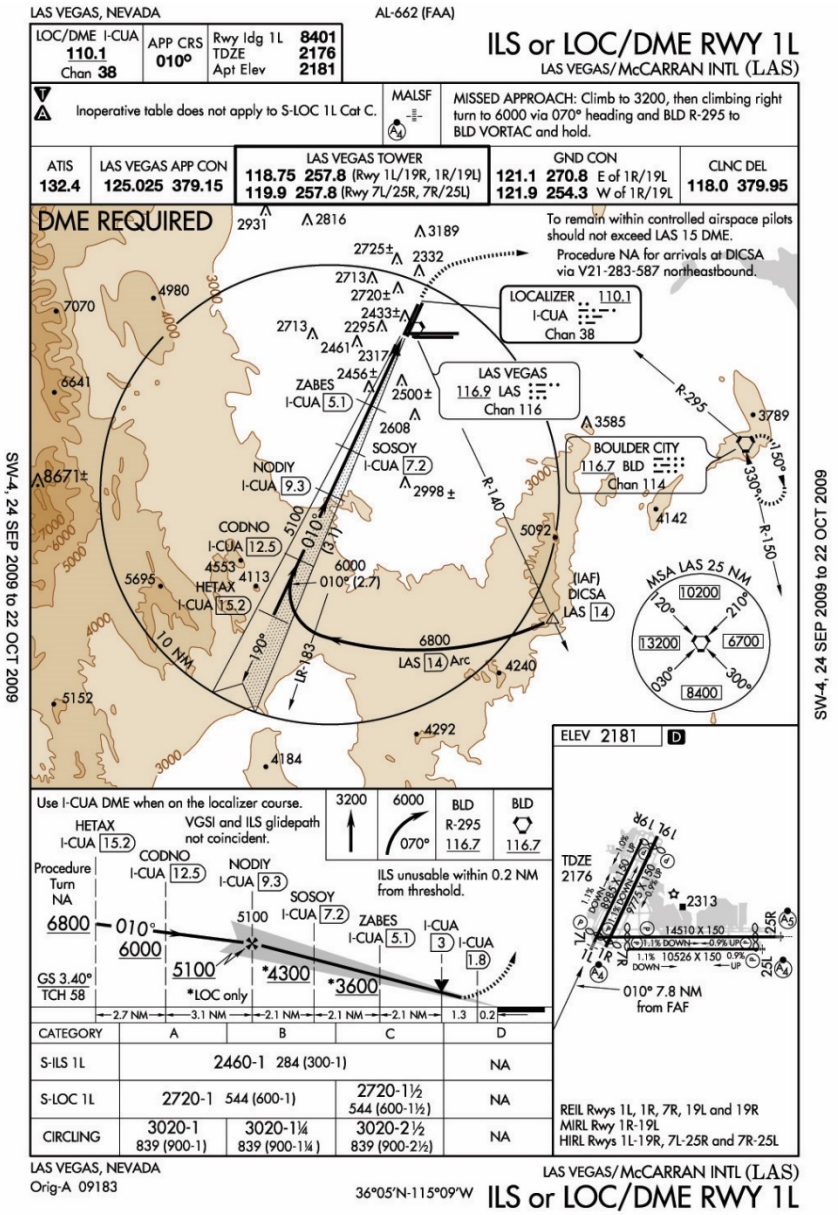

2.4 Winds

All airfields exist in environments with variable weather conditions. While wind is only one component of weather, wind plays an especially important role in determining the orientation of an airstrip. Thus, it is treated separately.

Each aircraft type has flying characteristics that dictate the degree to which they can safely operate near the ground with head-, tail-, and cross-winds. Ideally, aircraft would land and take off only with a direct head wind, which adds to the ground speed to make the airspeed high and thus maximizes lift on the wings. In locations where wind directions vary widely, or frequently, it may be difficult to select a single airstrip direction if airfield operators want to maximize the availability of the runways. Thus, it is common at large, busy, or strategically sited airfields for there to be at least two airstrips, usually close to perpendicular to each other. These airfields typically are said to have "main" and "crosswind" runways, allowing them to usually accommodate more-or-less into-the-wind landings and takeoffs at all times for all aircraft types.

Like at the Pegasus site, it was NSF's desire to minimize the amount of construction and maintenance needed for a replacement airfield. At Pegasus, wind analysis during development of the airstrip showed that strong winds were nearly always from a few degrees east or west of due south, and prevailing winds were a few degrees north or south of due east. Further, the prevailing winds rarely exceeded the allowable crosswind speed for the aircraft USAP operate. Thus, the Pegasus Airfield had only one airstrip, aligned in the 150°–330° direction. It was our desire to have just one airstrip with favorable crosswinds at the new site, also, so that the orientation could be into the storm winds as was the case at Pegasus, thereby eliminating any need for constructing a crosswind runway.

2.5 Weather

Aspects of weather, other than wind, that are of most importance in siting an airfield include temperature, precipitation traits (e.g., how much, what type, how frequent, and the duration of each precipitation event), visibility (horizontal distance that can be seen clearly), and ceiling (cloud base height above the ground). Excellent weather records exist for the MIS for many years, both from automated weather stations (AWS) and from McMurdo weather office observations.

We know the temperature regime in the region and understand that, unlike at Amundsen-Scott South Pole Station, only occasionally do austral winter temperatures dip below the safe operating temperature for typical USAP aircraft. Otherwise, the only concern related to temperature is for levels that are near or surpass the melting point. Figure 7 provides a cyclic analysis of the air temperature data for the Pegasus airstrip and computes

the daily average over the period of record and the maximum and minimum reported air temperature for each day through the period of record. Summer temperature records for the Pegasus airstrip show a 10-week period when peak daily temperatures can be above the freezing point. For comparison, Figure 7 also plots hourly data from the U.S. Navy's Space and Naval Warfare Systems Command (SPAWAR)* AWS at Pegasus from 2012 to 2014. During 2012–2014, there were several days where the maximum air temperature for a particular day exceeded that seen in the record spanning 1992–2011.

Figure 7. Cyclic analysis of austral summer air and ice temperatures at the Pegasus airstrip for the period from 1992 to 2011. The *average* is the mean average daily air temperature over the period, and the *max* and *min* are the maximum and minimum observed values for that day during the period. The SPAWAR data are hourly data measured over two austral summers.

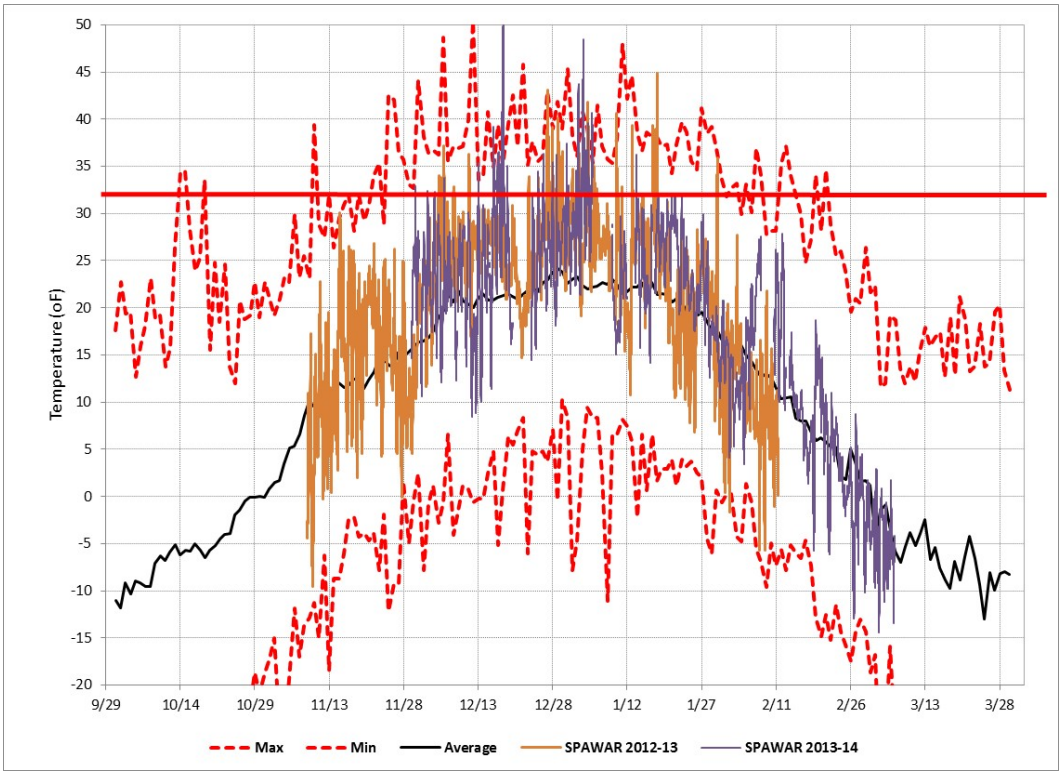

Snow accumulation amounts in the McMurdo area are not known for as many individual locations as are temperatures (most AWS do not measure precipitation), but there are adequate measurements to characterize much of the area within approximately 30 km (18 miles) or so of McMurdo. Of most value are many years of measurements of annual snow accumulation

* SPAWAR is NSF's reimbursable support provider for air traffic control, NAVAIDS, flight following, and aviation weather.

along the snow road connecting Williams Field and Pegasus airstrip. Data from a long-term McMurdo surveyor (Jeffrey Scanniello, Antarctic Support Contract, pers. comm., undated) indicate that a typical year sees about 1.3 m (4 ft) of snow accumulation at Williams Field and that this depth diminishes gradually to about 0.3 m (1 ft) when moving westward until a point about 1.5 km (1 miles) east of the Pegasus airstrip. There, accumulation drops off sharply to about 0.15 m (6 in.) at the Pegasus site.

Additionally, the SPAWAR center out of Charleston, South Carolina, maintains aviation weather models, measurements, and historical records. They have an excellent understanding of the minimum visibility and ceiling requirements for various USAP aircraft and how McMurdo-area weather patterns during typical flight-operation periods impact these minimums. In a study they completed in 2002 when USAP was considering options for an alternate landing strip for aircraft that could not make a round-trip mission from New Zealand without refueling in McMurdo (i.e., LC-130 Hercules), they "binned" regional weather into areas that had progressively more favorable flying weather when any of the primary USAP airfields (Williams Field, the annual Sea-Ice Airfield when it existed, and Pegasus) were below minimums. This study concluded that patterns for aviation weather at Williams Field and the Sea-Ice Airfield were too similar to distinguish. Pegasus weather tended to be enough different that it could be designated as likely to be flyable when either of the other two airfields were below minimums. However, in terms of a reliable alternate landing area, SPAWAR data showed that it would need to be located well outside of the MIS to be unaffected by a weather system that compromised flying at any of the primary McMurdo-area air facilities (Art Cayette, SPAWAR, pers. comm., undated).

2.6 Contamination potential

In siting the Pegasus airstrip, there was knowledge of mineral dust deposition in the airstrip area during strong wind events from the south (Klokov and Diemand 1995; Blaisdell et al. 1998). An analysis of the dust collected at Pegasus in 2009 showed them to be conglomerates of individual mineral particles in a filamentatious carbon-rich matrix (Susan Taylor, CRREL, pers. comm., 2012).

In more recent years, closer examination of these deposits has shown that an active dark-colored organic material (Diana Wall, Antarctic Suport Contract, pers. comm., 2016) is now very common in the Pegasus area and

for some distance to the east. Ad hoc study of the organic material, shown in Figure 8, reveals that it appears to travel onto the MIS attached to mineral particles. Biological examination and study of the organic material has identified it as cyanobacteria (Barbato and Thurston, CRREL, pers. comm., 2016). When austral summer solar gain and higher ambient temperatures prevail, the dark mineral particles appear to generate a tiny microclimate (Figure 9) that is warm enough to create a small amount of water, which accelerates growth of these organic colonies. Being itself dark colored, the organic matter contributes to solar gain; and a positive feedback loop is formed that can, within a week or so, generate a large area of dark and wet snow that migrates downward to create a "badlands" of warm, deteriorated, and weak snow as shown in Figure 10. Left completely unchecked, "mats" of organic matter form (Figure 11). Specifics of how the material is actually transported to this area of the MIS and how it blooms and propagates will be the subject of future studies.

Figure 8. Moist organic matter (dark-olive to dark-brown clumps) associated with tiny dark black mineral particles (individual particles on the finger).

Figure 9. Pocket of "rotted" snow where mineral dust and cyanobacteria have made a foothold, creating a small, wind-protected, microenvironment conducive to melt.

Figure 10. Area of snowpack "rotted out" by localized melting and ablation caused by the microclimate induced by a concentration of contaminants.

Figure 11. A several-centimeter-thick mat of cyanobacteria in the base of a "rotted" snow pit just to the east of Pegasus airstrip. This area was untouched throughout the austral summer, allowing the cyanobacteria to flourish (image taken 26 January 2016).

Obviously, such features are highly undesirable on or near an airfield complex. Therefore, the aerial extent of organic contamination was of immediate interest when considering siting a new airstrip. CRREL and NSF performed satellite imagery and helicopter reconnaissance missions to determine if the area of snowpack on the MIS impacted by mineral dust deposits and cyanobacterial growth was predictable or stable. While not exhaustive, studies suggest that over the past ten or so years, the area showing contamination has steadily spread eastward from the Pegasus airstrip (at the western edge snow cover on the MIS). By 2016, it was possible to see clearly from satellite images that contaminated snow extended up to 5 km (3 miles) east from the Pegasus airstrip. Further, the areas covered take on curious geometries (Figure 12 and Figure 13) with very sharp boundaries (Figure 14) not proximal to any landforms. The spatial extent is most likely related to general wind currents associated with weather fronts moving through the region. Cursory examination of imagery prior to 2015 shows that there is some consistency in the shapes and distribution of the contaminated areas.

Figure 12. MODIS (Moderate Resolution Imaging Spectroradiometer) satellite image of the McMurdo area on 14 January 2016 showing (*1*) dark areas of contaminants, (*2*) White Island, (*3*) Black Island, (*4*) Minna Bluff, and (*5*) McMurdo.

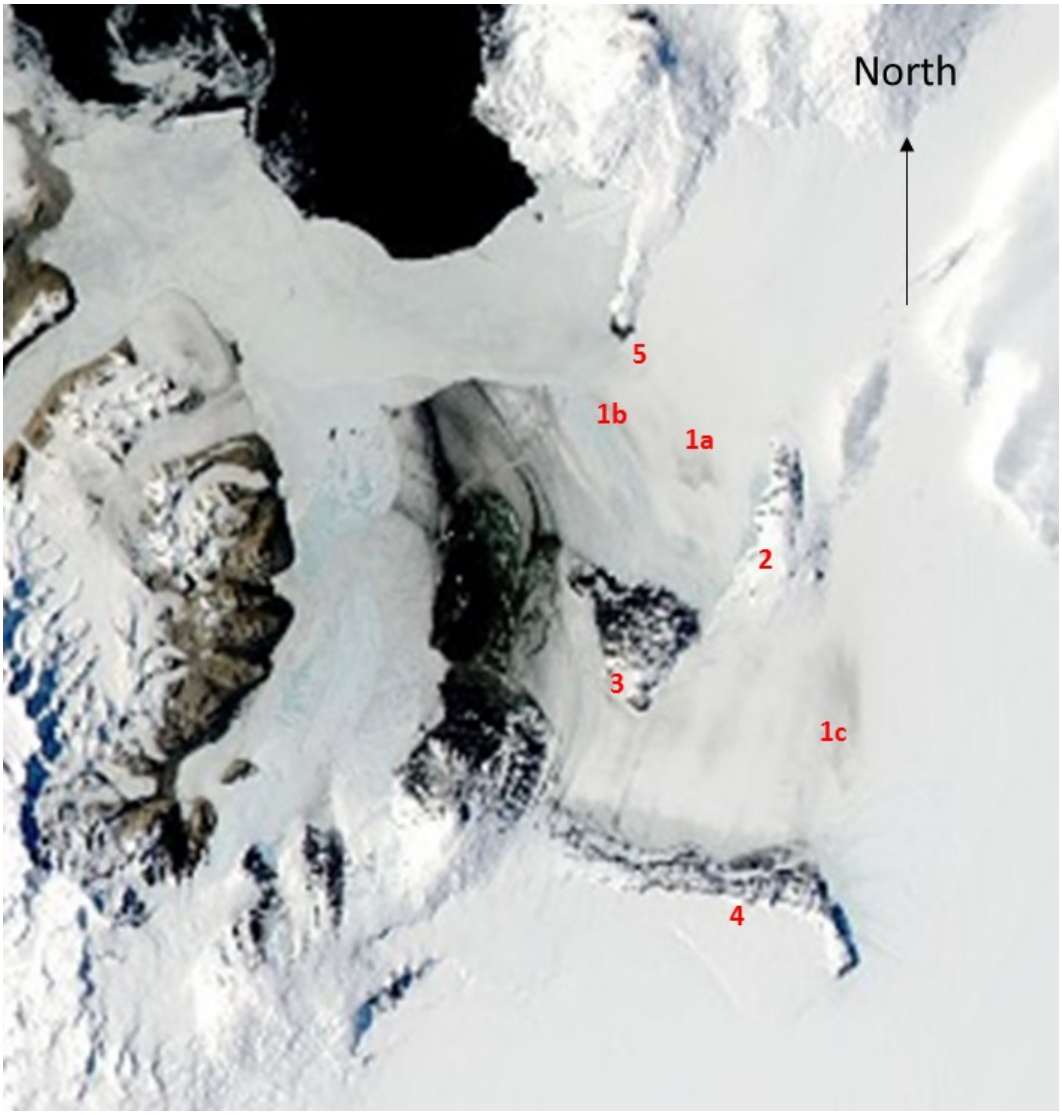

Figure 13. Oddly shaped contamination area 1a from Fig. 12.

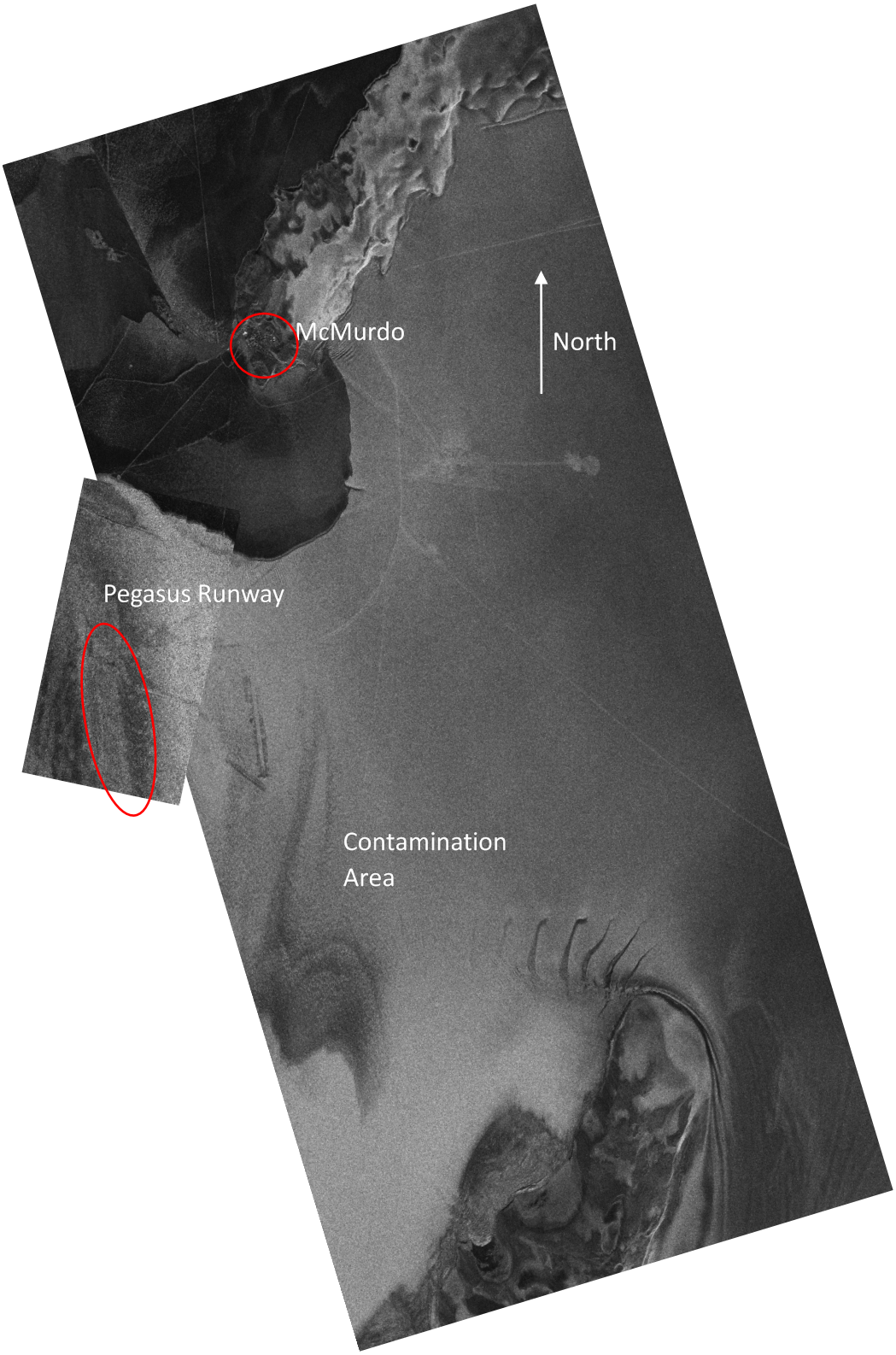

Figure 14. Curvilinear south edge of contaminated area 1a depicted in Fig. 12 and Fig. 13 (*top*: view looking east-southeast toward White Island) and sharpness of the boundary between contaminated and clean snowpack (*bottom*: view looking north towards Mt. Erebus).

Experience at the Pegasus airstrip and along the road leading to it led us to believe that limited amounts of mineral dust and associated cyanobacteria could be managed with a reasonable amount of effort to remove its potential to damage a snow runway. Thus, we were not adamant that a replacement runway site have no evidence or history of mineral dust contamination, but we certainly favored finding a site that showed minor deposits as evidenced from past satellite images and from core samples.

Other types of contamination that we wished to avoid were sites of former fuel spills or other disturbance from human activity (e.g., entrainment of non-native materials, even in microscopic sizes, and topographic alterations) and large-scale melt and refreeze events that reduce albedo and coarsen snow particles.

2.7 Surface friction

Aircraft braking ability is a major concern when constructing a snow or ice runway. Aircraft do have guidelines on safe-landing runway friction levels. On conventional runways (paved or not), it is only when considerable snow, ice, or significant surface water is present that friction levels drop to levels that are of concern. However, ice and snow runways are inherently low friction, even in the best conditions.

Our experience with McMurdo-area airfields whose surfaces include moderately compacted snow (Williams Field), bare sea ice (annual Sea-Ice Airfield), graded glacial ice (original Pegasus Airfield), and strongly compacted snow (post-2001 Pegasus Airfield) shows that low but acceptable levels of surface friction can be maintained on snow and ice runways. Thus, in searching for a site for a new airstrip, we were unconcerned about the ability to achieve adequate friction levels to support robust air operations.

2.8 Accessibility

As mentioned earlier, all interested parties strongly desired any new airfield to be in close proximity to the population and work centers in McMurdo. Travel times for airfield maintenance workers, flight support services (fire fighters, cargo and passenger handlers, weather observers, NAVAID maintainers, aircraft fuelers, food service, and generator mechanics), and aircrews all strongly impact productivity and the duty day. In addition to wanting to minimize distance from McMurdo to the airfield, consideration also needed to be given to how personnel and materials are transported (i.e., a road system or other means) between the two locations and the reliability of that infrastructure with changing weather and climate.

2.9 Chosen site

Accounting for the constraints listed above drastically reduces the possible locations to build a replacement airstrip for the failing Pegasus facility. We were confident that we could accommodate the required performance and

dimensional requirements in a zone of modest snow accumulation in the central part of the MIS. Accessibility and our basic understanding of airspace design led us to confine our search along the immediate south side of the existing snow road connecting Williams Field and Pegasus.

In early 2015, a team from CRREL deployed to closely survey and perform glaciological evaluation of this area from a point about halfway between Williams Field and Pegasus, moving westward to the Pegasus Airfield. This site was initially named the Alpha site. The team closely inspected the snow surface, looking for evidence of recent dust and organic deposits and any from the past 20 years or more. They extracted cores ranging in depth from 1 to 3 m (3–9 ft)and studied the stratigraphy (looking for ice lenses [evidence of melt-refreeze events], mineral dust horizons, depth hoar layers, summer/winter snow layering, and the thickness of these layers), density, and ice grain shape and size distribution.

Results of the 2015 field study* in the area approximately one-third of the way from Pegasus to Williams Field showed that along a roughly north–south transect, natural snow density was consistently about 0.4 g/cm^3 (25 lb/ft^3) near the surface and close to 0.5 g/cm^3 (31 lb/ft^3) at a 1 m (3 ft) depth (Figure 15). From the 46 cores taken, over half of the snow mass in the top 0.5 m (18 in.) was fine grained with both faceted and rounded ice particles (Figure 16). The next highest concentration of mass in the snow column (slightly less than half) was melt-refreeze material (Figure 16), characterized by large, rounded polycrystalline frozen ice grains. Both consolidated and loosely bonded melt-refreeze layers were detected. This coarse-grain component of the snow mass is concerning as snow that contains a large fraction of coarse grains has a lower albedo and sinters (i.e., gains strength) very slowly in comparison to snow that is mainly (85% or more) composed of fine-grained snow. Because this compacted natural snow would be buried deep under the final snow-pavement surface, we considered that the effects of the lower-albedo, coarser, natural snow would not influence the final albedo of the airstrip. Also, because the construction period was expected to take almost two years, the slow sintering of these coarser grains would likely not detrimentally affect the overall

* J. Hardy, T. Melendy, and G. Blaisdel, "Phoenix Runway Coring: Data, Methods and Procedures: January 2015 Data Collection" (unpublished white paper prepared for the National Science Foundation, 16 September 2016), PDF file.

strength of the runway as this natural snow would gain adequate strength by the time the construction was completed.

Figure 15. Variation of undisturbed snow density with depth at the Alpha site. Data were acquired in January 2015 along the length and width of the 10,000 ft runway site.

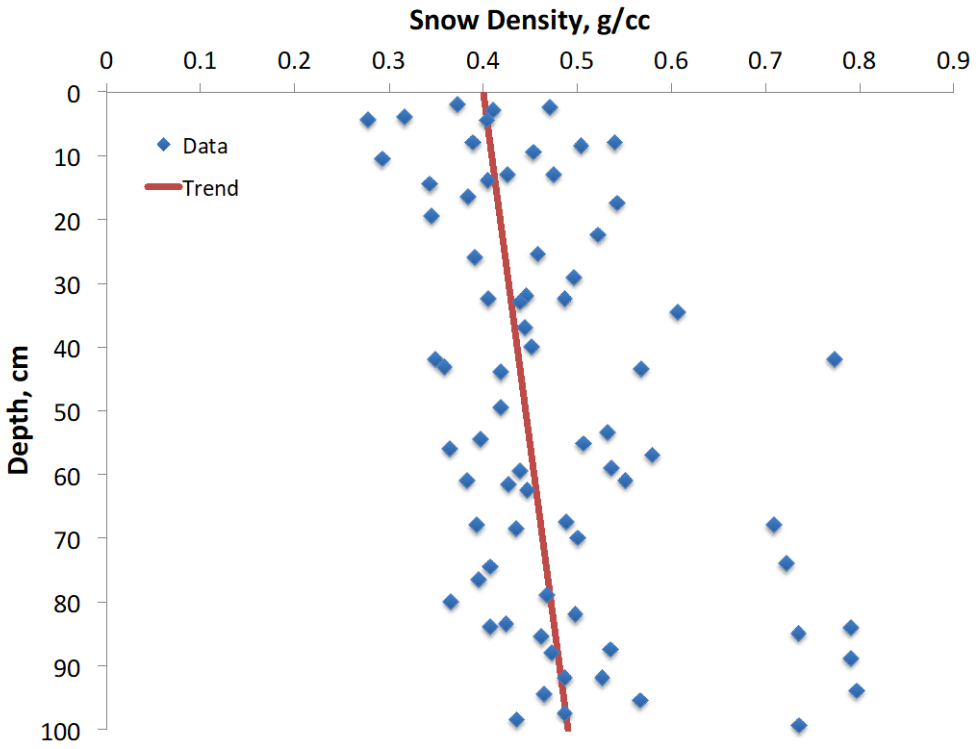

Figure 16. Percent occurrence of snow types in the top 0.5 m (18 in.) of 46 cores taken along a 3050 m (10,000 ft) north–south transect along the Williams Field to Pegasus snow road. Color gradation indicates different cores.

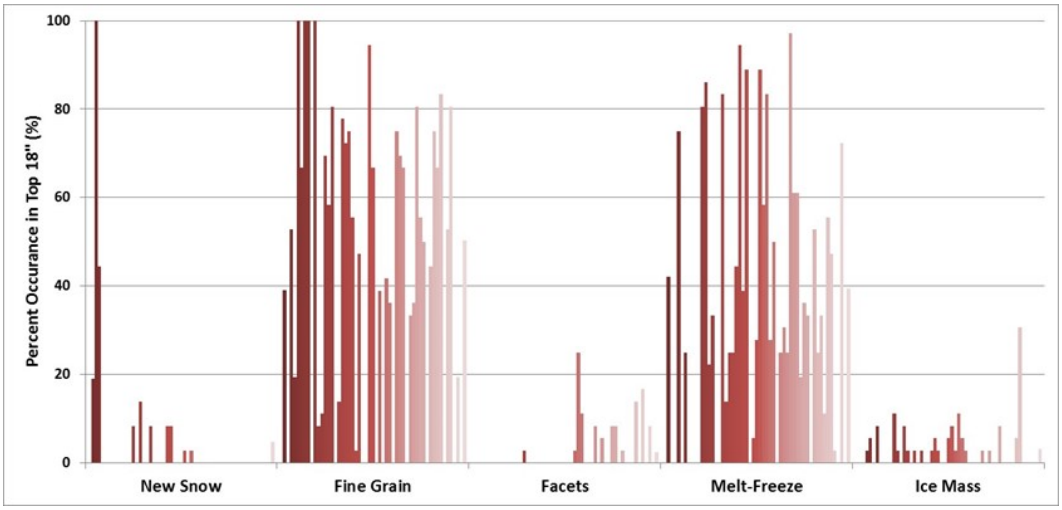

Hoar layers, which would be evidence of metamorphic activity that produces weak internal structure, were sparse. Some large, loosely consolidated, faceted ice grains were observed; but their presence was not extensive, either in vertical or lateral extent, and they were seen in only about 25% of the cores. Likewise, the presence of ice masses (horizontal layers or vertical pipes that were small, i.e., on the order of a few centimeters) was limited. This suggested that prolonged or aggressive melting most likely is rare in the area where Hardy et al.* took cores.

In addition to the snow characterization, for each of the 46 cores, we noted any dark particles in the cores. In most cases, there were no distinct particles. When present, the particles were categorized into two types:

- *Scattered dark particles (mineral or organic)*—The majority of the particles were organic and were easily distinguished with a hand lens by the irregular surface and brown color; the mineral particles were generally black. Organic material was much more common than mineral particles.
- *Distinct particle layer*—This concentration of particles in a horizontal layer were typically not more than a millimeter (0.04 in.) thick.

The small percentage of contaminants seen in this area was also very encouraging, suggesting that the area is likely adequately removed from the zones most prone to contamination (e.g., Figure 12).

We obtained satellite imagery and conducted ground surveys at the Alpha site to ascertain the patterns of mineral dust contamination and to determine if they were stable. With the assistance of the Polar Geospatial Center (PGC, https://www.pgc.umn.edu/), we studied high-resolution imagery of the MIS during the times of year when mineral dust and associated organic blooms are most obvious. This exercise demonstrated clearly how much the contaminated region has extended east over the past several years. Finally, we used the most recent depictions of contaminated areas (Figure 17) as the best guide of where to place a new airstrip.

* Hardy et al., "Phoenix Runway Coring."

Figure 17. MODIS image of the McMurdo area from 7 February 2016 showing distinct areas of contamination (gray snow east and west of the Pegasus Runway) on the McMurdo Ice Shelf.

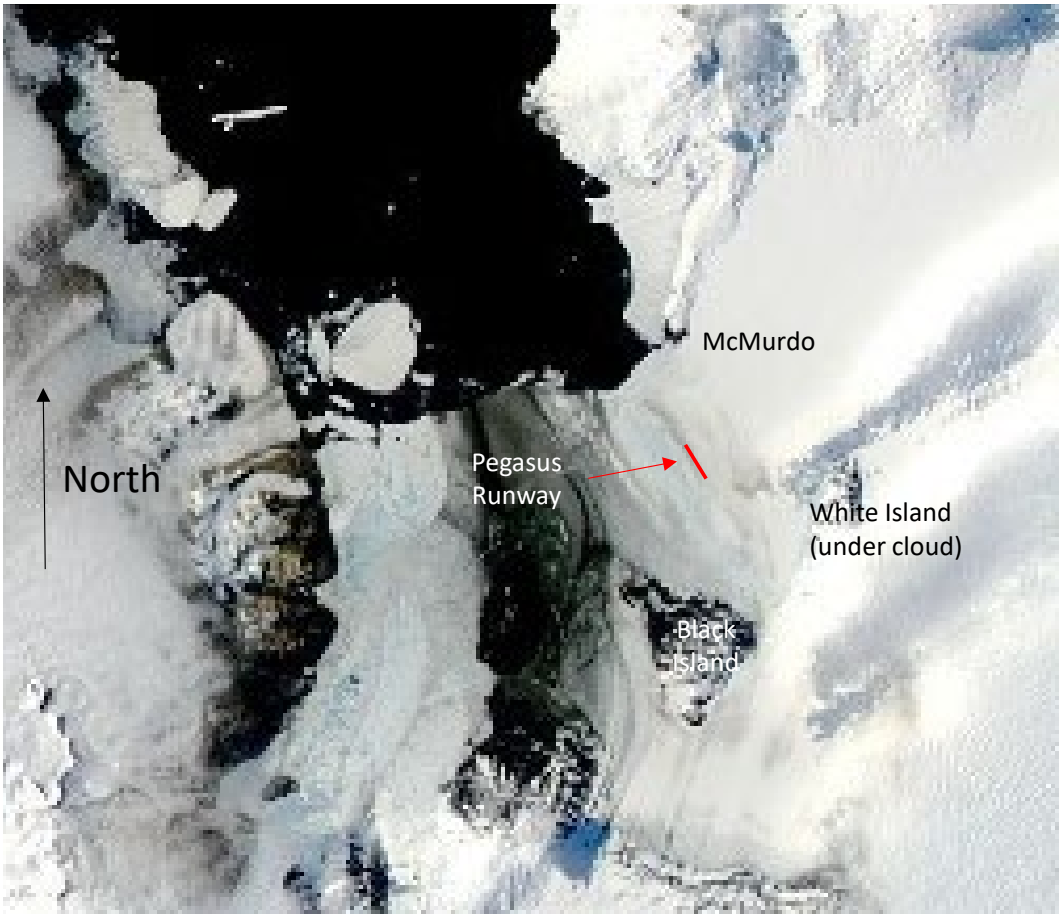

We ultimately determined that the combined results of the glaciological and contamination studies favored placing the new airstrip's north end just south of Mile Post 11 on the Williams Field to Pegasus snow road (Figure 18). This location had an annual snow accumulation rate of about 0.5 m (1.5 ft) and was located, at least at this time, in a gap between contamination bands to the west (engulfing the Pegasus Airfield, feature 1b in Figure 12) and to the east (the oddly shaped dark feature, 1a in Figure 12, Figure 13, and Figure 19).

Figure 18. Location of the site selected for development of a new airstrip (called Alpha site at the time).

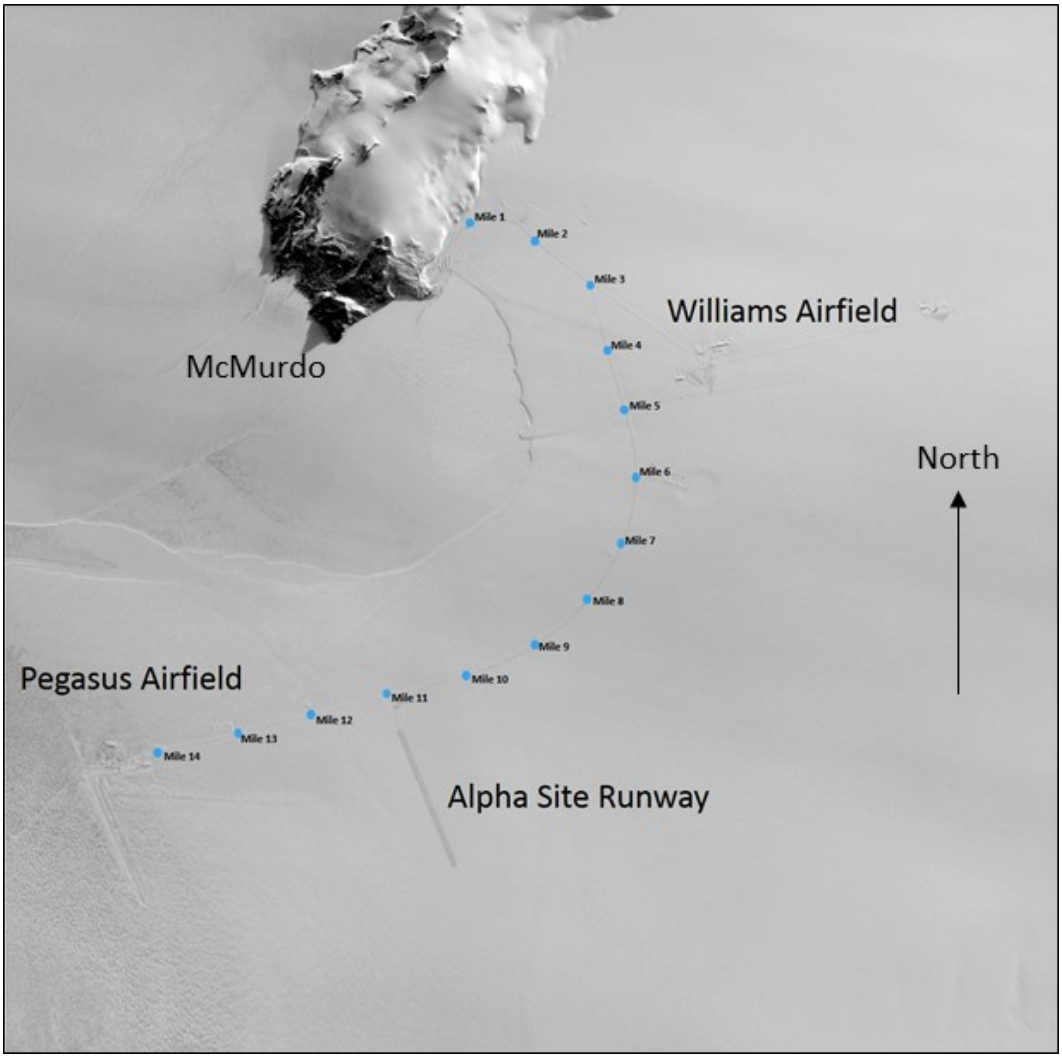

Figure 19. January 2015 satellite image of the McMurdo Ice Shelf just south of McMurdo, showing regions of concentrated contamination in relation to the Pegasus airstrip and the site selected for a new airstrip (called Alpha site at the time).

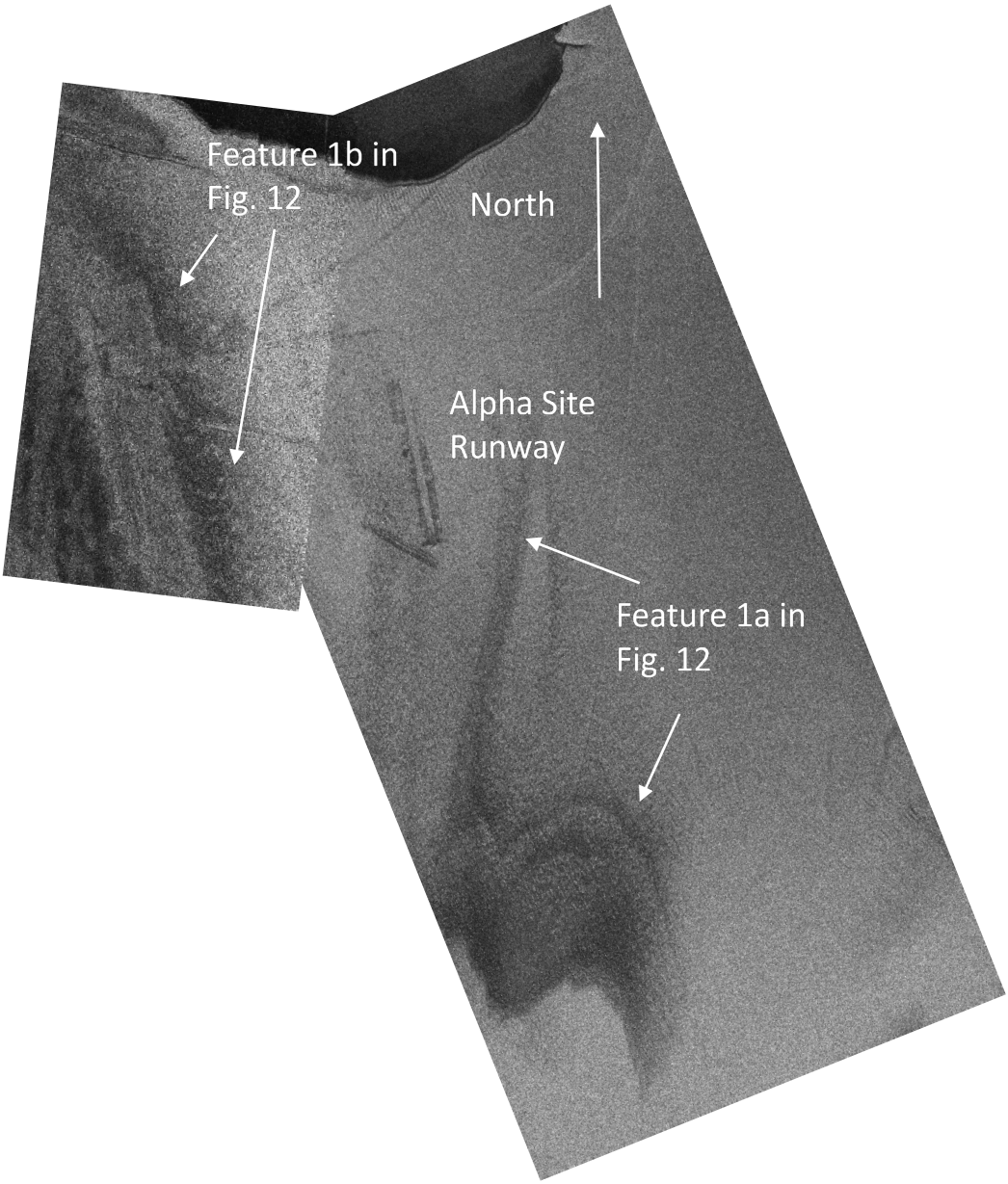

This area, while only 5 km (3 miles) east of Pegasus, possessed very different glaciological conditions. This suggested that wind and weather conditions could not be assumed to be the same. With assistance from SPAWAR, we established an AWS at the site. Wind directions and speeds were collected for 12 consecutive months during 2014 and 2015. The results (Figure 20) showed wind conditions at this location were much like those at Pegasus, meaning that runway alignment could remain at a 150°–330° headings.

Figure 20. Wind rose for the Phoenix site, showing the amount of time winds of various speeds prevail from various azimuth directions. In this case, the strongest winds (from about 170° to 190° headings) are much less frequent than the prevailing, weak winds (which arrive from headings of 20° to 80°). Intermediate-speed winds predominate from the 130° to 170° headings.

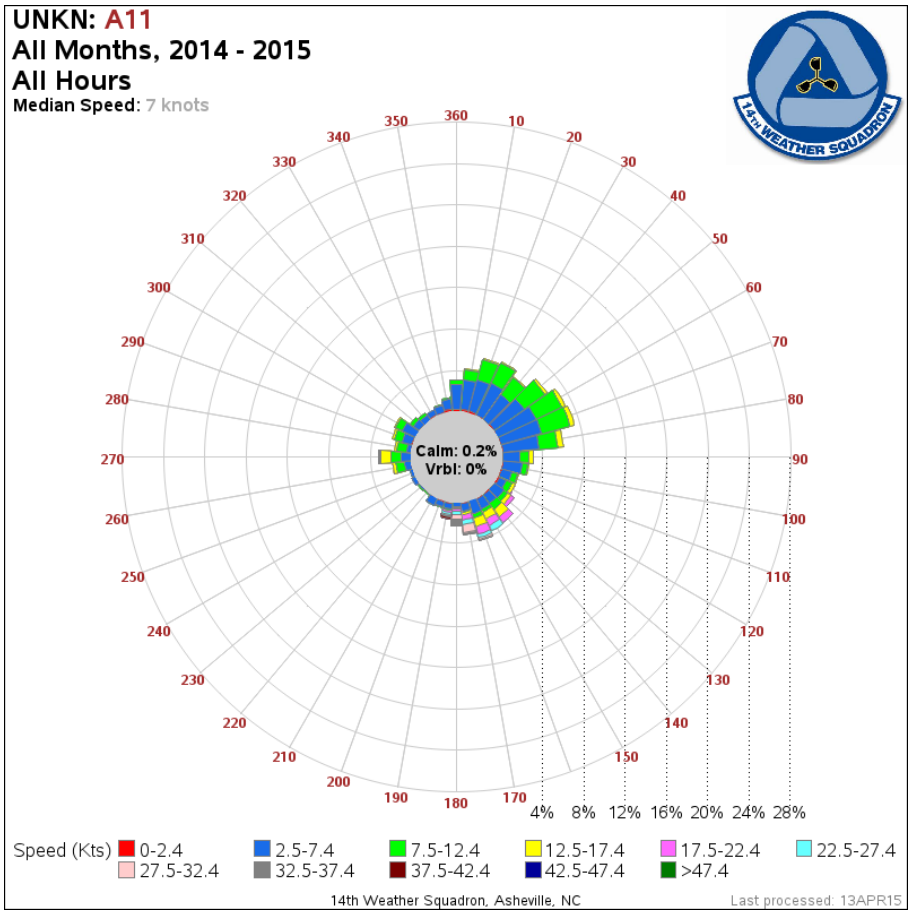

Using the location and runway heading, we had the McMurdo-area surveyors generate the GPS positions for the corners of the airstrip that would be the likely best fit. Having a specific site outlined, we proceeded to evaluate the other vital aspects necessary to support an airfield. Airspace design was most important to consider first since the fixed geographic features that would impede aircraft approaches and departures could hardly be remediated.

SPAWAR, together with the New York Air National Guard (NYANG*) in Schenectady, New York, are responsible for establishing approach and departure procedures for USAP airfields. We provided these groups with the

* The NYANG is NSF's reimbursable support provider for on-continent heavy airlift—LC-130 Hercules aircraft.

proposed airstrip corner points, and they conducted an analysis that assessed all potential takeoff and landing pathways. They determined through a TERPS analysis that all the desired procedures (e.g., Figure 21) could be completed at this proposed site. However, owing to the high terrain a short distance away to the south (White Island) and very high terrain starting a short distance north (Ross Island and Mt. Erebus), even a slight shift in placement or airstrip orientation would have compromised these procedures.

Figure 21. Approach plate for Phoenix Runway 15 (true azimuth heading of 150°).

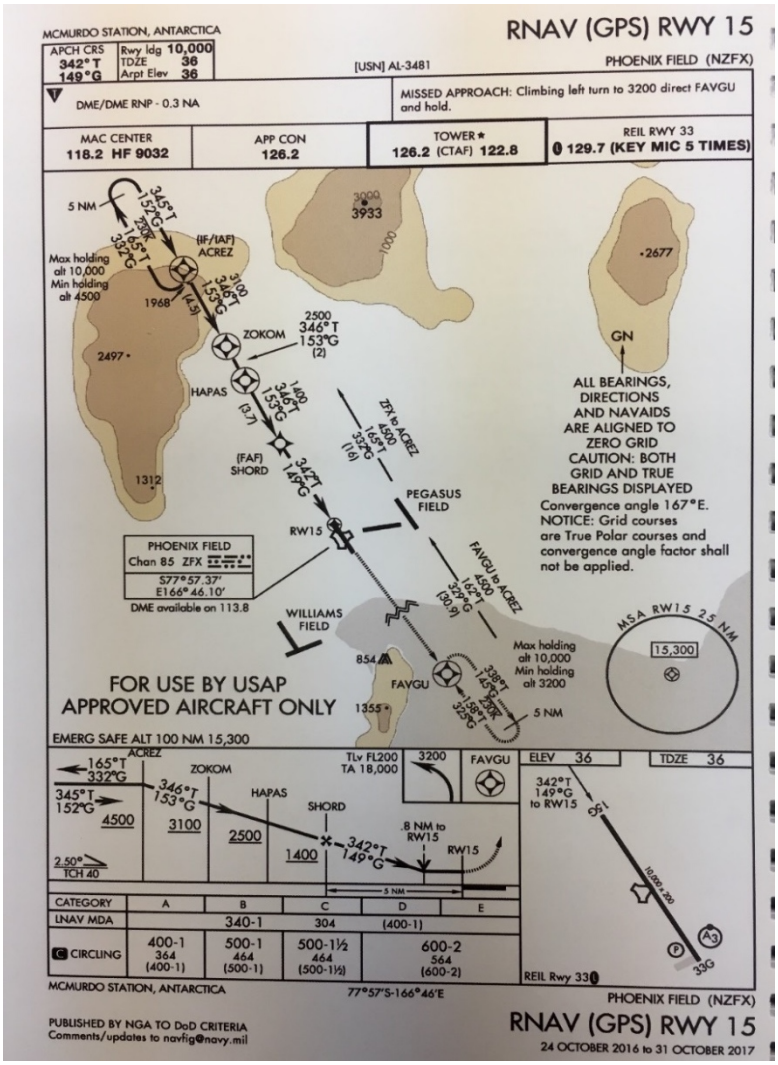

As mentioned earlier, we had reason to think the selected site may have notable weather differences from Pegasus. In the early days of planning for a new airstrip, NSF engaged the National Center for Atmospheric Re-

search (NCAR, https://ncar.ucar.edu/) to study weather patterns along the Williams Field to Pegasus snow-road corridor. That study (Manning and Powers 2011) used historical McMurdo-area forecast data from the Antarctic Mesoscale Prediction System (AMPS)—an advanced numerical weather-prediction model that provides real-time weather forecasting for the USAP—to determine if detectable differences in weather could be expected along the corridor of interest. Specifically, Manning and Powers (2011) compared weather at Williams Field, Pegasus, and two sites approximately equally distributed between the two airfields ("Alternate 1," closest to Pegasus, and "Alternate 2," closest to Williams Field). They focused on wind speed, wind direction, temperature, wind chill, precipitation and relative humidity. The study found the following:

- Little difference in mean wind speed is seen among the four sites.
- The strength of southerly winds at Alternate 1 and Alternate 2 is generally less than at Pegasus.
- Strong winds are more prevalent and persist longer at Pegasus, and this trend decreases with distance east toward Williams Field.
- Little difference in temperature, or temperature range, is present within the corridor studied; however, the frequency of colder temperatures generally becomes higher when moving from Williams Field to Pegasus.
- Small differences in wind chill exist at the four sites, yet slightly lower mean wind chill temperatures are present at the two Alternate sites compared to the two established airfields.
- Precipitation shows a strong gradient along the corridor, with total precipitation at Williams Field more than twice that at Pegasus. Specifically, Alternate 1 received 125% of the precipitation that occurred at Pegasus; Alternate 2's was 156%; and Williams Field's was 223% of Pegasus.
- Relative humidity is highest near Pegasus and lowest near Williams Field; however, the largest difference seen was only 2.4%.

Unfortunately, the NCAR study did not discuss visibility or ceiling. However, aviation weather experts at SPAWAR with intimate knowledge of this study and of McMurdo weather were able to interpret the study's findings and to conclude that sites along the corridor of interest would very rarely be expected to have conditions that were anything other than an interpolation of weather experienced at Pegasus and Williams Field. This, along

with our long collective experience on the MIS, caused us to be unconcerned that the selected site would present a notable difference in available operating days to what is experienced now at Pegasus.

Siting the airfield at this location would rely heavily on a transportation system over snow roads, as is the case now and in the past. While snow roads have their limits in terms of seasonal strength and thus the types of vehicles and supportable travel speeds, they are well understood within the USAP and are generally very reliable. A long-held concern exists around the potential for a single-point failure at the place where the majority of McMurdo's snow-roads connect directly to Ross Island, known at the Scott Base Transition. No convenient alternative is obvious; and while at times maintenance intensive, the current road "transition" has not threatened transportation success for more than 50 years. Therefore, we do not view continued use of snow roads and the Scott Base Transition as a limitation for providing access to the new airfield.

2.10 Naming

During development of the Pegasus Airfield in the 1989–1990 season, the closest "landmark" was an abandoned C-121 Constellation aircraft named "*Pegasus.*" This led to the site, and eventually the airfield, being named for that aircraft. The international airfield designation for the Pegasus Airfield is NZPG.

During the time the *Pegasus* aircraft was being operated in Antarctica (1964–1970), a sister Constellation aircraft, named *Phoenix*, also performed missions between New Zealand and McMurdo (Figure 22). In continued homage to the early USAP's Constellation aircraft, the new airfield was named Phoenix. It is also entirely fitting that, like Greek mythology's Pegasus, the Phoenix is a flying creature. Remarkable, also, is that the Phoenix is a long-lived bird that is cyclically reborn by arising from the ashes of its predecessor (in our case the "burned up" Pegasus Airfield). The signage and logo now associated with the Phoenix Airfield is inspired by the nose art on the C-121 *Phoenix* (Figure 23). The international airfield designation for the Phoenix Airfield is NZFX.

Figure 22. C-121 Constellation aircraft *Phoenix* in McMurdo, operated by the Navy expeditionary air squadron VX-6 (California) circa 1960.

Figure 23. Logo for new McMurdo-area airfield, Phoenix.

3 Snow Runway Strength

In this section, we determine the minimum strength requirements needed for a snow runway that will support operations of a C-17 and outline methods for assessing that these target strengths are achieved. Mosher and Sherwood (1967) recommend that the maximum load carrying capacity (i.e., runway strength) of the top 40 cm (60 in.) of a snow runway pavement needs to be equal to or greater than the tire inflation pressure. This is consistent with the design strength profile for the Molodezhnaya Airfield—operated from 1981 to 1991—wherein the top 40 cm (60 in.) of the snow pavement had an unconfined uniaxial compressive strength of at least 0.9 MPa (130 psi) to support landing the Il-18D aircraft and at least on one occasion an Il-76TD aircraft (Mellor 1993; Russell-Head and Budd 1989). The tire pressures for the Il-18D and Il-76TD are 0.79 MPa (114 psi) and 0.66 MPa (95 psi), respectively (Table 1). The Il-18D requires a higher surface strength owing to the higher tire pressure. However, aircraft with higher overall weight require that deeper layers be stronger to prevent subsurface rupture; this means that the Il-76TD, with a gross weight that is about three times that of the Il-18D, provides a more demanding strength requirement deeper in the pavement.

The variation in the design strength with depth for the Molodezhnaya Airfield is shown in Figure 24 (red line). We also note that for the Molodezhnaya Airfield, the minimum pavement thickness, T—the entire thickness of material that is strengthened to support aircraft operations—is 1 m (39 in.) (Mellor 1993).

Aver'yanov et al. (1983) provides some further limited insight on the Soviet experience building snow runways (i.e., the thickness of the "strengthened" part of the runway depends on the depth of the "active stress zone" and can vary from 400 to 800 mm [15–30 in.], depending on the aircraft type). It is unclear what is meant by the "strengthened" part and whether that refers to the thickness, t, of the contact surface on the top of the runway or, T, the total pavement thickness. Aver'yanov et al. (1983) also indicate that the required strength of the top layer can vary from 0.5 to 1.2 MPa (72–174 psi), depending on the airframe, though no firm guidance is provided on the relationship between the aircraft characteristics (e.g., gross weight, tire pressure, etc.) and the required top-layer strength.

Table 1. Summary of characteristics for aircraft that have landed on snow or ice runways. Where possible, the characteristics provided are for operating on snow or ice; otherwise, the maximum operating characteristics for these aircraft are provided.

Aircraft	Tire pressure, main landing gear, kPa (psi)	Maximum Gross Aircraft weight, kg (lb)	Weight on main landing gear, kg (lb)
KC-135	824–1070 (134[b]–155[a])	125,263 (275,579[b])	30,000 (67,000[b])
C-17	993 (144)	223,000 (490,000)	106,000 (233,000)
LC-130	724 (105)	70,500 (155,000)	33,500 (73,600)
IL-18D	786 (114[d])	61,180 (134,600[b])	29,060 (63,940)
Il-76TD	530 (77)	171,360 (376,990)	81,395 (179,070)
An-74	490–786 (71[d]–114)	34,571 (76,058[c])	16,422 (36,128)
C-5A	765 (111[e])	382,000 (840,000[d])	181,000 (399,000)
C-141	1240 (180[f])	146,000 (322,000[f])	69,500 (153,000)
757-200	1310 (190)	116,000 (256,000)	55,000 (121,000)
767-300ER	1413 (205[e])	176,000 (388,000[e])	83,770 (184,300)
A-319	1380 (200)	62,700 (138,000)	29,800 (65,550)

[a] DOD (2001), Table 4-1

[b] Abele (1990), Table 7

[c] Palt (2017)

[d] Mellor (1993)

[e] USAF (2015a), Table B-1

[f] Klokov and Diemand (1995)

Figure 24. Comparison of snow runway pavement strength profiles (1 psi = 0.006895 MPa).

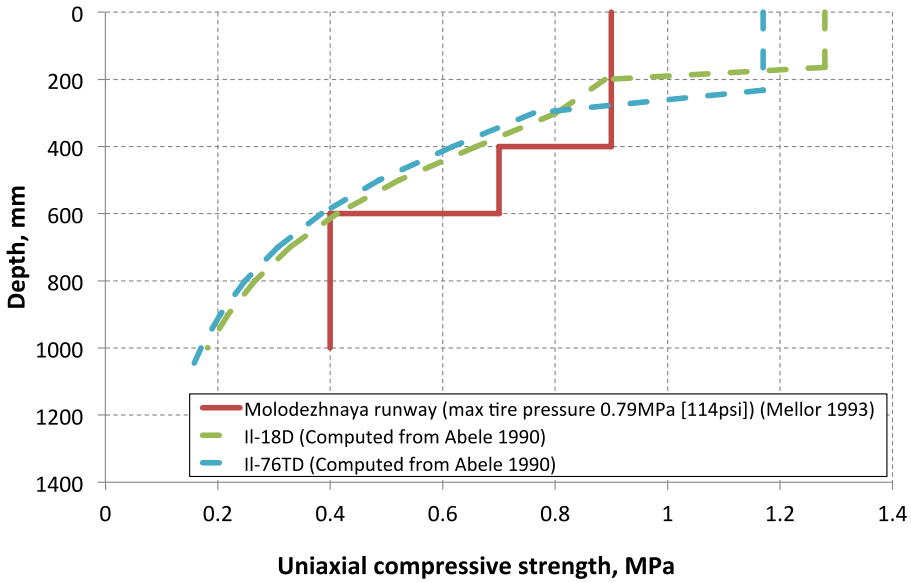

The other documented landing of a wheeled aircraft (an An-74) occurred at Vostok Station on a skiway that is ordinarily maintained for operations

with ski-equipped aircraft. Mellor (1993) notes that "the subsequent take-off was a bit of an adventure" and that the aircraft took off on the third try. The aircraft left ruts 20–30 cm (8–12 in.) deep. It appears that that was the only landing and takeoff of a wheeled aircraft at Vostok. Mellor (1993) goes on to say that the density of the runway was on the order of 450 kg/m^3 (28 lb/ft^3) while the density required to support an An-74 is about 580 kg/m^3 (36lb/ft^3). Mellor (1993) provides no detail on how this required density was determined. The maximum tire pressure for an An-74 is 79 kPa (114 psi) but can run as low as 49 kPa (71 psi).

Beyond the above information, we were unable to find more detailed data on what formed a basis for the strength profile for the runway at Molodezhnaya. Abele et al. (1968) and Abele (1990) do provides guidance on strength requirements for aircraft operating on a snow runway; Abele et al. (1968) suggests that for this approach, FS = 1.2 or less. We apply this guidance to the Molodezhnaya case here and compare that value to the design strength (red line) in Figure 24. First, Abele (1990) dictates that the thickness necessary for the top "high-strength" pavement layer is $t = r$ where r is the equivalent circular contact area radius of the tire contact patch, as in

$$r = \sqrt{A/\pi}, \tag{1}$$

and A is the contact patch area, which is approximately the load borne by each tire divided by the tire pressure. Within this thickness, the strength can be determined using the nomogram from Abele (1990, Figure 126). The input information for the nomogram is as follows:

1. The average tire contact pressure—lacking additional information, we assume this is close to the tire pressure
2. The load on each wheel
3. Number of wheel coverages, C, which is the number of wheels in the landing gear that are in-line so they roll over the same patch of snow (e.g., a dual landing gear, a common nose-gear configuration, has two tires side-by side, so $C = 1$; for a tandem landing gear, one tire follows in the track of the preceding one, therefore $C = 2$)

Both the Il-18D and the Il-76TD have tandem main landing gear; therefore, based on the guidance of Abele (1990), $C = 2$ should be used. For the Il-18D, the nomogram gives the strength of this top layer as 1.3 MPa (185 psi), while it is 1.2 MPa (170 psi) for the Il-76TD. These are plotted as

the vertical portion of the dashed lines in Figure 24. These values are considerably higher than the 0.9 MPa (130 psi) strength that was used at Molodezhnaya for the top layer (Figure 24, solid red line), suggesting that the Abele (1990) guidance may be overly conservative.

Below this top layer, Abele (1990) assumes the strength of the pavement varies with the depth according to the Boussinesq relationship for soils. The dashed lines in Figure 24 show the computed strength using the method proposed by Abele (1990) for the two-aircraft used at Molodezhnaya, the Il-18D and Il-76TD. Note that the stress variation with depth, σ_z, for the dashed lines was computed using the modified Froehlich equation (Smith et al. 2000),

$$\sigma_z = \sigma_o \left[1 - \left(\frac{z}{[r^2+z^2]^{1/2}}\right)^{\nu}\right], \quad (2)$$

to estimate the Boussinesq variation of stress with depth in soils. In equation (2), σ_o is the applied surface stress (force over area), and z is depth. Note that the Froehlich concentration factor, ν, was chosen for these two aircraft to get a reasonable match of the stress distribution (dashed lines) for each aircraft to the strength profile (solid red line). For the Il-18D, ν = 17, while for the Il-76TD, ν = 8. It is hard to know the correct value for ν for any particular case since ν is a parameter that captures the effects of the variations with depth in the stiffness (e.g., elastic modulus) of the supporting soil structure on the varying stress profile. Hence, the parameter ν needs to be calibrated for each soil or snow structure and, it appears, for each load configuration and therefore is hard to determine a priori.

The guidance of Abele (1990) recommends that the surface strength at Molodezhnaya should have been a factor of 1.4 higher than the actual design value used at that airstrip. This is likely because Abele (1990) includes provision to specify an increase in the surface strength if there are multiple passes in the same tire track made by the landing gear (i.e., one or more tires following the lead tire). The rationale for this is that the lead tire may cause some small degree of failure in the surface and the following tires will progressively continue to cause the surface to fail. The landing gear of the Il-18D and Il-76TD both have a tandem configuration where one tire follows immediately behind the lead tire. It appears that the surface strength specified for Molodezhnaya does not account for multiple passing of wheels over the same track as the specified surface strength is only 1.14 times higher than the maximum tire pressure (0.79 MPa [114 psi] for the

Il-18D). However, if we apply the Abele (1990) approach accounting for only one pass of the wheel on a track, the surface strength would be 1.0 MPa (150 psi) for the Il-18D and 0.97 MPa (140 psi) for the Il-76TD, about 15% higher than the specified surface strength for Molodezhnaya Airfield. The high-strength surface layer at Molodezhnaya is quite a bit thicker than the minimum thickness, r, recommended by Abele (1990), which, depending on the aircraft, is $t = 1.7r$ to $2.4r$. Based on this comparison of the Abele (1990) guidance to the Molodezhnaya design, we conclude that there are too many uncertainties in the available design guidance for snow runways and that a more rigorous approach is required to estimate the strength requirements needed to support a specified aircraft.

We now turn to U.S. Department of Defense (DOD) and USAF guidance for airfield construction for the C-17. Based on DOD (2001), Table 2 shows the runway strength with depth for a C-17. The specifications given in this table are for a light- to medium-load runway with a maximum of 200 passes (with 1 pass including landing and takeoff, provided there is a separate taxiway), which is the minimum number of passes designed for in the DOD (2001) specification. The overall thickness of this pavement structure is approximately 0.9 m (36 in.) as specified in DOD (2001) Table 6-2, which is the cumulative thickness of the subbase to surface layers (obtained from DOD 2001 Figure 10-18). The thickness of base and surface layers are determined from DOD (2001) Table 8-5. DOD (2001) specifies the strengths of the subsurface layers in units of California Bearing Ratio (CBR); an approximate correlation of CBR to uniaxial strength is equation (7) and is used to convert the CBR in Table 2 to the strength in units of stress (Table 3).

Table 2. Paved runway strength with depth to support a C-17, based on guidance provided in DOD (2001). This is for a fully loaded C-17 (580,000 lb) and medium runway loading. Note that a CBR is not reported for the top layer (pavement surface); the strength of that layer is denoted by the material properties (e.g., elastic modulus) of the pavement.

Layer	Layer Thickness, mm (in.)	Strength, CBR (%), [Uniaxial compressive strength, psi]
Surface	100 (4)	NA
Base	150 (6)	80 [505]
Subbase	225 (9)	30 [163]
Subgrade	125 (5)	13 (95% compaction) [62]
Subgrade	300 (12)	13 (90% compaction) [62]
Total thickness	900 (36)	—

NA = Not applicable, runway pavement specified based on flexural strength not compressive strength (Parker et al. 1979).

Table 3. Strength correlations

Equation No.	Strength Parameter	Correlation	Reference
(3)	Rammsonde	$\sigma = 0.37R^{0.55}$	eq. (4) in Abele (1990)
(4)	Russian, RSP index (kg)	RSP index = $W\,h\,n/L + W + Q$	USAF (2002a)
(5)	RSP index	$\sigma = 4.1 + 0.45N$	Mellor (1993) Fig. 62
(6)	California Bearing Ratio, CBR (%)	$CBR = 1.44R^{0.48}$	eq. (7) in Abele (1990)
(7)	CBR	$\sigma = 0.23CBR^{1.15}$	Combining eq. (4) and (7)* from Abele (1990)
(8)	Dynamic Cone Penetrometer, DCP (mm/blow)	DCP = 2678.9 × RSP index$^{-1.1312}$	USAF (2015a)
(9)	CBR	CBR = 0.0423RSP index$^{1.267}$	USAF (2015a)

1 kgf/cm^2 = 14.223 psi = 98.1 kPa.

σ = unconfined uniaxial compressive strength (UUCS) (kgf/cm^2).

R = Rammsonde hardness index (kg).

N = number of Russian hammer drops to drive 10 cm ($N \geq 2$).

Q = total mass of the penetrometer without hammer (kg) (typically 1.75 kg).

W = mass of the drop hammer (kg) (typically 1.58 kg).

h = drop height (mm) (typically 500 mm).

n = number of hammer blows to penetrate depth, L (mm).

* The coefficient of 0.173 that comes out of combining these equations does not properly estimate the uniaxial compression strength (Abele 1990, Fig 32). We have adjusted the coefficient to 0.23 to get better overall agreement.

The paved runway structure specified by DOD (2001) is more demanding than may be needed for the Phoenix Airfield, which is better characterized as an unpaved or contingency airfield. Furthermore, Table 2 is for a fully loaded C-17 while the design specification for the Phoenix Airfield is a maximum gross weight of 227,000 kg (500,000 lb). Based on USAF (2002b), the minimum strength requirement for a contingency airfield for a fully loaded C-17 for ten passes (minimum number of resolvable passes in the USAF charts for contingency airfield evaluations for a C-17) is CBR = 12.5%. Designing to this strength would be conservative since the Phoenix Airfield will be maintained between passes (flights), and therefore it is more likely that the design criteria for the Phoenix Airfield can be for a single pass. We also estimate that the C-17 will arrive at McMurdo at a maximum weight of only 227,000 kg (500,000 lb) (Margaret Knuth, NSF, pers. comm., 2016); this lower weight means the design will be more conservative as USAF (2002b) is for a fully loaded 264,000 kg (580,000 lb) C-17. This serves only as a starting target value for minimum strength requirements for the surface layer since the design strength profile had not

been determined prior to this point. Development of a design profile follows. The full, layered section is analyzed later in this report for capacity after we discuss in section 3.3 the target design strength layers.

Figure 25 shows the computed CBR for the snow on the Phoenix apron. The top surface of the apron had been compacted using a sheepsfoot roller and pneumatic-tire weight cart. The strength of the deep snow may give some indication of the baseline strength of undisturbed snow. Note that for depths shallower than about 430 mm (17 in.), the lower bound in strength appears to increase the closer one gets to the surface. Below that, the lower bound in the strengths appear to be more uniform. This may indicate that the initial compaction of the base layer were effective at increasing the snow strength to a depth of about 430–460 mm (17–18 in.). Below this depth, the average measured CBR for the undisturbed snow is 14%; the minimum is 7.4%. However, to address variability in snow strength, we use a standard earth materials approach and report the strength value above which 85%, or two standard deviations, of the data lies (AFCESA/CES 1997). We term this the 85% rule. This is more conservative than using the mean to characterize the data as with the mean 50% of the data is weaker than the computed statistic for the pavement layer. By using the 85% rule, or reporting the "85% strength," only 15% of the sampled data is weaker than the reported value. Using this approach, the strength at the 15th percentile is CBR = 9.7%, which indicates that 85% of the measured strength values are at or above that level, providing a reasonable statistical estimate of the expected minimum strength of the undisturbed snow. These are reasonable values for the subgrade coarse, indicating that the strength of the undisturbed snow is in the ballpark of what is needed for the subgrade (CBR = 12.5%) but that some strengthening of that layer may be required to achieve acceptable subgrade strength. Furthermore, specifying a uniform strength with depth does not account for the higher strength needed at the surface due to the contact patch of the landing gear on the runway. To better understand what near-surface strength is needed to support the C-17, we used computational methods to estimate the stress in the snow-pavement structure when subject to the design load conditions.

Figure 25. Estimated CBR for the compacted snow on the Phoenix apron calculated from Rammsonde (RAM) measurements of the snow strength and the correlation of RAM to CBR (equation [6]). The documented snow in this figure supported a rubber-tired (inflation pressure of 450 kPa [65 psi]) Ox cart with a gross weight of 20,000kg (44,000 lb).

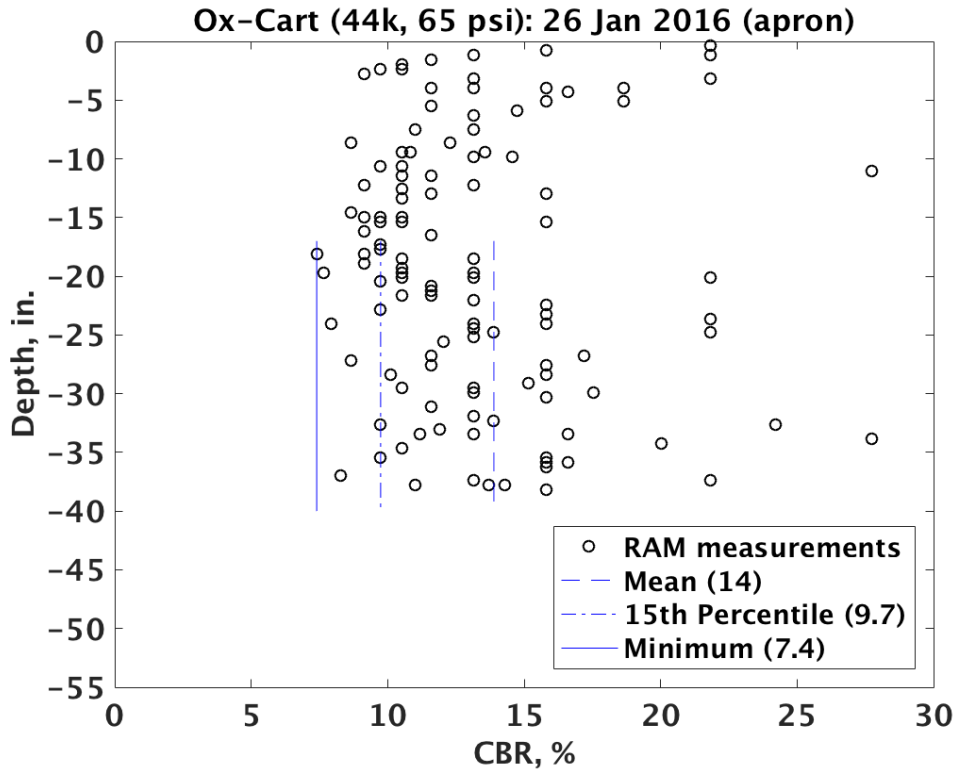

3.1 Computation of the runway stresses

To estimate the stresses imposed on the runway, we used a computational model developed by the FAA, Layered Elastic Analysis Formulation (LEAF version 2003.6.11.0) (Hayhoe 2002), that is used to calculate the stress in a pavement structure. This computational tool is implemented in FAA computer programs, including "FAA Layered Elastic Design" (LEDFAA V. 1.3) and "FAA Backcalculation" (BAKFAA V. 2.0*). Both of these allow forward calculation of the pavement stresses generated under an aircraft's main landing gear given the layered structure of the pavement. BAKFAA 2.0, or hereafter referred to as BAKFAA, also allows back calculation of the pavement structure given measured deflections and the imposed load (i.e., a falling weight deflectometer analysis).

* Available from https://www.airporttech.tc.faa.gov/Products/Airport-Safety-Papers-Publications/Airport-Safety-Detail/ArtMID/3682/ArticleID/11/BAKFAA-version-2101.

We used BAKFAA in the forward calculation mode to estimate the stresses in a snow runway for aircraft of interest (e.g., the Il-18D and Il-76TD on the Molodezhnaya Airfield and a C-17 on the planned Phoenix Airfield). We were also able to use BAKFAA to compute the stresses generated in the runway by the weight carts used to compact the snow runway at Phoenix, so we could compare the stresses generated by the weight cart to the stresses we expect to see when the C-17 is operating on the same surface. More specifically, we used the LEAF program within BAKFAA to compute pavement response for various landing-gear geometry and load configurations. LEAF was used independently, and each landing gear and load case was analyzed to a 1.02 m (40 in.) depth.

BAKFAA uses computationally efficient methods to compute the stresses at user-defined predetermined locations and depths in the runway. The runway pavement structure is entered into BAKFAA and saved in a structure file (.str). The pavement structure is defined in terms of

1. layer thickness,
2. elastic modulus of the layer, and
3. Poisson ratio of the layer.

Up to ten layers can be defined for the pavement structure.

BAKFAA treats all of the layers as elastic media. Though snow is a visco-plastic-elastic material, the loading and unloading cycle of any point on the snow runway imposed by a landing or departing aircraft is generally very quick; therefore, provided there is minimal deformation in the runway*, the elastic response is a reasonable assumption for takeoff, landing, and taxi maneuvers. This analysis is not applicable to long-term parking, however, wherein the creep behavior of the snow would play an important role in the overall deformation of the surface.

BAKFAA also assumes that the analysis is for the main landing gear; and since half of the full landing gear is simulated, it is also assumed in BAKFAA that the loading is symmetrical. Furthermore, the main landing gear supports 95% of the aircraft weight, an assumption that has been FAA policy since 1964 (FAA 2016). The geometry of several aircraft is readily available within the BAKFAA program. However, if other aircraft, nose gear, or

* That is to say, the imposed stress is well below the plastic limit for the runway materials such that rutting or other large-scale deformation or damage is not occurring.

geometries are of interest, such as a compaction weight cart, these geometries must be manually entered into the aircraft configuration file (LEAFAircraft.ext).

BAKFAA treats the contact patch of each tire as a circular area with an effective radius computed from equation (1); and the contact area is

$$A = 0.95 \frac{W_A}{2N_g p}, \tag{10}$$

where

W_A = the gross weight of the aircraft supported,
N_g = the number of wheels in the main landing gear on one side of the aircraft, and
p = the tire pressure of the wheels on the main landing gear.

Therefore, BAKFAA assumes the load on each individual tire is the same and is $0.95W_A/2N_g$.

At each specified evaluation point, BAKFAA computes the six stress components (vertical, horizontal in the lateral and longitudinal directions, and the three shear components), six strain components, displacements in the vertical and horizontal directions, and the principle stresses and strains.

In general, the above enumerated assumptions do not pose undue limitations on calculating the stresses associated with the main or nose landing gear on an aircraft or other tire configurations (e.g., a weight cart with each tire loaded to the same weight). However, we note that BAKFAA cannot simulate the condition where a train of wheels is not loaded equally (e.g., a weight cart that has wheels that are not equally loaded). For this more complicated case, more generalized computational methods, such finite element analysis (FEA), can be used. Though all of the features of BAKFAA can be replicated using FEA, in general FEA requires more effort to set up the simulation and takes more computational effort to run (several hours for an FEA analysis vs. under a minute for BAKFAA). Therefore, we limited use of FEA in this effort to cases where tire loading is nonuniform or for verification that governing assumptions in BAKFAA (such as treatment of the tire contact patch as a circle rather than an ellipse) is sufficiently accurate for our purposes. For the few cases where this effort used an FEA, it used the ABAQUS finite element software.

3.2 Snow-pavement structure

In addition to the tire load data discussed above, information on the variation in the material properties of the runway pavement structure (i.e., pavement layering) needs to be determined to accurately compute the imposed stresses within the pavement structure. As noted previously, in particular we need information on the elastic modulus and Poisson ratio for each pavement layer. This information has not been directly measured in the Phoenix Airfield. However, Shapiro et al. (1997) provide a summary of data correlating elastic modulus and snow density. The data summarized in Shapiro et al. (1997) show that elastic modulus increases with snow density; for the data presented by Shapiro et al. (1997), there is not a clear dependence of elastic modulus on snow temperature. Drawing from the data of Shapiro et al. (1997), we obtained an estimate of the elastic modulus of the snow from the design or measured snow density in the runway. Haehnel (2017) also compiled a look-up table for use in the ABAQUS finite element software to characterize the change in elastic modulus with snow density, which is reproduced in Table 4.

Table 4. Dependency of elastic modulus on snow density extracted from Shapiro et al. (1997).

Snow Density, kg/m³ (lb/ft³)	Elastic Modulus, MPa (psi)
200 (12.5)	1.379 (200)
380 (23.7)	98.20 (14,200)
410 (25.6)	146.9 (21,300)
470 (29.3)	303.3 (43,990)
540 (33.7)	633.6 (91,890)
620 (38.7)	1,319.0 (191,300)
770 (48.1)	4,165.0 (608,400)
900 (56.2)	9,532.0 (1,382,000)

For BAKFAA model input, we used the lower limit in elastic modulus of the Shapiro et al. (1997) data. For the FEA models discussed here, the information in Table 4 is provided directly as tabular input in the ABAQUS model. ABAQUS performs a linear interpolation between tabular entries to obtain a value for E for a snow density that is between table entries. For the calculations performed in this study, the snow densities were confined within the upper and lower bounds of the densities given in Table 4; therefore, no extrapolation beyond the bounds of Table 4 was required. Note

that ABAQUS does not extrapolate beyond the bounds of tabular input; rather, for values outside the limits of the independent variable (in this case density), the dependent variable is held constant at the limiting value (e.g., for a snow density less than 200 kg/m^3 [12.5 lb/ft^3], E is held at 1.379 MPa [200 psi]).

Shapiro et al. (1997) also provides information on Poisson ratio, γ, for snow. Though the data show that measured values of γ vary from 0.2 to 0.4, there is no clear trend with density. It appears that over the range of snow densities provided in Table 4, γ is on average around 0.30 to 0.35. For the purposes of this effort, we use $\gamma = 0.3$ independent of snow density.

Table 5 provides the design structure of the snow pavement. The proposed construction plan is to compact the snow in layers or lifts of 75 mm (3 in.). Figure 15 shows the measurements of the undisturbed snow taken during January 2015*. The average density from the surface to a depth of 1 m (39 in.) of the undisturbed snow at the Phoenix site is about 480 kg/m^3 (29.9 lb/ft^3)†; the average density at the surface is about 400 kg/m^3 (25.0 lb/ft^3); and at a depth of 1 m (39 in.), it is 490 kg/m^3 (31 lb/ft^3). Therefore, we assume for the design that the subgrade has a density of 490 kg/m^3 (31 lb/ft^3). For the purposes of model computations, the bottom layer is considered infinite, and the properties for this layer do not change with depth. Initially, we assume the density at the depth of the undisturbed layer is the same as what was observed in Figure 15 at a depth of 150 mm (6 in.) below the original snow surface. The right-most column in Table 5 shows the planned increase in snow density during construction of successive lifts, with the top of Lift 4 being the planned final runway surface when flight operations commence.

Note that this analysis is purely elastic; and although the modulus depends on density, the model does not compute changes in the density with loading (as in compaction) as that is a plastic response. The development of an elastic-plastic FEA constitutive model for the Phoenix Airfield has not yet been performed and is out of the scope of this project.

Though Table 5 provides the planned structure of the runway, observations taken on 2 February 2016 show that the actual densities achieved during construction for the base layer and Lift 1 are higher than the

* Hardy et al., "Phoenix Runway Coring."

† Hardy et al., "Phoenix Runway Coring."

planned densities, with Lift 1 achieving a depth-averaged density of 630 kg/m^3 (39 lb/ft^3), which is considerably higher than the target values of 575 kg/m^3 (36 lb/ft^3). To accurately determine the stresses generated in the runway by the C-17, the design values need to be updated to the actual values. To understand the effect of the variability in snow density on the stress calculations, we performed a sensitivity study on snow density.

Table 5. Design runway cross section as proposed April 2015 (NSF 2015a). Elevation is given relative to the surrounding undisturbed terrain, with negative (−) elevations indicating that the planned final elevation of the constructed surface is below the surrounding terrain. The density of the subgrade later provided in this table is determined from the measured density of undisturbed snow at that depth in January 2015.

Layer	Top elevation		Layer thickness		Target density (kg/m^3)
	mm	in.	mm	in.	
Lift 4	230	9	76	3	675
Lift 3	150	6	76	3	650
Lift 2	76	3	76	3	600
Lift 1	0	0	76	3	575
Base	−76	−3	76	3	525
Subgrade	−150	−6	Infinite	Infinite	490

Source: Hardy et al., "Phoenix Runway Coring."

Owing to the expected differences between the design snow density and actual snow density achieved in the runway, we explored the effect of density variability on the elastic modulus of the snow and how that may affect the computed stress profile (Sopher and Shoop 2017). Using BAKFAA, we computed the stress for the C-17 on the design density profile given in Table 5 (and also included in Table 6 along with the estimated moduli and strengths inferred from this density information) for the Phoenix Airfield and the IL-18D and the IL-76TD on the Molodezhnaya Airfield. Figure 26 compares the landing-gear configuration for each of these aircraft. Table 7 compares the aircraft load and strength requirements.

The C-17 was modeled with 95% of the weight on the main landing gear and each set of main landing gear supporting one half of this, equally distributed to each tire. Two weights were used in the BAKFAA modeling: the C-17 at the weight expected for landing at McMurdo, 500,000 lb, and an empty C-17 at 280,000 lb.

The BAKFAA model results show a very comparable stress distribution beneath each tire, indicating that the relative weakness (low stiffness) of the

snow does not significantly influence stresses between each wheel. The maximum of the major principle stress at anywhere on tire contact patch was chosen as the most conservative (highest) estimate of stress for use in the following analysis.

Figure 27 provides the results of this analysis. This shows that the surface stress is largely independent of the variation in elastic modulus typical of expected snow density variability. There is some variation in the strength attributable to density variations deeper in the snow, though the variation is small.

Table 6. Updated design density and strength profile for the runway at the Phoenix Airfield from April 2016.

Lift	Phoenix Target Lift Thickness, mm (in.)	Depth to Bottom of Layer, mm (in.)	Target Density, kg/m³ (lb/ft³)	E_s[K], MPa (ksi)	E_c[B], MPa (ksi)	E_x[E], MPa (ksi)	Unconfined Compressive Strength[A], MPa (psi)
5	75 (3)	75 (3)	675 (42.1)	NA	1900 (280)	3000 (440)	2.5 (363)
4	125 (5)	200 (8)	675 (42.1)	NA	1900 (280)	3000 (440)	2.5 (363)
3	125 (5)	325 (13)	650 (40.6)	NA	1700 (250)	2700 (390)	2 (290)
2	125 (5)	450 (18)	600 (37.5)	NA	1000 (150)	2100 (300)	1.4 (203)
1	125 (5)	575 (23)	575 (35.9)	NA	600 (87)	2000 (290)	1 (145)
Base	225 (9)	775 (31)	525 (32.8)	100 (15)	360 (52)	1800 (260)	0.6 (87)

[K] E_s = Static elastic modulus (data set K in Shapiro et al. 1997, Figure 6).

[B] E_c = Elastic modulus determined from uniaxial compression data (data set B in Shapiro et al. 1997, Figure 6); strain rate approximately 3×10^{-3} to 2×10^{-2} s^{-1} at −25 °C.

[E] E_x = Complex Modulus (data set E in Shapiro et al. 1997, Figure 6); complex modulus evaluated at 103 Hz and −14 °C.

[A] Abele (1990), most conservative estimate (see also Appendix A).

NA = No data available in that range in data set K (Shapiro et al. 1997, Figure 6).

Table 7. Comparison of aircraft weight and strength requirements as determined by Abele (1990) and this study (C-17 at McMurdo, with CBR value determined from the guidance of Abele 1990). Note that some of the gross weight and tire pressure values in this table differ from that of Table 1; the values in this table are as given by Abele (1990) while those in Table 1 are representative of conditions used for reported landings on snow and ice runways.

Aircraft	Gross Wt (lb)	Wheel Load (lb)	Tire Pressure (psi)	Required CBR	Equivalent Sigma (MPa)	Rammsonde
C-5A	732,500	26,000	150	45	1.424	>>1000
C-141	318,000	40,000	150	47	1.724	>>1000
IL-18	134,000	15,000	114	38	1.276	750
C-17 at McMurdo	500,000	40,000	160/144	37.5		

Figure 26. Landing-gear configuration for the C-17 (*top*), Il-76TD (*middle*), and Il-18D (*bottom*).

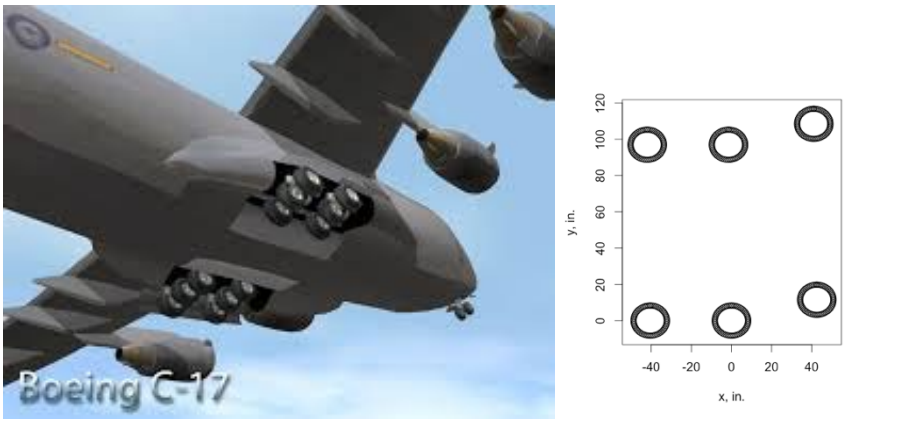

Figure 27. BAKFAA model results for the C-17, assuming elastic modulus based on target snow density from Table 6 (for a range of E based on density) and Il-76 and Il-18 for the same snow conditions. Compressive stress is positive.

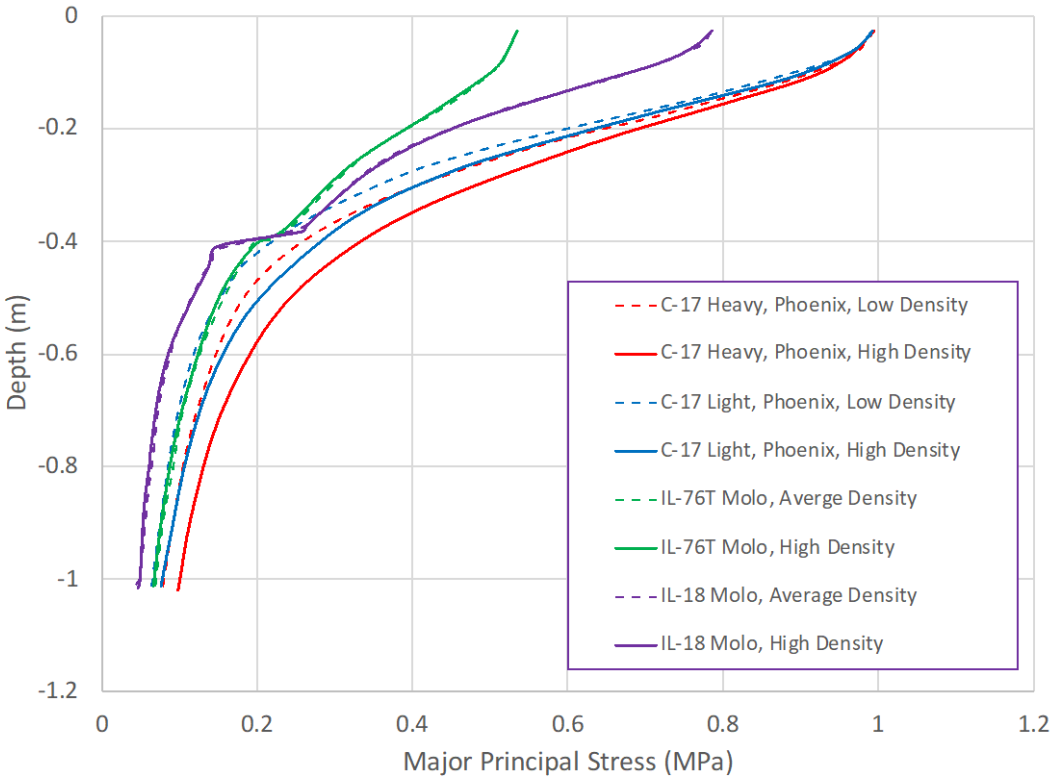

Additionally, the airfield design requirement was compared to the requirement specified by Abele (1990). The CBR = 37.5 surface layer for the C-17 is lower than Abele's requirements of a CBR of 45 and 47 for a C-5A and C-141 aircraft, respectively. We note that the tire pressures used by Abele (1990) for the C-5A and C-141, and given in Table 7, are different than what is given in Table 1; but still we provide the values as is in Table 7 as these are the values that Abele (1990) used to estimate the required snow strength for those aircraft. We also observe that though the C-17 has a higher tire pressure than the Il-18D, it is closest to the requirements for the Il-18D with a CBR of 38. The Il-76 is closer to the weight of the C-17 although the tire pressure is much less.

3.3 Acceptable runway strength

In addition to the stresses computed for the C-17 main landing gear presented in the previous section, owing to the higher tire pressures of the nose gear (1.1 MPa, or 160 psi), we also compute the stresses associated with the higher tire pressure. The configuration of the nose gear is dual wheels that are 737 mm (29 in.) apart (USAF 2015b). We assume the nose

gear carries as much as 5% of the total aircraft weight, or 11,000 kg (25,000 lb) for an aircraft loaded to the runway design gross weight of 200,000 kg (500,000 lb). Using these computed stresses, we now develop a target runway-strength profile for a C-17 operating on the Phoenix Airfield.

We computed the stresses under and around the C-17 tires at several locations to determine where the maximum stresses may occur: at the tire centerline, offset from the centerline but still under the tire, at the tire's edge, and beyond the edge of the tire as indicated in Table 8. The location of the tire edge is based on the assumptions applied in BAKFAA and is determined from equation (1) to calculate the effective contact-patch radius. These stress computations were made on both sides of the tire in the lateral direction, which is perpendicular to the direction of travel by the aircraft, to determine if the stresses differed at these various locations depending whether there was a tire adjacent to a tire edge or whether there was no adjacent tire (e.g., the outer side of an outside tire). These same computation points were used in front of and behind the tire (in the longitudinal direction, or direction of travel).

Table 8. Locations in the horizontal plan along which stresses were computed around landing-gear tires using BAKFAA for the C-17.

Stress Computation Location along the Lateral and Longitudinal Tire Axes	Nose gear, mm [in.]	Main gear, mm [in]
Centerline	0	0
Under tire	± 76.2 [3]	± 127 [5]
Tire edge	± 127 [5]	± 244 [9.6]
Beyond edge of tire	± 254 [10]	± 381 [15]

In addition to the stress components computed by BAKFAA, we computed the von Mises (abbreviated as Mises) stress, σ_v, at each computation point

$$\sigma_v^2 = \frac{1}{2}\begin{bmatrix}(\sigma_{xx}-\sigma_{yy})^2+(\sigma_{xx}-\sigma_{zz})^2+(\sigma_{yy}-\sigma_{zz})^2+\\ 6(\sigma_{xy}^2+\sigma_{xz}^2+\sigma_{yz}^2)\end{bmatrix}, \quad (11)$$

where σ_{xx}, σ_{yy}, and σ_{zz} are the normal stresses acting in the cardinal X, Y, and Z directions and σ_{xy}, σ_{xz}, and σ_{yz} are the shear stresses. The Mises stress is a stress measure that accounts for the interplay of the three-dimensional stress field on the deformation and failure of the material and is often used as a failure criteria in materials (i.e., failure is expected to occur

when the computed Mises stress is higher than the material strength). Figure 28 compares the Mises and principle stress components at these various stress computation points to determine the most severe stress condition under the landing gear.

Figure 28. Computed von Mises and principle stresses in the runway under a tire in the main landing gear of a C-17. The gross weight of the aircraft is 230,000 kg (500,000 lb), and the tire pressure is 993 kPa (144 psi). The notation *1*, *2*, and *3* indicate the three principle stresses, with *1* being the major and *3* being the minor. The *solid lines* indicate the computed stresses where there is a tire adjacent to the tire of interest. The dashed lines indicate the stresses on the outside of an outer tire of the landing gear; therefore, there is no adjacent tire on that side of the wheel. All calculations were made using BAKFAA. Table 6 provides the snow structure used for these calculations.

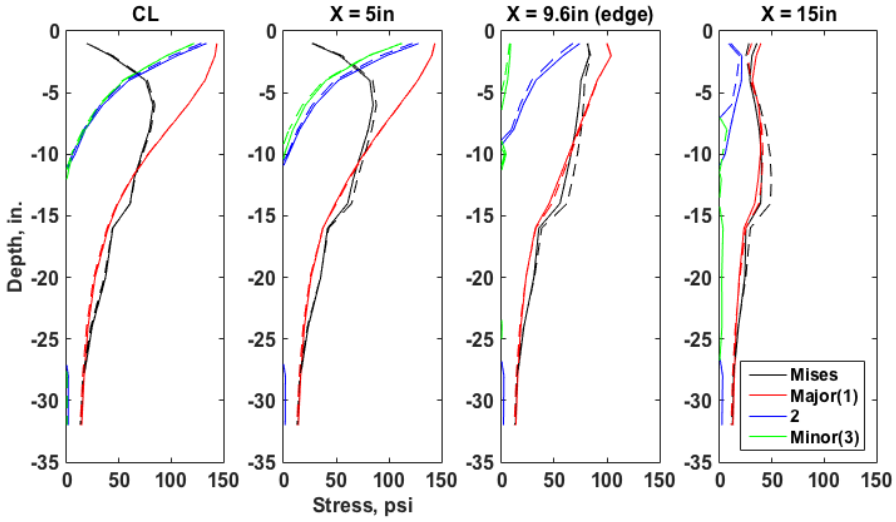

Figure 28 shows the computed stresses associated with the main landing gear for the design case and a density profile indicated in Table 6; offsets from the tire centerline, X, are as indicated as in Table 8. The solid lines are stress profiles obtained between adjacent tires while the dashed line indicates the stress for the side of a tire where there is not an adjacent tire (outer side of the landing-gear configuration).

The left pane in Figure 28 shows the stresses under the centerline (CL) of two tires: one that is in the center of the landing gear (solid line) and therefore has tires on either side of it and an outer tire (dashed line), which thus has only one adjacent tire. For all practical purposes, there is not a difference in the stresses at the centerline of each tire. Also, comparing the left two panes, we see that under the tire, the Mises stress is near zero at the surface while the major principle stress (which is closely aligned with the vertical direction) near the surface is approximately equal

to the tire pressure. Though under the tire the maximum stress is approximately the major principle stress, the Mises stress is slightly higher than the major principle stress below 300 to 675 mm (12 to 27 in.). Between tires, the Mises stress measure can be equal to or slightly greater than the computed principle stresses.

Another feature worth noting is that on the side facing outward on an outside tire, the computed Mises (dashed black lines in the right two panes) is higher than that between two tires (solid black lines in the right two panes). This is a result of the confinement between adjacent tires elevating the lateral stresses and thereby reducing the Mises stress.

What we are able to conclude from Figure 28 is that the maximum Mises stresses are realized at the tire edge, and the maximum principle stresses occur under the tire centerline. Furthermore, the outside edge of the outside tires produces the highest Mises stresses. We note that the difference in Mises stresses between adjacent tires is not very profound for the C-17 main landing gear, owing to the ample spacing between adjacent tires. This difference is more prominent as the spacing between tires is reduced. These same basic trends are observed for the nose gear as well. The most conservative design criteria would be to use the maximum stress measure (Mises or major principle stress) with depth at the tire edge and centerline.

Figure 29 compares the stresses imposed by the main landing gear (solid lines) and the nose gear (dashed lines). Here we compare only the Mises stress at the tire edge and the major principle stress at the tire centerline. As was stated previously, these provide the most extreme stress conditions. Figure 29 shows that, in general, the main landing gear imposes a higher stress on the runway, except at the surface where the higher pressure of the nose gear imposes higher stress in the top 75–100 mm (3–4 in.) of the runway. This suggests that generally we can design for the main landing-gear loads, but the top few inches need to have an elevated strength to account for the higher stresses associated with the nose gear. Note that the green (dash dot) line indicates the maximum of all stress measures and provides a conservative upper limit on the stresses for both sets of landing gear.

We note that close to the surface, the major principle stress defines the most conservative failure criteria. At a depth of about 375 mm (about 15 in.) and below, the Mises stress fluctuates around the major principle

stress; for all practical purposes, it can be considered the same as the major principle stress. Therefore, based on this analysis, using the major principle stress computed under the tire centerline provides a conservative estimate of the failure criteria for the pavement surface.

Figure 29. Comparison of von Mises stress at the edge of the landing-gear tire and major principal stress under the tire centerline for the main landing gear (*solid lines*) and the nose gear (*dashed lines*).

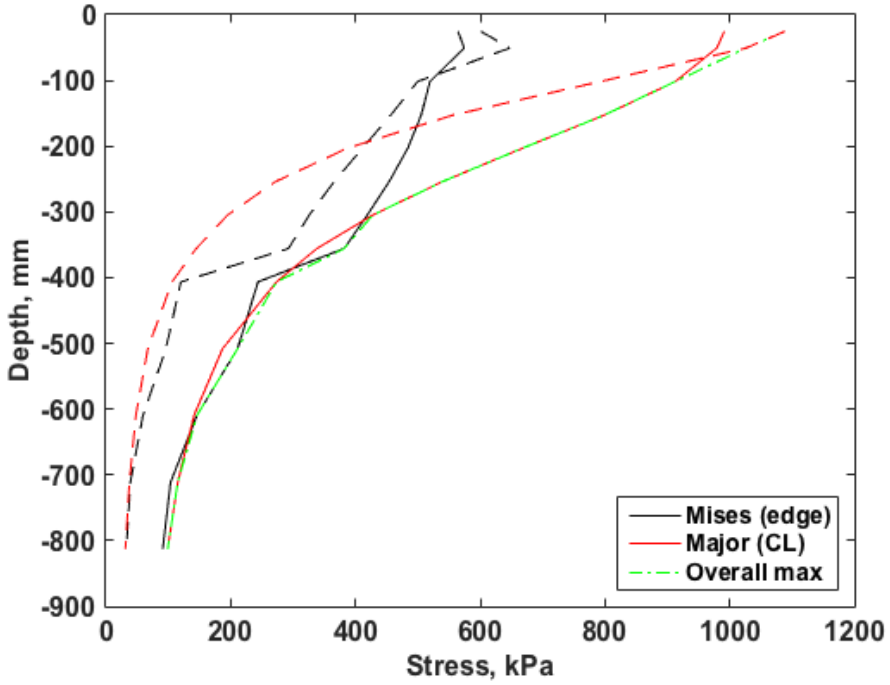

We emphasize, however, that though BAKFAA provides valuable insight on runway stress, we are cautious about these findings because

1. BAKFAA is not a validated model for snow and has never been applied to snow before now;
2. there are many assumptions used to convert strength measures and density, and none of these include snow metamorphism impacts on strength, which can be extremely significant;
3. BAKFAA is a purely elastic model, and snow is known for plastic and viscous behavior;
4. BAKFAA does not account for tire construction and nonuniform contact stress; and
5. BAKFAA assumes all tires in the landing gear are uniformly loaded (this is considered a valid assumption for the C-17 per USAF staff).

3.4 Recommended runway design strength

Based on the analysis in the previous section, we found that the design strength for the runway needs to exceed the major principle stresses under the tire centerline (e.g., as shown in Figure 29) by at least the design FS = 1.25. We consider a design runway strength that meets these requirements as follows.

First, we accept that the minimum strength of the runway down to a depth of 1 m (39 in.) needs to be at or above the CBR = 12.5% associated with a contingency airfield, as discussed previously.

Then, we consider the guidance of Abele (1990) for the runway surface. For a C-17 with the design load, the surface strength computed from Abele (1990) would be 1.3 MPa (185 psi) for the nose gear and over 1.4 MPa (210 psi) for the main gear. For each of these, we use the number of wheel coverages, $C = 1$ (Abele 1990). For the nose gear, $C = 1$ is appropriate as it is dual wheels. Using $C = 1$ for the main landing gear, however, may be open for debate as the C-17 is a modified tandem configuration wherein the following wheels are offset laterally 38 mm (1.5 in.) from the leading wheels (Figure 26) and the wheel tracks are not exactly one on top of another but do overlap.

The higher strength value of 1.4 MPa (210 psi) is a factor of 1.3 higher than the maximum stress at the surface (1.1 MPa [160 psi]) indicated in Figure 29, very close to the planned FS = 1.25. Based on Abele (1990), this should extend to a depth of 250 mm (9.6 in.) as determined from equation (1).

Finally, we need to preserve FS ≥ 1.25 in between these limits. Figure 30 shows a candidate structure (red solid and dashed lines) for the Phoenix airstrip that meets the design criteria. Also provided for comparison is the computed stress imposed by the C-17 landing gear on the runway for the design conditions and the computed stresses imposed by a fully loaded Southwest (SW) weight cart wheel that might be used for proofing the runway (the use of the SW cart will be discussed in greater detail in the following section).

The vertical dashed red line is the guidance of Abele (1990) as discussed above: runway strength is 1.4 MPa (210 psi) to a depth of $r = 250$ mm (9.6 in.). The solid red line indicates the rest of the candidate structure

with the vertical section from a depth of 500–1000 mm (20 to 35 in.), representing a CBR = 12.5% with the strength converted to megapascals (using equation [12]), allowing comparison to the computed stresses. The vertical segment between these upper and lower depths was determined as follows. First, at a depth of 250 mm (9.6 in.), FS = 1.25 was applied to the larger of the two computed stress measures for the C-17, in this case, the major principle stress (0.626 MPa [91 psi]): 0.78MPa ≈ 1.25 × 0.626 MPa, so this vertical segment has a value of 0.78 MPa (113 psi). The lower bound for this middle segment was determined using the fully loaded SW cart as the limiting stress; during proof testing of the runway, we do not want failure of the lower layers of the runway to compromise the runway. Having the step change from the lower strength to the middle segment at a depth of 500 mm (20 in.) avoids overstressing the runway with the proof cart at any depth in the runway.

Figure 30. Comparison of the proposed runway structure needed to support a C-17 (*red solid and dashed lines*) to the computed runway stresses created by the C-17 landing gear with a maximum aircraft gross weight of 227,000 kg (500,000 lb). Also provided for comparison is the design structure for the Molodezhnaya airstrip. For this figure, the density profile used to calculate the pavement stresses for the C-17 and Southwest (SW) cart is from as-built observations made in November 2016.

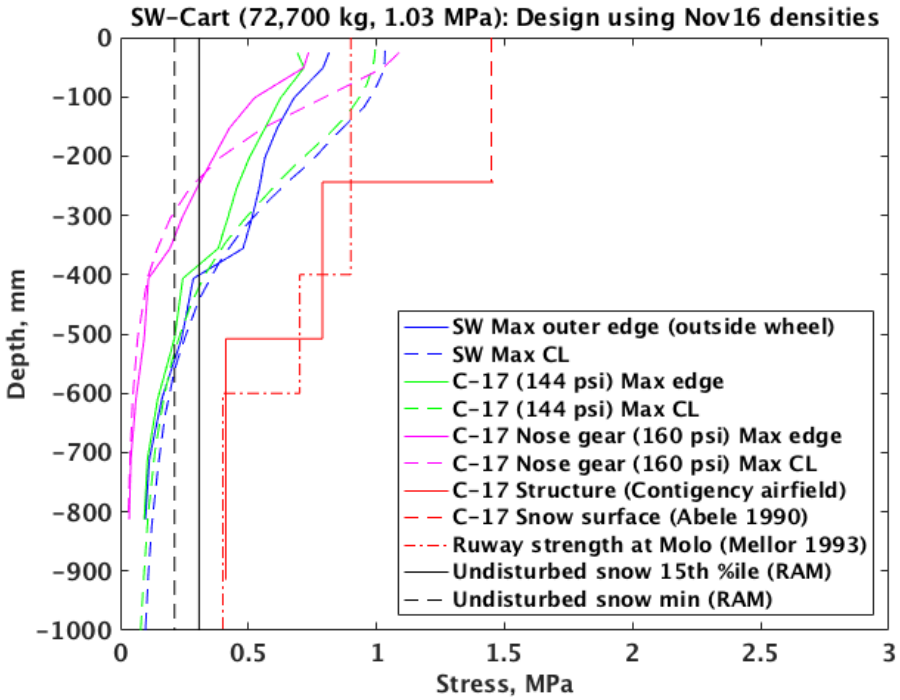

The proposed runway structure in Figure 30 (and summarized in Table 9) uses only three changes in strength with depth. In Figure 30, we also provide for comparison the runway-strength profile used at Molodezhnaya. The lower surface strength needed at Molodezhnaya is likely due to the lower tire pressures of the Soviet aircraft used there. The Soviets also extended the high-strength layer deeper than what Abele (1990) recommends. Interestingly, at lower depths, the strengths chosen in the present study (CBR = 22 for mid-depths and CBR = 12.5 for the deepest part of the runway) match up well with the values used by the Soviets at Molodezhnaya. The only difference is that the Molodezhnaya Airfield carried the high strengths deeper into the runway than the design proposed for Phoenix.

Table 9. Strength and minimum factor of safety for a C-17 loaded with a gross weight of 227,000 kg (500,000 lb) and a strength profile as indicated in Fig. 30.

Depth range, mm (in.)	Strength, MPa (psi)	RSP Index (kg)	Minimum FS
0–250 (0–10)	1.45 (210)	99	1.32
250–500 (10–20)	0.782 (113)	65	1.25
500–1000 (20–39)	0.41 (60)	42	1.75

Figure 31 also shows this target strength profile and indicates that, even taking into account the expected variability in runway density, the target densities should provide strength above what is required.

We also want to be able to relate the design strength to a suitable measurement method. Though it is preferable to measure the strength of the pavement directly (e.g., a uniaxial compression test), the additional effort that would be needed to obtain such a direct measure makes the use of an index test such as the Russian Snow Penetrometer (RSP) more appealing. However, direct application of a correlation of ice strength to RSP, such as applying equation (5), must consider the stress state of the pavement structure. Correlations such as Equations (3) and (5) are made to a uniaxial compressive stress (i.e., no lateral confining pressure on the sample). However, the runway stress computed using BAKFAA and shown in Figure 30 are subject to lateral confinement when a vertical stress is applied and represents a triaxial stress state. Hawkes and Meller (1972) and Masterson et al. (1997) showed that, in general, the measured strength of laterally constrained ice is about three times higher than that measured in the uniaxial stress state. Owing to the high density of the compacted snow in the runway (nearly 700 kg/m^3 [44 lb/ft^3]), we thought it reasonable to treat the snow pavement the same as ice. Therefore, to compute the RSP index from

the pavement stresses determined in BAKFAA, the stresses have to be reduced by a factor of three before applying a correlation based on the uniaxial compressive strength (i.e., equation [5]). This method was used to determine the RSP index associated with the strength profile given in Table 9.

Figure 31. BAKFAA model calculations of the estimated stress distribution in the Phoenix runway under the C-17 for a range of snow and aircraft weights compared to the target strength profile for Phoenix runway. Compressive stress is positive.

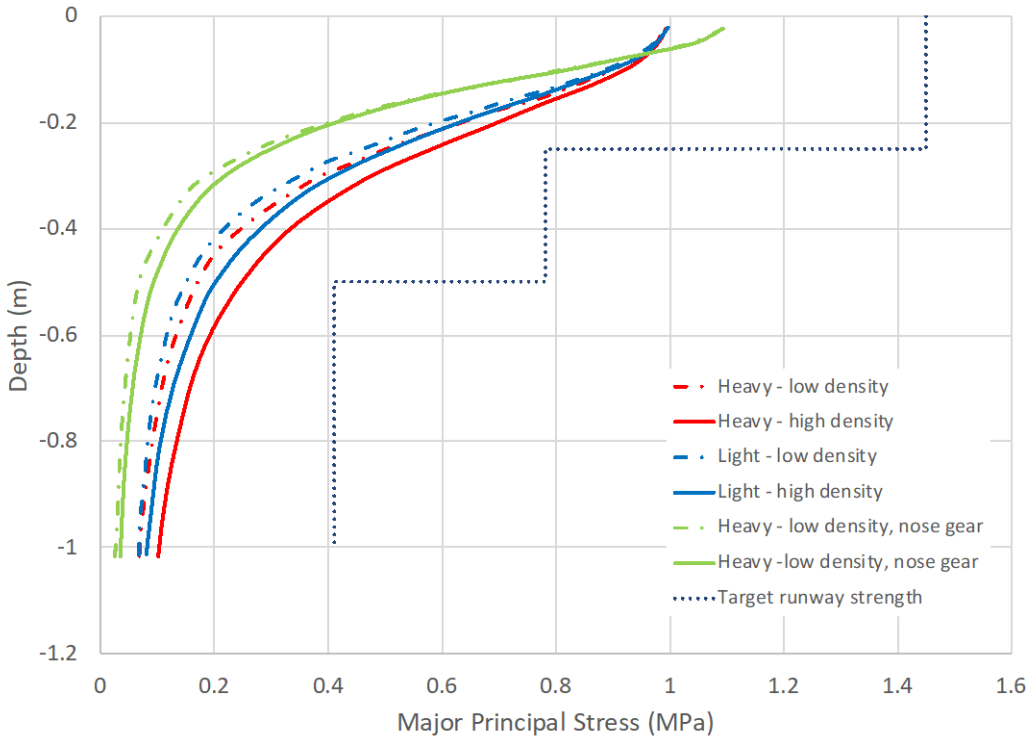

3.5 Evaluating runway design strength

Based on the evaluation above, Table 10 provides a design runway-strength profile. This profile was used in standard USAF and FAA design analysis as a cross check to evaluate the suitability for C-17 operations. Three standard and commonly used airfield design tools are used to evaluate this profile: the PCASE (Pavement-Transportation Computer Aided Structural Engineering) (USACE 2010) software, ETL2-19 for *Airfield Pavement Evaluation Standards and Procedures* (USAF 2002b), and the BAKFAA tool used to calculate the stresses within a runway structure based on the stiffness of the layers. All analyses considered the design aircraft to be the C-17 at 227,000 kg (500,000 lb). The following subsections discuss each of these analysis techniques.

Table 10. Recommended structural design strength for Phoenix Airfield.

Depth range, mm (in.)	CBR	Equivalent σ [eq. 7] MPa, (psi)
0–250 (0–10)	14.4	1.45 (210)
250–500 (10–20)	8.4	0.782 (113)
500–1000 (20–39)	4.8	0.41 (60)

3.5.1 PCASE

The PCASE software allows computation of the expected performance of a pavement-systems design against the criteria used in the design and evaluation of transportation systems, such as roads, runways, and railroads, based on the Unified Facilities Criteria (USACE 2001). PCASE was developed by USAF, Army, Navy, and FAA; and this analysis used version 2.09 to evaluate the capacity of the proposed runway structure at the Phoenix Airfield based on aircraft type, load, and number of passes using a standard traffic pattern for an assault or semiprepared unpaved landing zone (USACE 2010).

All cases were modeled using the structure given in Table 10. The results show that the airfield could support 24 passes or more for a C-17 with a gross weight of 227,000 kg (500,000 lb) and about 380 passes for an empty C-17 (126,500 kg, or 279,000 lb). Figure 32 illustrates the allowable passes based on the aircraft weight.

Figure 32. Allowable passes of the C-17 based on weight for the Phoenix design strength profile.

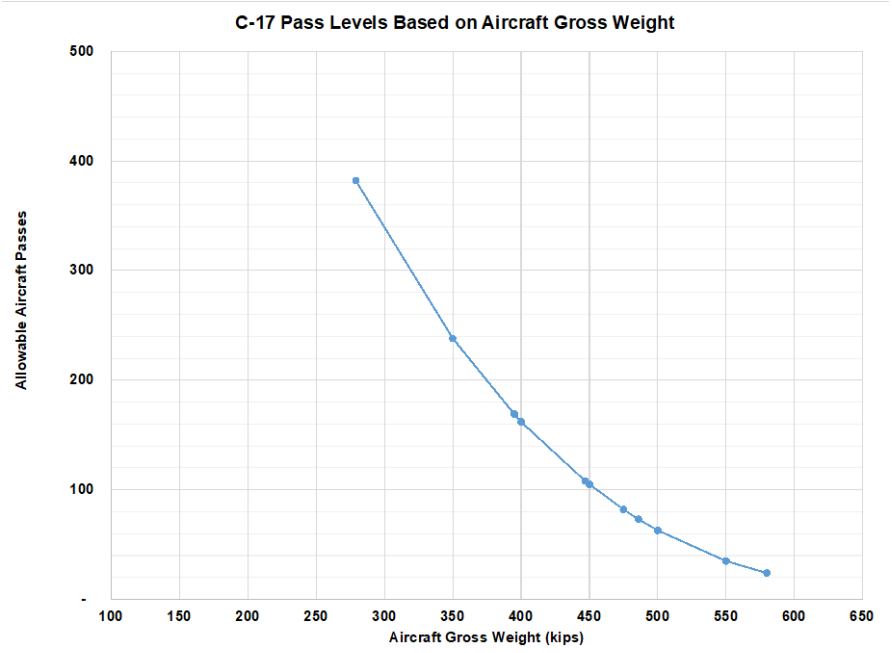

3.5.2 ETL2-19

Applying ETL2-19 (USAF 2002b), we evaluated the airfield structure for the allowable passes for each layer based on the strength and depth of that layer. The nomograph curves for the C-17 were used along with a weight of 227,000 kg (500,000 lb) on an unsurfaced, expedient, or aggregate surfaced airfield. The two charts needed for the analysis are the "Soil Surface Strength Requirements for the C-17" (USAF 2002b) shown in Figure 33 and the "Aggregate Surfaced Evaluation Allowable Load for the C-17" (USAF 2002b) shown in Figure 34. Using Figure 33, the allowable passes for a 250 m (10 in.) surface layer with a CBR of 14.4 is 90 passes. A layer at 250–500 mm (10 to 20 in.) with a CBR of 8 will allow 150 passes (Figure 34); and a layer of CBR= 5 at 500 mm (20 in.) and deeper will allow 1000 passes.

Figure 33. Soil surface strength requirements for the C-17 (USAF 2002b).

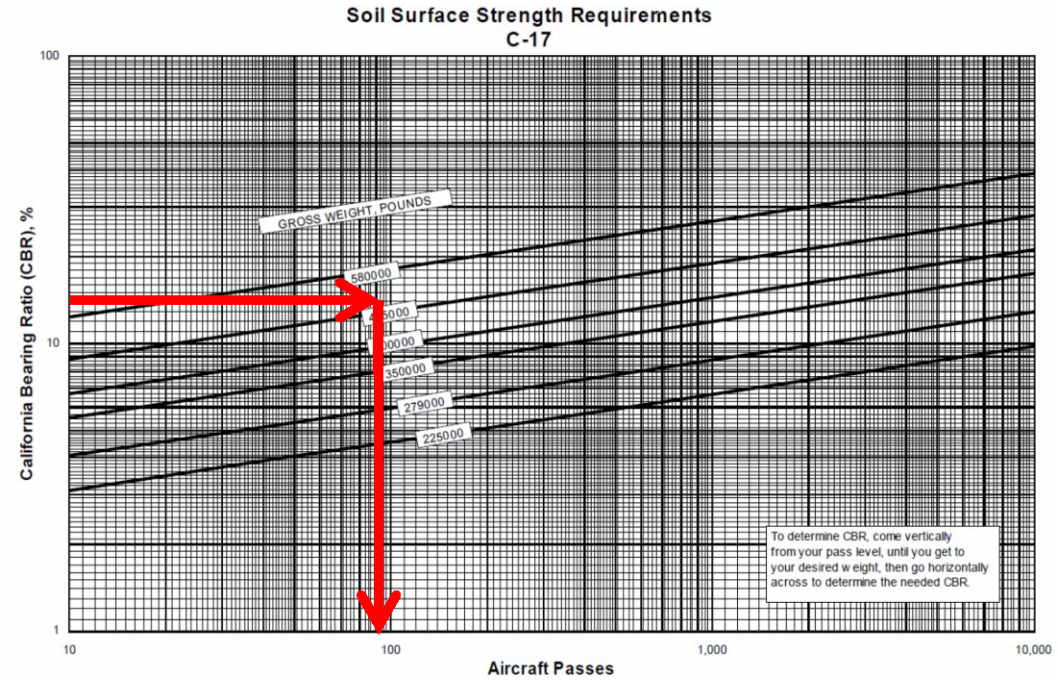

Figure 34. Aggregate surfaced evaluation allowable load for the C-17 (USAF 2002b), indicating the allowable passes for the CBR = 8 layer at a 10 in. depth for a 500,000 lb C-17.

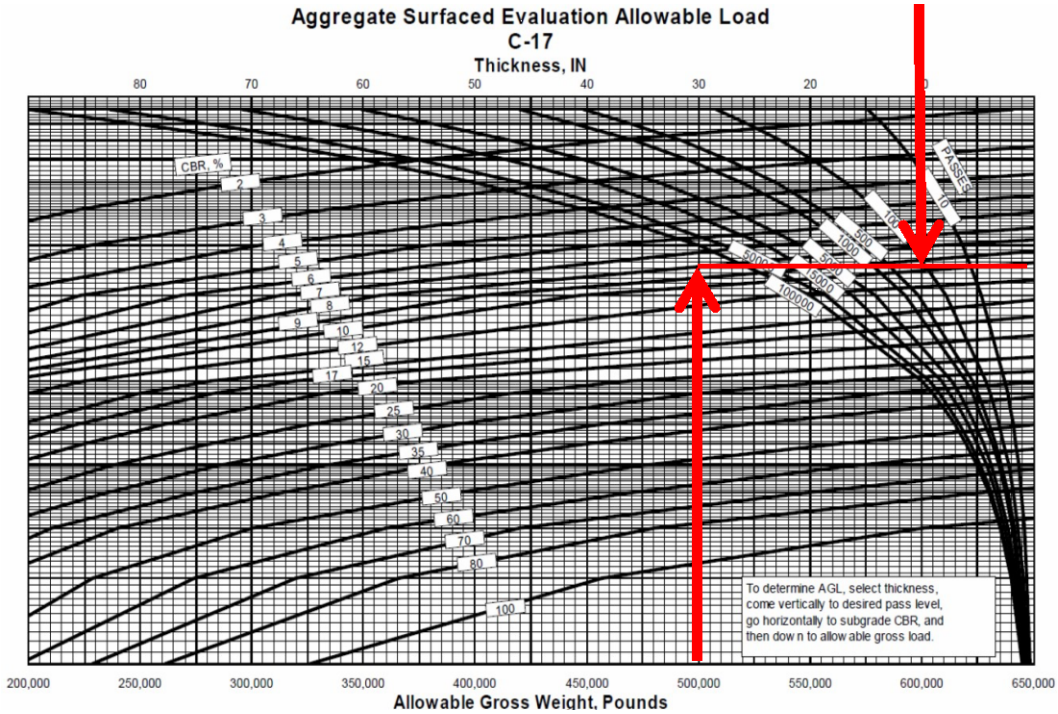

4 Field evaluation of runway strength

Having established an acceptable runway-strength profile, we now discuss methods to verify that target strengths are achieved and maintained. USAF (2015a) FC 3-260-06F specifies use of a proof cart to test the strength of glacial ice runway surfaces (without a snowcap). Based on that specification, the minimum individual tire pressures of the proof cart must be 0.76 MPa (110 psi), and the minimum individual tire loads must be 15,875 kg (35,000 lb). USAF (2015a) provides no information on tire geometry or other details of the proof cart except that the distance between adjacent passes cannot exceed 1 m (3 ft).

USAF (2015a) also discusses using a "proof weight cart" for compaction of the runway surface. However, the use of the word "proof" seems out of context here; and more appropriate would be use of just the term "weight cart" (e.g., the multiwheel Ox or SW weight carts used in McMurdo to compact the runways and snow roads). In the remainder of this work, we will draw the following distinction: a *weight* cart is used for runway construction and maintenance to compact the snow used in construction while a *proof* cart is used to verify that the runway meets minimum strength requirements to support planned aircraft operations on the runway. We note that it may be possible to use the same piece of equipment for runway compaction and proofing the runway; however, the configuration of the cart, in terms of the load on each wheel, may differ between compaction and proofing operations.

According to USAF (2015a), the snow strength for a glacial ice runway that is capped with a thin layer of compacted snow, such as Pegasus, may also be evaluated using an RSP or a Dynamic Cone Penetrometer (DCP). As these are point measurements, adequate spatial coverage of these measurements is necessary to provide an acceptable sampling pattern to characterize the entire runway strength. In addition to the DCP and RSP, the RAM penetrometer may be used as it is well suited to measuring lower snow strengths than the RSP and DCP. Each of these tools is based on a similar design, using a known weight dropped a known distance and recording the number of drops and associated penetration depth, though the penetrometer cone and dimensions vary between tools. The RAM penetrometer was specifically designed for use on natural and compacted snow structures, the RSP for highly compacted snow and ice runways, and the DCP for airfield pavement evaluation below the asphalt or concrete surface

layer. The DCP and RAM have established correlations to CBR (e.g., equation [6]) while the RSP correlations to CBR are achieved through combining correlations (e.g., combining correlation of RSP to DCP and a second correlation of DCP to CBR). The scatter among the correlations is likely extensive for all of the tools, however, partially due to the significant natural spatial and temporal variability in snow as a medium, which is not considered in any of the correlations.

The potential role of using proof carts and penetrometers to verify that the runway strength is at or above minimum requirements is discussed below.

4.1 Evaluating runway strength with a proof cart

Historically, a proof cart has been a piece of equipment assembled to replicate the full load of the complete main landing gear of an aircraft. For example, the original certification of the Pegasus Airfield used a proof cart that simulated the complete main landing gear of a C-141 (Blaisdell et al. 1998). For this case, a cart was assembled that had both sides of the main landing gear and was weighted to simulate a C-141 loaded to the proof load. A similar proof cart was assembled for the C-130 for proofing the runway for Casey Station (Russell-Head and Budd 1989).

It is not clear that a complete simulation of the entire main landing gear is needed to proof a runway. Provided individual tires in the landing gear are far enough apart that one is not influencing the stress bulb near another (i.e., there is no or very little superposition of stresses due to an adjacent wheel in the landing gear), the stress exerted on the runway by each tire can be considered independently of the others. Figure 28 compares the stresses of adjacent tires on a C-17 main landing gear with the design load. As discussed previously, this figure compares the stresses at the outer edge and beyond the outer tire (dashed lines) to that computed at an inner edge and between tires (solids lines); Figure 28 shows that there is very little difference between the computed stresses between adjacent wheels compared to outer wheels, suggesting that each wheel can be treated independently of the other. This allows a way to use a proof cart to verify that the runway strength is at or above minimum requirements (i.e., the proof cart needs to simulate the stresses induced by only a single wheel loaded to the proof load as is recommended by Jeb Tingle [ERDC, pers. comm., 2017]). This should be possible using the SW weight cart as outlined below.

At the design load, each tire of the C-17 main landing gear carries 17,700 kg (38,800 lb); this is the load per tire needed to proof the runway. Each tire on the SW cart (Figure 35) can be independently loaded to as little as approximately 6800 kg (15,000 lb) and as much as 18,500 kg (40,750 lb). The SW cart tires could be loaded to a little more than the equivalent wheel load of a C-17. We performed an analysis using BAKFAA with the SW cart fully loaded to 74,000 kg (163,00 lb). Because of the limitations of BAKFAA discussed previously, we could not simulate a case where adjacent wheel loads differed, so our initial evaluation of using the SW cart for proofing the runway was done simulating the cart fully loaded.

Figure 35. SW weight cart used for compaction on the roads and runways at McMurdo.

In Figure 36, we compare the computed stresses for the SW cart to that of the C-17. The maximum normal stresses at the tire centerline imposed on the runway is higher for the SW cart than the C-17. Figure 36 also shows that the Mises stress generated in the runway by the SW cart varies significantly between the outside edge of an outside tire and that on either side of an inner tire. This is a result of the close spacing of the SW cart tires (330 mm [13 in.] spacing between adjacent tires), resulting in high lateral stresses and reducing the near-surface Mises stresses between tires. Figure 36 shows that the Mises stress induced at the tire edge for inner tires is about the same as that of the C-17 for a depth of about 100 to 355 mm (4 to 14 in.), effectively testing for FS = 1 over that depth range. Right at the surface and below about 355 mm (14 in.), the Mises stress imposed by the outer tires of the SW cart is noticeably above that generated by the main landing gear. It is only the outer edge of these outer tires that maintains a

Mises stress well above that generated by the main landing gear for the entire depth. What this suggests is that a system of alternating the weight on the SW cart tires (Figure 38), thereby separating the heavily weighted tires, would provide a weight cart that has more regions that stress the surface slightly above that of the C-17—in terms of both the Mises and maximum principal stresses—cutting down on the number of passes needed to proof the entire runway to at least FS = 1.

Figure 36. Comparison of stresses imposed on the runway by a C-17 at design load for the Phoenix Airfield and a SW cart loaded to 73,000 kg (160,000 lb.).

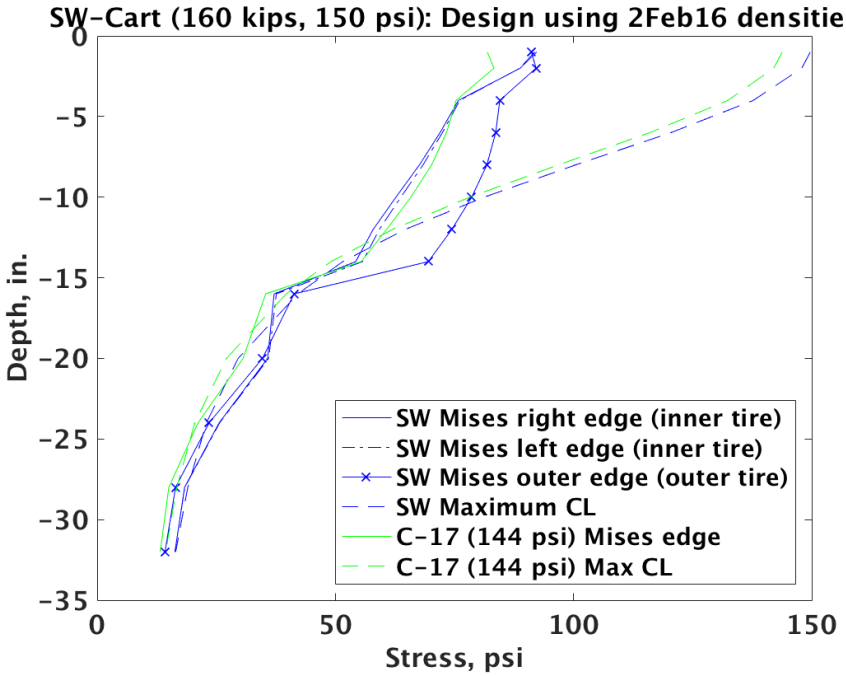

To determine the spacing needed between fully loaded tires to have an effectively isolated tire on the SW cart, we performed an FEA of the weight cart. Figure 37 shows the results of this simulation. The contours shown are Mises stress; the red lines at the top of the figure indicate the tire contact patch at the top of the runway surface. In Figure 37a, one can notice that the stress bulb under the outside tire extends out further on the left (outside) than on the right. Clearly, the presence of the adjacent tire has reduced the lateral extent of the bulb between the tires. In Figure 37b, the bulb under the fully loaded tire is nearly symmetrical, suggesting that lightly loading the inside tires provides enough separation that the two outside tires load the runway independently. Figure 37c shows the stress field for a cart that has alternating tires fully loaded. This

seems to show that the stress bulb for the fully loaded tires are also symmetric and that lightly loading alternating tires provides enough separation between the fully loaded tires so that the stresses under the tires are not appreciably changed.

This then provides a strategy for loading the SW cart to allow it to be used to proof the runway for a C-17. Alternating the fully loaded tires, or only fully loading the outside tires, can provide twice as many high Mises stress edge conditions per pass, providing more coverage of the runway with each pass. By pulling the carts in tandem and with the "opposite" heavy/light loading pattern, the gaps between these heavily loaded tires can be tracked by the following cart. Several tire-loading combinations can be envisioned when considering tandem carts, as shown in Figure 38. The optimum configuration that most widely distributes the high-stress edge pattern is either the "combination" or "reversed alternate." Either pattern should provide a good pattern for proofing the runway using the SW weight cart that is also used for compacting the runway. For compaction operations, the tires are all loaded equally.

Using the SW cart in this way would allow it to be used to proof the runway for a C-17. However, to verify that the runway has adequate strength for other aircraft would require either evaluating alternative configurations of the SW cart (different tire loads and load patterns) or, if the SW cart proves inadequate, construction of a proof cart that has greater flexibility to simulate the load for a wide range of aircraft types and payloads.

Figure 37. Finite element simulations of the SW cart (*a*) fully loaded, (b) with the outside tires fully loaded 18,000 kg (40,000 lb) and inside tires loaded to 6800 kg (15,000 lb), and (*c*) alternating tires fully loaded. For (*a*) and (*b*), the right edge of the model is a symmetry plane; therefore, the cart is effectively mirrored about that side. Contours of von Mises stress are shown. The scale for the stresses is the same for (a) through (c).

(a) Fully loaded cart

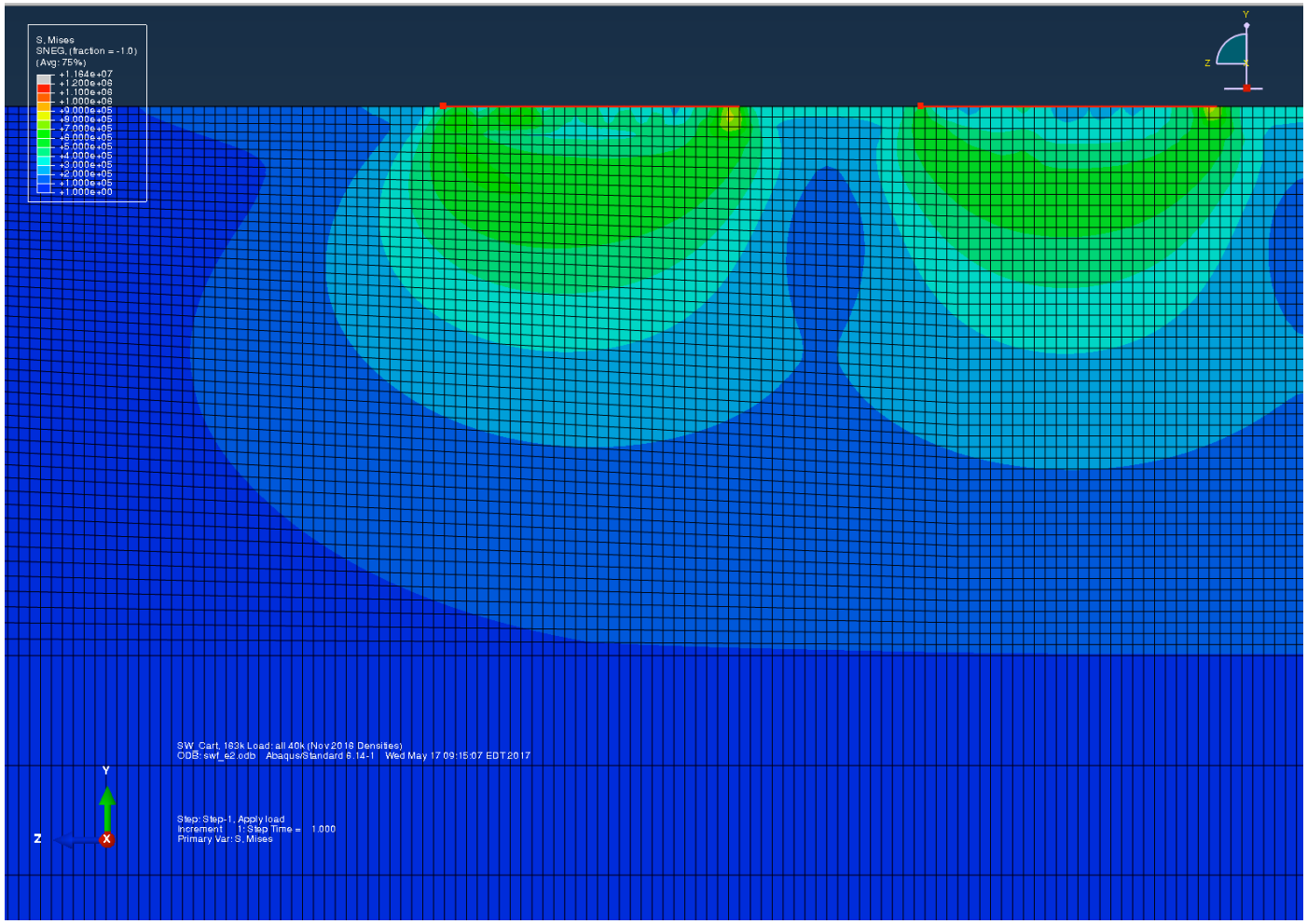

Figure 37 (cont.). Finite element simulations of the SW cart (*a*) fully loaded, (b) with the outside tires fully loaded 18,000 kg (40,000 lb) and inside tires loaded to 6800 kg (15,000 lb), and (*c*) alternating tires fully loaded. For (*a*) and (*b*), the right edge of the model is a symmetry plane; therefore, the cart is effectively mirrored about that side. Contours of von Mises stress are shown. The scale for the stresses is the same for (a) through (c).

(b) Outer tires fully loaded

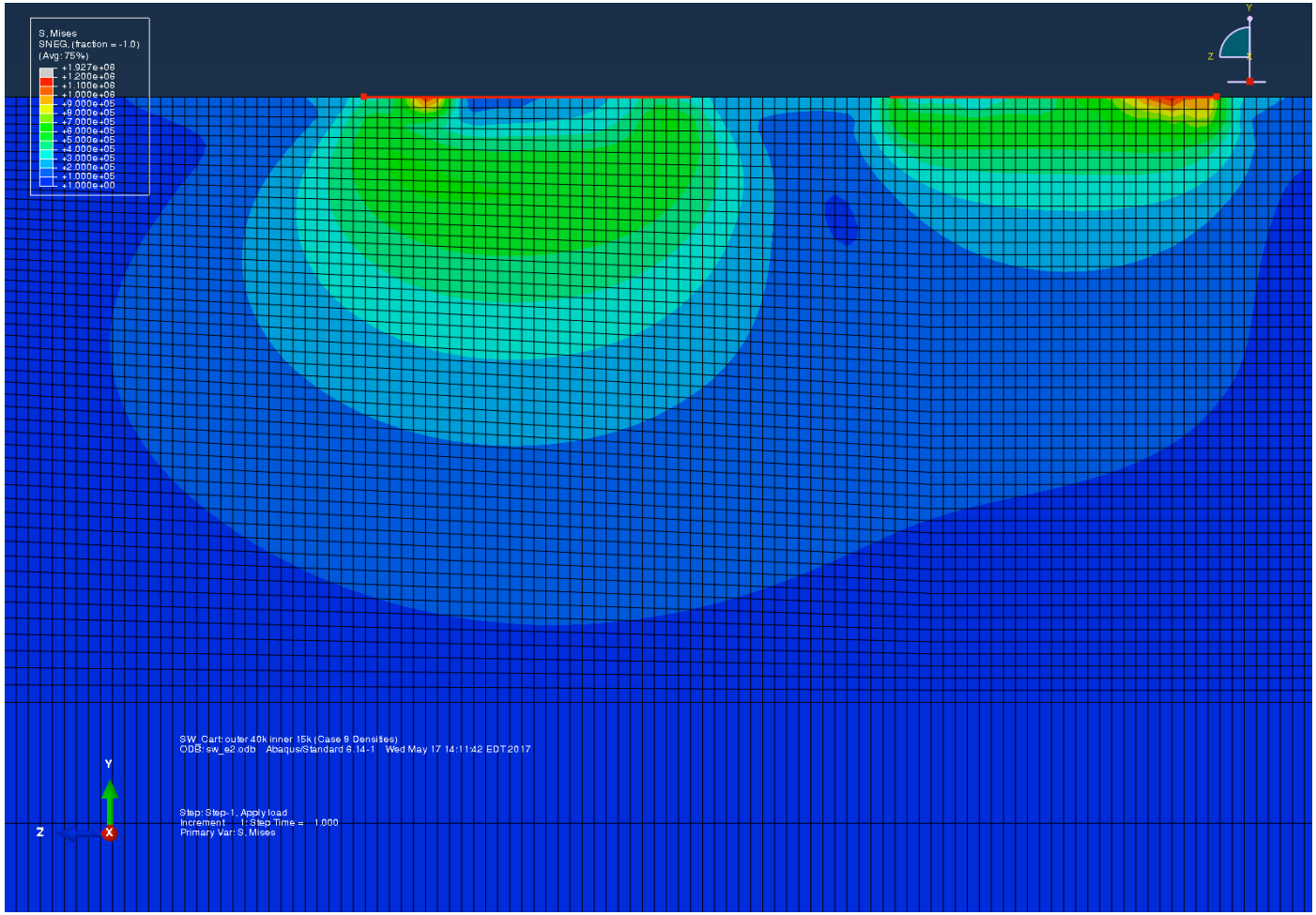

Figure 37 (cont.). Finite element simulations of the SW cart (*a*) fully loaded, (b) with the outside tires fully loaded 18,000 kg (40,000 lb) and inside tires loaded to 6800 kg (15,000 lb), and (*c*) alternating tires fully loaded. For (*a*) and (*b*), the right edge of the model is a symmetry plane; therefore, the cart is effectively mirrored about that side. Contours of von Mises stress are shown. The scale for the stresses is the same for (a) through (c).

(c) Alternating tires fully loaded

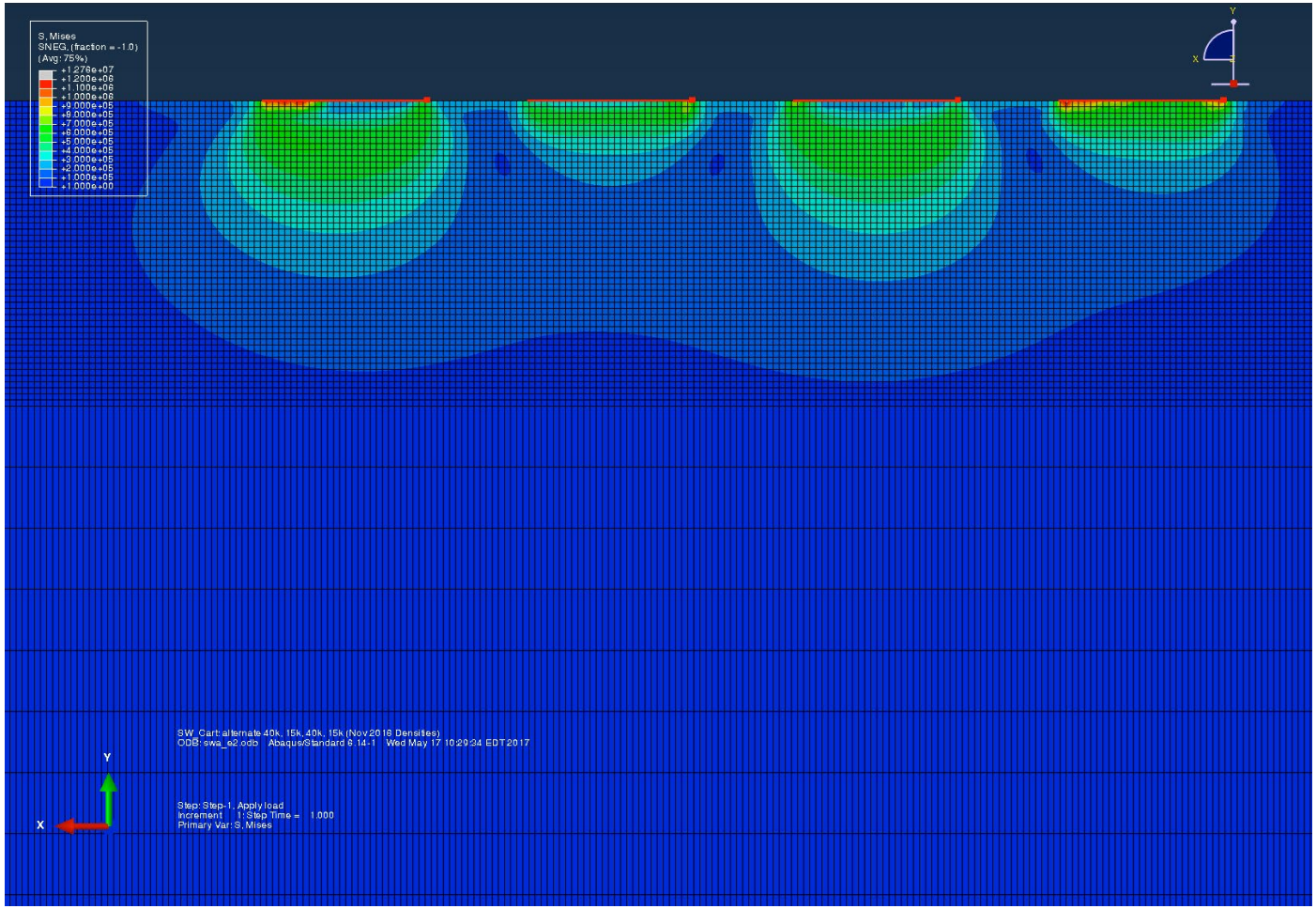

Figure 38. Layout of tire loading for the SW weight cart. The *green lines* indicate tracks for maximum Mises stress load. The thickness in the *green lines* indicates the uncertainty in the location of the following cart.

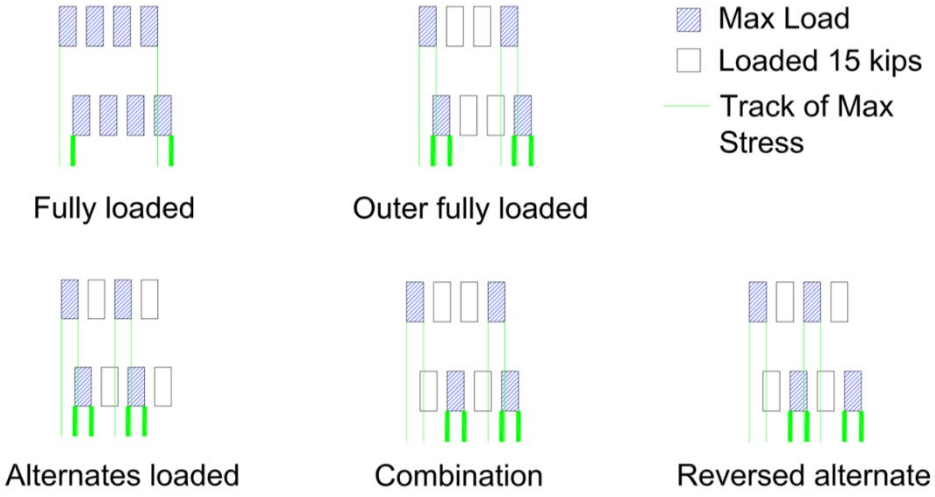

We note that with respect to proof-cart application, AFCESA/CES (1997) provides guidance on acceptable performance for a C-17 operated on contingency airfields. In particular, rutting in the runway that is at or exceeds a 229 mm (9 in.) depth is a red severity condition, and immediate repair to the runway is necessary. Rutting exceeding 89 to 100 mm (3.5 to 4 in.) but less than 229 mm (9 in.) is an amber condition that "requires monitoring and should be repaired if possible." Ruts shallower than 89–100 mm (3.5–4 in.) are classified as a green condition: "low-risk operation." These severity conditions were developed for contingency operations on a runway constructed from soil. Lacking any similar guidance for snow construction, we provisionally adopted this severity classification for the Phoenix Airfield. We expect that assessment of the runway with an appropriately designed proof cart will allow classification of the runway condition according to this guidance. Therefore, in general, if the proof cart does not produce ruts deeper than 50 mm (2 in.), the runway should be proofed to FS = 1 and should conservatively meet the rutting guidance for the C-17 in AFCESA/CES (1997).

4.2 Evaluating strength with penetrometers

As discussed, penetrometers are widely used to indicate the relative strength of granular materials, such as soils and snow. Such devices have a conical pointed end that is driven into the soil or snow, creating a combination of shear and compressive stress within the material. Thus, a penetrometer does not produce a "standard" measurement of material strength

but rather an "index" value that has been shown over many years and granular material types to be repeatable and representative (Abele 1963; Herrick and Jones 2002).

4.2.1 Penetrometer choices

The three penetrometer types mentioned previously (DCP, RAM, and RSP) each have one or more standardized cone sizes and geometries. These variations allow each device to perform efficiently and effectively within a particular range of material strengths. The DCP was developed for soils in construction situations and is a standard tool for assessing unpaved airfields and subgrades on paved runways (ASTM International 2015). The RAM was first used for natural snow studies and was initially configured for low-strength materials (Wong and Irwin 1992). During early field studies using snow as a construction material, strengths were encountered that were difficult to measure with the initial RAM design. A new design for the RAM tips were developed to penetrate stronger materials more easily but still with enough resistance to allow resolution of small differences in material strength. As fieldwork moved toward making high-strength snow pavements capable of supporting large wheeled aircraft, Russian researchers developed the RSP (Mellor 1993) to allow adequate resolution of penetration resistance with less test effort, compared to the DCP or RAM, in very strong snow.

We have used all three of these penetrometer types in snow in past studies but have the most experience with the RAM and RSP for work in Antarctica. During development and subsequent monitoring and maintenance of the white ice pavement on the Pegasus Airfield, the RSP was found to be the most effective in the high-density and high-strength snowcap. This was associated with the RSP's ability

1. to penetrate the thin (<15 cm, or 6 in.), strong compacted snow layer of the cap with minimal spalling at the top surface;
2. with a modest number of blows (roughly 3 to 8) to incrementally move 25 mm (1 in.) into the snow pavement; and
3. to clearly signify hitting the glacial ice surface under the compacted snow pavement by dramatically slowing the penetration rate (i.e., 8 or more blows were required to penetrate 25 mm [1 in.] or less).

During site investigations for determining a suitable location for a Pegasus Airfield replacement, we used the RAM in the natural snowpack of the

MIS. The RSP's small, sharply pointed tip penetrated too far (>50 mm, or 2 in.) with each blow to provide us with a reliable understanding of snow strength layering or overall variation with depth in soft snow. Once snow compaction began at the Phoenix site, the RAM was used until its blow counts exceeded about 8 for each 25 mm (1 in.) of penetration. At that point, the snow pavement being developed had a strength level that was better measured with the RSP. However, at times, the RAM was used to monitor the strength of the natural snow underneath the developing snow-pavement layer. Thus, the RSP and RAM were used together during runway construction to quantify the snow-pavement strength and the underlying subgrade.

Although penetrometer tests only generate an "index" value of material strength, it can be shown that each of the three devices discussed here provides a means to "measure" snow strength similarly. Figure 39 shows an example of the strong correlation between DCP and RSP strength measurements; the data and curve fit presented in Figure 39 are the basis for equation (8).

Figure 39. Results of side-by-side measurements of index snow strength in compacted snow at two locations in Greenland with the Dynamic Cone Penetrometer (DCP) and the Russian Snow Penetrometer (RSP).

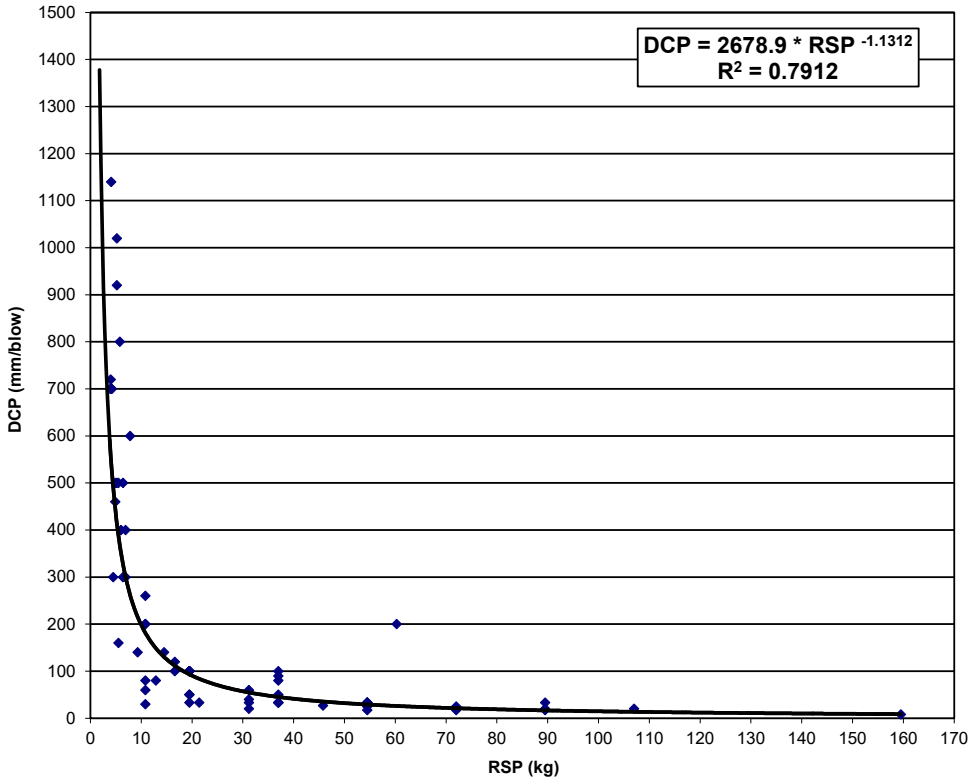

4.2.2 Analyzing penetrometer data

The strength index determined from penetrometer measurements (e.g., Table 3) are basically an indication of the energy required to penetrate a unit distance into the material being studied. Standards exist for each penetrometer type, recommending how to operate the device and collect the data needed as input for the index equation. Variations in these standards are often practiced so as to tailor the index values to the portions of the terrain system of most interest to the user.

During early construction of the Phoenix runway, the RAM and RSP were used to monitor the overall strength and uniformity of the runway along the length and across the width. However, as the runway gained strength, the only penetrometer that could be used to assess strength efficiently was the RSP. As the runway construction approached completion, we used the layering and strengths in Table 9 as a guide for what we expected the strengths should be and also validated those values as follows.

We elected to accumulate penetrometer blow counts over 25 mm (1 in.) increments of penetration before starting a new set of blows. This resulted in a series of 6–12 individual calculated index values, providing a vertical strength profile within the developing pavement and extending into the underlying natural material.

While continuing to collect blow counts for every 25 mm (1 in.) of penetration, we separated the entire vertical suite of RSP data into three layers and concentrated our analysis on those layers. These layers were defined as 25–125 mm (1–5 in.), 125–275 mm (5–11 in.), and 275–400 mm (11–16 in.)* and were related to the pavement, base, and subbase layers in a conventional runway construction profile. Within each layer, the RSP values calculated from each blow set were aggregated† to give three RSP strength values to characterize the vertical variation in snow-pavement strength at each sample location. In addition to using this data to evaluate the developing pavement system horizontally and vertically for uniformity, variability, and progress toward achieving target strength levels to inform

* The RSP is limited to collecting data to a depth of only 400 mm (16 in.).

† The strengths for each of these layers were computed by using the aggregated number of blows to penetrate the indicated layer, either 25–125 mm, 125–275 mm, or 275–400 mm.

the construction and maintenance activities, this was also monitored for progression toward the target values in Table 9.

Earth materials are well known to typically demonstrate property variability on both small and large scales. Even a simple (nominally) two-phase material like snow can show wide variations in strength; for example, existence of ice lenses and hoar layers within an otherwise homogeneous snowpack causes disparity in strength properties. Our construction process was designed to greatly reduce property variability in the ultimate pavement system despite the first two lifts being sourced from aged snow that clearly included both very strong and very weak but discontinuous layering. Still, variability is bound to remain. By using the RSP (with a sampling size of less than 1 cm^2, or 0.16 $in.^2$) to measure the properties of an initially nonuniform material that was processed by construction equipment with a footprint of between 70 and 2700 cm^2 (11 and 418 $in.^2$), the potential for major variations in index value could be expected. However, because of the scale difference (aircraft tires being much closer to the construction equipment than the RSP in how they load the snow), some degree of variability in RSP value should not be cause for alarm.

Our approach for dealing with variability is to use a standard earth materials approach: the "85% rule" discussed previously. We determined the 85% value for each defined pavement layer by calculating the 15th percentile of all of the data sampled on the runway in that layer; 85% of the data lies above the 15th percentile value, and this single 85% RSP value was used to characterize the strength of each layer of the runway.

We recognize that this approach is conservative but does take into account that (a) measurement errors can be present, (b) natural variability in earth materials can never be entirely eliminated, and (c) only reasonable and acceptable levels of risk are present when the 85% rule is engaged. However, a routine part of the data review includes checking the entire collection of RSP data to be sure that the weakest 15% of strength values are not grouped together in one area of the runway. If the weakest 15% measurements are physically adjacent or nearly adjacent, that is an indication of a spatially large, weak location in the pavement system that requires immediate attention and remediation.

4.2.3 Establishing index strength limits for aircraft

At the time runway construction was underway, the heavy compaction roller (SW carts) and the RSP were the only two tools in McMurdo that could provide a means of establishing strength thresholds for various aircraft. As described in section 4.1, although the SW carts placed a similar magnitude load and contact pressure on the Phoenix pavement system, there were limitations to actually replicating the C-17 landing-gear loading (e.g., the unique orientation of tires shown in Figure 26). Additionally, the RSP tool was so grossly dissimilar in the area it evaluated, and as an index measure of strength was not directly related to the engineering property of the snow, that it was not obvious that it could reliably be used to predict pavement-system strengths adequate for various aircraft. However, knowing that the SW carts and the RSP each provided important insights into the pavement system's ability to support heavy loads, we performed a test series aimed at correlating the results from each tool for a range of snow strengths, with the goal of achieving a method for providing at least a "go/no-go" sense of runway readiness for a particular aircraft type.

We termed this exercise Fail/No-Fail testing. The concept was to find areas of processed snow of varying strengths from somewhat more robust than natural snow up to the heaviest compacted area of the runway and apron. In these areas, the approach was to perform closely spaced RSP measurements in a path that would be tracked by a SW cart ballasted with varying weight. Our aim was to discover along the path of the cart areas that were fully supported by the SW cart and areas where the pavement system failed (to a minor or major extent) and to be able to correlate the RSP values measured in those areas with the degree of support realized by the SW cart. This information then would be used to update the target RSP strength values given in Table 9 for the runway. What follows is a detailed accounting of how we related the Fail/No-Fail tests with the weight cart to an RSP strength criterion for the runway.

Our first attempt at Fail/No-Fail testing took place at the transition between the eastern edge of the very robust apron and the abutting western edge of the lightly compacted region next to the airstrip where airfield support buildings are placed, which is referred to as the "town site." We acquired a line of equally spaced RSP measurements perpendicular to the boundary between the two regions, leading from the apron/town-site boundary 25 m (84 ft) into the town site. Our measurements clearly

showed a rapid transition from very high RSP values (RSP > 175) to much lower values (RSP < 125) within the length of our sampling line (Figure 40).

Figure 40. RSP profiles across a transect from inside the apron to well inside the town site, showing diminishing strength.

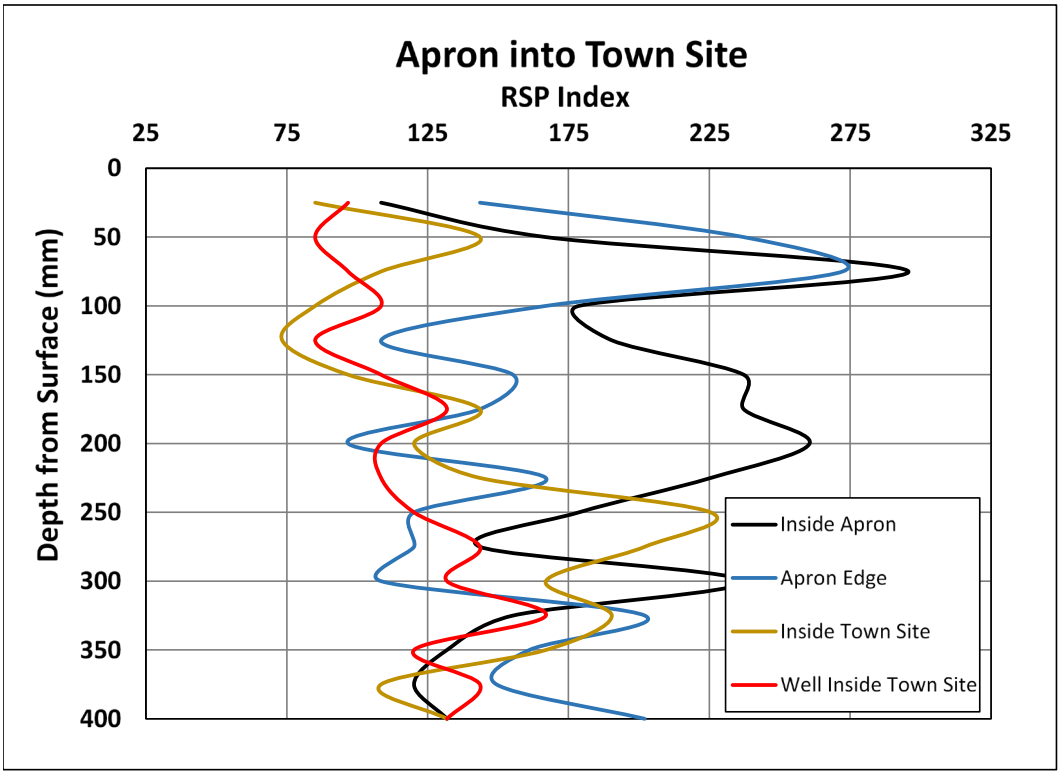

We started with a modestly loaded compaction roller (36,000 kg, or 84,000 lb). Anticipating that the roller would fail the pavement along the sampling line and knowing that we were running the risk of the tractor not having adequate traction should the roller rut the pavement, we elected to back the roller into the town site along the line of our RSP measurements. To our surprise, the roller was completely supported by the town-site pavement for more than 36 m (120 ft). We removed the roller and added ballast to bring the gross load on the four tires to 47,200 kg (104,000 lb). This load also caused no failure of the pavement system over the ±60 m (200 ft) we backed it into the town site. We next hitched to a roller having a gross load of 50,800 kg (112,000 lb) with 18,370 kg (40,500 lb) on each of the inner two tires and 7050 kg (15,500 lb) on each of the outside tires. While this load configuration was not part of any plan (e.g., Figure 38), it was expedient to produce as a step up from the prior trial. This load was backed over 60 m (200 ft) before several areas showed a modest amount of surface breakage, more so on the inner tires than the outside tires.

Dispensing with concerns about getting the tractor and roller stuck, we drove the 50,800 kg (112,000 lb) SW cart with unequally loaded tires forward into the town site parallel to but 2 m (6 ft) offset from the backing-in path. The roller failed the pavement only in areas that were aligned adjacent to failures in the first path. This provided us with areas for RSP testing of untracked pavement that could reliably be assumed to have inadequate strength. Likewise, there were ample untracked areas that clearly would have supported the roller (Figure 41).

Figure 41. Parallel 50,800 kg (112,000 lb) compaction-roller tracks generated when moving from a very strong airfield apron (out of sight in the foreground) into a modestly compacted town site showing alignment of areas that supported the tire load (near-field tire tracks) and areas that suffered rutting (depressions further out).

The data from this initial Fail/No-Fail test exercise (Figure 42) show that there is not a significant difference in the RSP values in the top 10 cm (5 in.) of the failed (three distinct locations) and unfailed snow (three distinct locations). There is a very big difference in the strength of the two areas in the 100–400 mm (5–15 in.) horizon below the surface. Below 400 mm (15 in.), the snow strength is statistically equivalent throughout the town site (the pavement construction in the town site extended down only 300 mm, or 12 in.).

For comparison, we include in Figure 42 the measured RSP strength of the runway at the centerline on the same day that we conducted the Fail/No Fail test.

Figure 42. RSP results from Fail/No-Fail tests (three distinct locations for both fail and no-fail results) with a 50,800 kg (112,000 lb) compaction roller (with the inner two tires loaded to 18,370 kg [40,400 lb] each and the outer tires loaded to 7030 kg [15,500 lb] each) traveling in the Phoenix Airfield town site (modest compaction) compared to the strength of the runway centerline (extensive compaction).

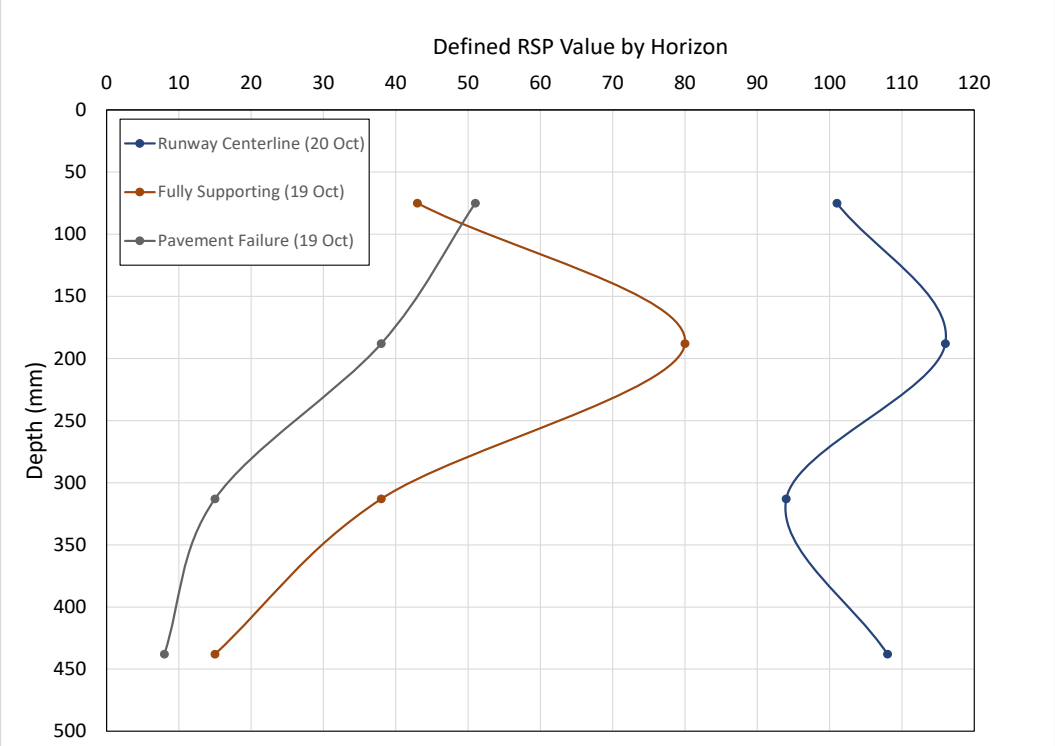

This initial Fail/No-Fail test, while appearing to clearly achieve our goal to link RSP and wheel loads that were similar to the C-17 (40,000 lb/tire), did not impose the overall amount of weight carried by a single main landing gear train that would be imparted by the C-17 on the runway. Therefore, a few days later, we performed another set of Fail/No-Fail tests, this time with a compaction roller ballasted to a gross mass of 74,000 kg (163,000 lb), about equal to the load carried by a single main landing gear train, with an equal load of 18,500 kg (40,750 lb) on the four tires on the weight cart. For this test, we drove multiple routes from the prepared runway apron into the town site where the compacted snow pavement is thinner and we presumed it to be weaker as it had not received as much compaction. Successive tests had increasing traverse length into the weaker regions of the town-site area. Prior RSP measurements and tests assured us that the town site strength dropped significantly when moving further

from the apron for the initial 75 m (250 ft) and then became more or less uniform beyond that. We ultimately drove six arcing paths into the town site (Figure 43). The two deepest incursions generated sections where the roller tires penetrated the surface. Only the final track caused an immobilization of the tractor when the roller tires sank between 120 and 150 mm (5 and 6 in.) below the pavement surface. (A second tractor was hooked in tandem, and the roller was handily moved along the rest of its designated track back into the apron.)

Figure 43. Arced paths of the 74,000 kg compaction roller traveling from the very strong airfield apron (in the *background* and to the *right*) into the modestly compacted town site (*foreground* and to the *left*).

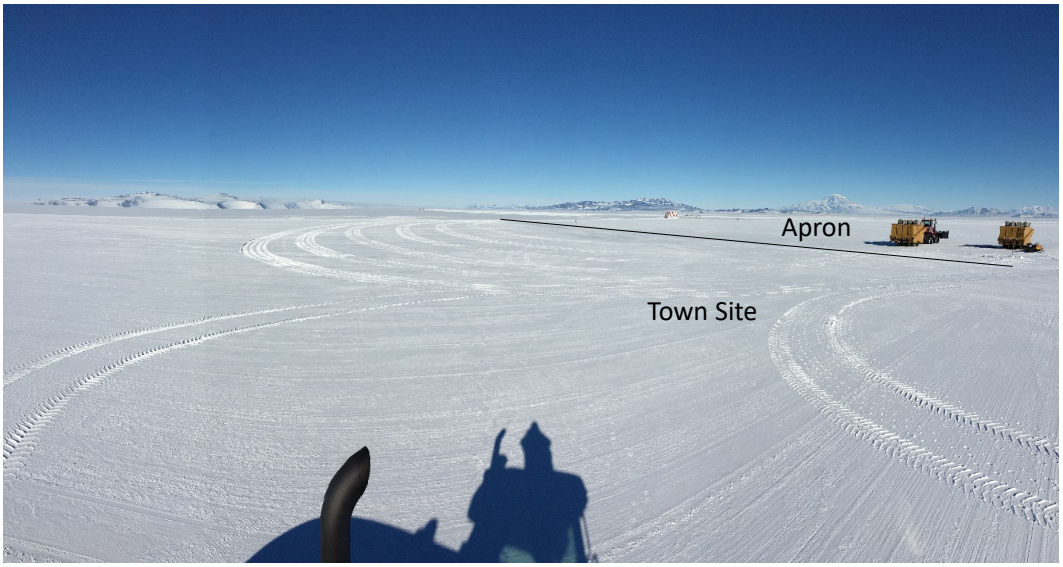

We observed that not only could the roller tracks be divided into Fail/No-Fail categories but also there seemed to be two types of failed surfaces. In the more benign case, the snow surface compressed enough to cause surface cracking along the edges of the roller tire's tread, but there was little or no spalling (lateral displacement and upheaval) of snow from below the surface. We defined this type of failure as a *Surface Disturbance* and set the limit of vertical displacement as between 25 and 130 mm (1 and 5 in.). A Surface Disturbance (Figure 44) is characterized by the subsurface compacting (volume reduction) rather than disaggregation and displacement of snow. This type of pavement compromise is very unlikely to be noticed by a flight crew when it occurs during flight operations. However, like all compaction activities, the newly densified subsurface snow will have lower strength until it has had a period of time to "heal" (sinter, or form and grow new intergranular bonds). Adequate healing time is a function of the snow and air temperatures but is typically 24–48 hours. Thus, a Surface

Disturbance should not be loaded by an aircraft (or other vehicle, including compaction roller) until the required healing time has passed. This would not preclude use of the runway, but aircraft should avoid traveling over the area displaying a Surface Disturbance. Additionally, adequate repair can be achieved by dragging fresh snow over the area and "packing" it into the depression with the tractor tracks and allowing the repair to heal for 24–48 hours.

Figure 44. Area of snow pavement showing a Surface Disturbance.

A more dramatic and concerning type of compromised surface is *Pavement Failure*, which results from a lack of bearing strength in the subsurface, allowing the pavement surface to crack and disaggregate and some of the subsurface snow to be dislodged up onto the surface along the sides of the tire (Figure 45). While these two features characterize distress of the pavement, we also believe that any area showing a tire penetration or rut depth greater than 120 mm (5 in.) has subsurface weakness that leads to disaggregation and dilatation of the snow by the passage of the heavy load rather than the compaction and consolidation of the snow, which is more indicative of a Surface Disturbance. Thus, a Pavement Failure should not be loaded by an aircraft (or other vehicle, including compaction roller) un-

til a repair has been effected and the area retested (section 7.4 of this report provides repair procedures). If the quantity and distribution of Pavement Failure areas allow, such surface compromises need not automatically close the runway. It is critical, though, that the damaged area of the runway is not traversed by any aircraft until repaired.

Figure 45. Compaction-roller tracks (movement in the direction from foreground to background) showing an area of Pavement Failure on the rightmost tire in an isolated region with the other tracks displaying only a Surface Disturbance response. Note the definitive difference between these two types of deformation where Pavement Failure displays disaggregation of the snow surface under the tire and "squeezing out" of this loose subsurface snow along the side of the tire.

Fully Supporting is the term we used to describe all areas of the surface that did not exhibit Surface Disturbance or Pavement Failure. In the best case, only a faint impression of the tire tread can be seen (Figure 46a), but any imprint less than about 25 mm (1 in.) deep suggests a loose covering of snow on the pavement itself rather than a lack of strength in the pavement system (Figure 46b) and is also classified as Fully Supporting.

Figure 46. Two examples of pavement areas fitting the Fully Supporting performance level: (*top*) faint tire tread and (*bottom*) obvious tread and imprints.

We performed a suite of RSP measurements at locations adjacent to each of the three defined pavement performance levels. Figure 47 shows these results.

Figure 47. Measured 85% RSP values from Fail/No-Fail tests. The lines are averages of several measurements with Surface Disturbance (n = 5), Pavement Failure (n = 4), and Fully Supporting (n = 4) with a 74,000 kg (163,000 lb) compaction roller (with all tires equally loaded to 18,500 kg each [40,000 lb]) traveling in the Phoenix Airfield town site (modest compaction) compared to the strength of the runway centerline (extensive compaction).

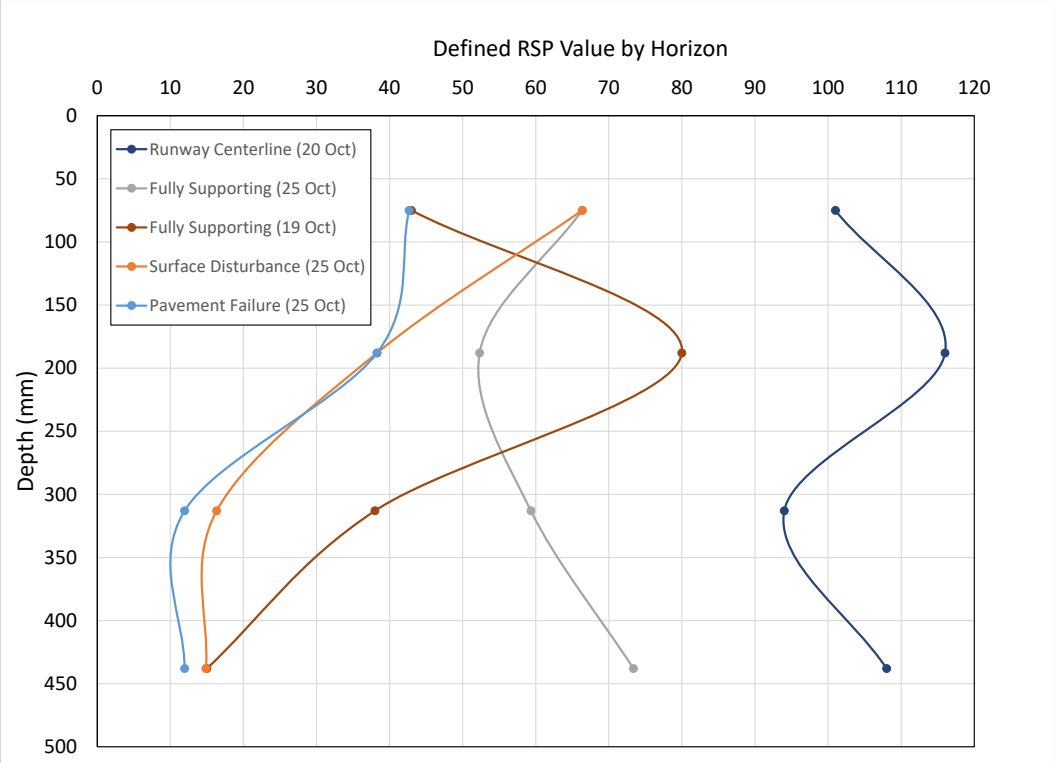

Results from both sets of Fail/No-Fail tests (Figure 42 and Figure 47) gave us confidence that a correlation could be found between RSP index strength values and pavement performance under compaction-roller load. We recognized that this correlation was likely to be minimally defined because

1. we performed a limited number of tests,
2. we are unable to know for certain the RSP value of a specific small-diameter "column" of snow that would later clearly demonstrate less than Fully Supporting behavior when trafficked by the compaction roller, and
3. the data set includes two different gross compaction-roller loads (although two of the tires in the lighter loaded roller had the same load as all four tires in the heavy roller case).

Nevertheless, we assembled all of the individual RSP values (for 25 mm, or 1 in., blow sets) associated with all Fail/No-Fail testing and plotted them on a single graph (Figure 48). In this data set, all of the measured values are shown, not just the top 85% strength data.

Figure 48. All data from the Fail/No-Fail tests, shown as RSP values for each 25 mm (1 in.) of penetration. *Red curves* are associated with pavement areas that demonstrated Pavement Failure, *gray curves* represent areas where the compaction roller created a Surface Disturbance, and *dark blue lines* depict where the pavement Fully Supported the load cart.

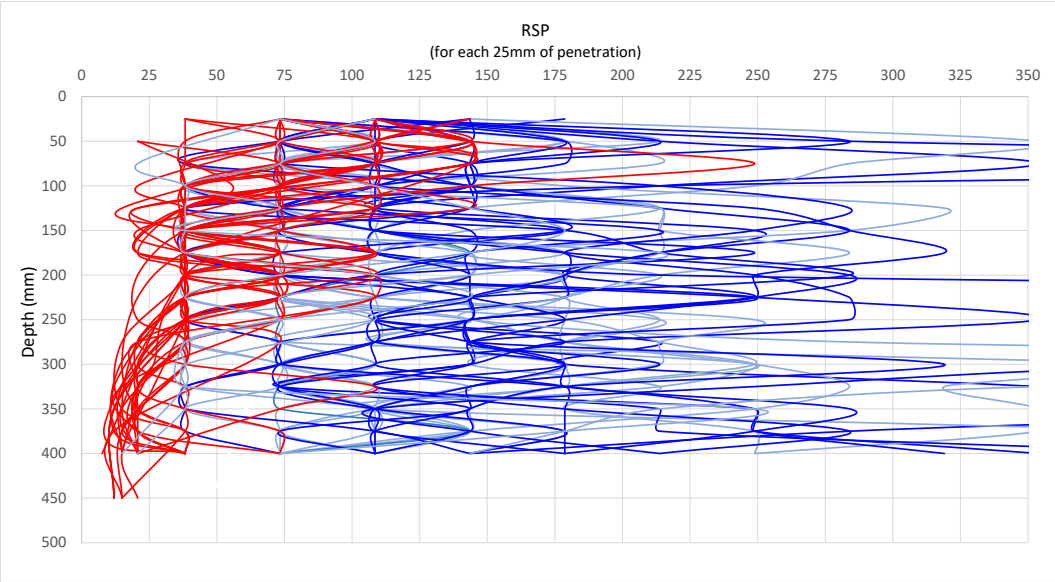

We recognize that this plot is busy, but it served to see all of the data together and to look for zones predominated by each pavement performance level. In reviewing the data, it is also valuable to recognize that measured RSP values are not continuous but discrete or quantized. That is, for a 25 mm (1 in.) penetration, RSP values will always only be integer multiples of 38, the RSP value associated with a single blow. This is clearly displayed in Figure 48 where strength values are clustered at discrete intervals.

Our first observation was that areas that had an RSP value less than about 60 at a depth in the pavement below 250 mm (10 in.) could be counted on to exhibit Pavement Failure. In the 150–250 mm (6–10 in.) horizon, it appears that the pavement system needs to have an RSP value of about 80 or above to avoid a Pavement Failure.

Within the 150–400 mm (6–16 in.) horizon, there is limited overlap between the red lines and the blue lines (Figure 48). This is not true above 150 mm (6 in.); although Pavement Failure curves, except in one case, never reach RSP levels higher than 150, it is common for the Fully Supporting and Surface Deformation pavement to have strengths higher than 150. We explain this by noting that we are placing very heavy loads on the snow and that, no matter how strong the surface, a weak underlying profile of snow will allow Pavement Failure. We colloquially refer to this

profile as an "egg shell": a strong thin layer over generally weak snow. Thus, in looking for a divider between Pavement Failure and the other curves in the upper 150 mm (6 in.) we focused on the blue lines, not the red lines. While not as obvious, we concluded that an RSP value of about 65 can be used to separate the Pavement Failure and Fully Supporting regions.

Recall that the Fail/No-Fail tests program aimed to generate a relationship between measured RSP values and a safe runway strength for the C-17 by using the compaction-roller loads as a surrogate. And, because at the time of these tests the Phoenix Airfield and apron already possessed an advanced level of compaction and strength and our immediate focus was on supporting the C-17 aircraft, the applicability of developing a correlation curve between RSP and compaction-cart weight that could be used for the purpose of proofing the runway for a broad range of aircraft weights and configurations was not possible, and these tests apply to the C-17 only.

To use this data to establish provisional RSP limits for the C-17, we reviewed the allowable operating environment for that aircraft. Fortuitously for the Antarctic application, the C-17 is designed to operate on unpaved and "contingency" runways. As discussed in section 4.1, its landing gear is capable of safe operation with up to 229 mm (9 in.) of rutting. While it was our goal to construct and maintain the Phoenix Airstrip to a strength level that would avoid any rutting by the C-17, it was helpful to know that the kinds of snow-pavement weakness we defined as Surface Disturbance would pose no adverse issue for the C-17. In fact, it appears than the C-17 has operated in soil/gravel runway situations where what we define as Pavement Failure levels of rutting were not unusual, though surface repair should still be effected as soon as is possible (AFCESA/CES 1997).

These tests and analysis led us to propose the minimum RSP target values for C-17 operations summarized in Table 11. Since the SW cart proofs the runway with a FS = 1, we assume initial correlations to RSP values (Figure 48) are also for a FS = 1. The snow-pavement layer from 25 mm (1 in.) below the surface to 125 mm (5 in.) in depth responds most directly to the contact pressure of loads placed on it (i.e., the actual pressure exerted by each of the main and nose landing-gear tires of the aircraft). For this layer, the RSP value when calculated from a suitable sample size (discussed later) using the 85% rule must be equal to or greater than 60 (middle column, Table 11).

Table 11. Recommended strength for 85% of the data for the Phoenix Airfield to support C-17 operations.

Layer, mm (in.)	Proof Cart RSP index, kg FS = 1	Minimum RSP index, kg FS = 1.25
25–125 (1–5)	60	75
125–275 (5–11)	73	91
275–400 (11–16)	55	69
400–1000 (20–39)	34	42*

* From Table 9

The next deeper layer (125–275 mm, or 5–11 in.) is most responsible for providing bearing strength to the gross load exerted by each of the three aircraft landing-gear gangs (nose and two main landing-gear groupings of tires). As such, its strength needs to be greater than for the top layer. Additionally, requiring this layer to be stronger than the top layer allows the strongest levels of compaction to take place on the top layer. Further, because the Phoenix Airfield is located in an accumulation zone, this requirement for a very strong bearing layer ensures that an increasing strength profile with depth for at least the first ±300 mm (12 in.) will always persist. The RSP strength level for the 125–275 mm (5–11 in.) layer is 73.

Modeling shows (see section 3) that aircraft landing-gear stresses below 275 mm (11 in.) are still about a third of their maximum and close to the strength limit of the natural snow at the Phoenix site. An RSP value of 55 for the snow horizon between 275 and 400 mm (11 and 16 in.) is appropriate.

We multiplied the values for FS = 1 in Table 11 by 1.25 to obtain recommended minimum RSP values for the design FS = 1.25 of the Phoenix runway (right column of Table 11).

We compare these findings to the target RSP values provided in Table 9. The results of the Fail/No-Fail tests divide the top layer in Table 9 into two layers, both layers with an RSP index lower than the value of 99 estimated from the computational analysis of runway strength (section 3.3), though the 125–275 mm (2–11 in.) layer is quite close in strength to RSP = 99 (Table 9). The third layer identified in the Fail/No-Fail tests (275–400 mm [11–16 in.]) roughly coincides in depth with the second layer in Table 9 (250–500 mm [10–20 in.]), and these are of comparable strength (RSP = 69 for Fail/No-Fail tests vs. RSP = 65 in Table 9). Given the uncertainty in the RSP instrument and through the Fail/No-Fail tests, we conclude that

the conversion from runway stress to RSP index outlined in section 3.3 is conservative and that the Fail/No-Fail tests provided a refinement on those initial values obtained in section 3.3.

4.3 Sampling locations

The Phoenix Airstrip and apron cover 204,400 m^2 (2,200,000 ft^2); and with a pavement system extending to a depth of 1 m (39 in.), there are 204,400 m^3 (7,150,000 ft^3) of material whose properties are of interest, with the properties in the top 0.5 m (20 in.) being of critical interest to understand.

With a proof cart, if care is taken to overlap the wheel tracks with successive passes, nearly 100% of the runway surface can be evaluated. By contrast a penetrometer provides information at a single, small point. To determine the spatial variation in strength with a penetrometer, many penetrometer measurements need to be taken. Figure 49 shows the recommended sampling pattern for a contingency airfield, and Figure 50 shows the sampling pattern used on the white ice airstrip at Pegasus. The sampling pattern used at Pegasus is similar to what is recommended for a contingency airfield, but there are a few more measurement points at Pegasus. For consistency, we recommend a sampling pattern similar to what is used at Pegasus and the apron sampling pattern similar to what is used for the contingency airfield. Figure 51 shows a recommended strength sampling pattern for Phoenix that combines the patterns shown in Figure 49 and Figure 50 and reflects the actual layout of the Phoenix Airstrip and apron. Table 12 provides more detailed information on the recommended locations and schedule to measure runway strength (e.g., the table specifies that a full suite of measurements is taken before flight operations commence for a summer season). During routine flight operations, we recommend documenting the strength 24 hours before each flight as well. The smaller number of sampling points indicated in “Routine Sample” (Table 12) are recommended for these preflight strength assessments.

Figure 49. Recommended penetrometer sampling pattern for a contingency airfield (after USAF 2002b).

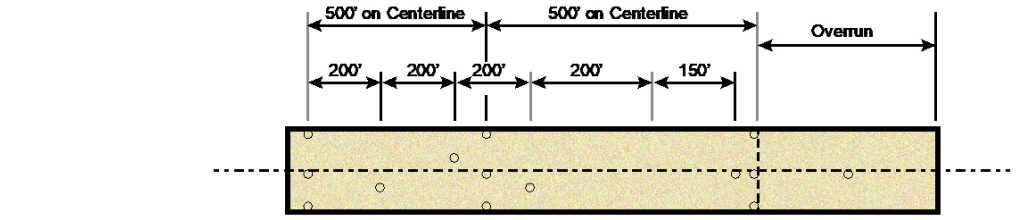

Typical Semi-prepared Airfield

Note: For unimproved airfield, continue this pattern throughout the length. For aggregate surfaced airfields, the pattern may be more widely spaced on the remaining portion of the airfield.

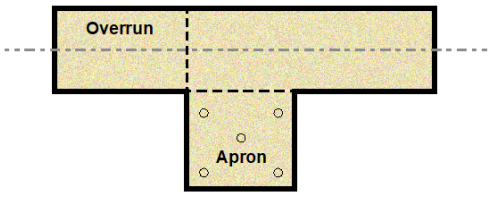

Typical Apron/Turnaround

Priority Testing

1. Soft spots
2. Offsets (should be in wheel paths of main gear)
3. Centerline
4. Aircraft turnarounds
5. Any area where the aircraft must stop
6. Overrun, one test in center (If overrun is used as a turnaround or for takeoffs, more tests are required)
7. Along edges at 500-foot intervals

Figure 50. Recommended penetrometer sampling pattern for the Pegasus white ice airstrip (USAF 2015a).

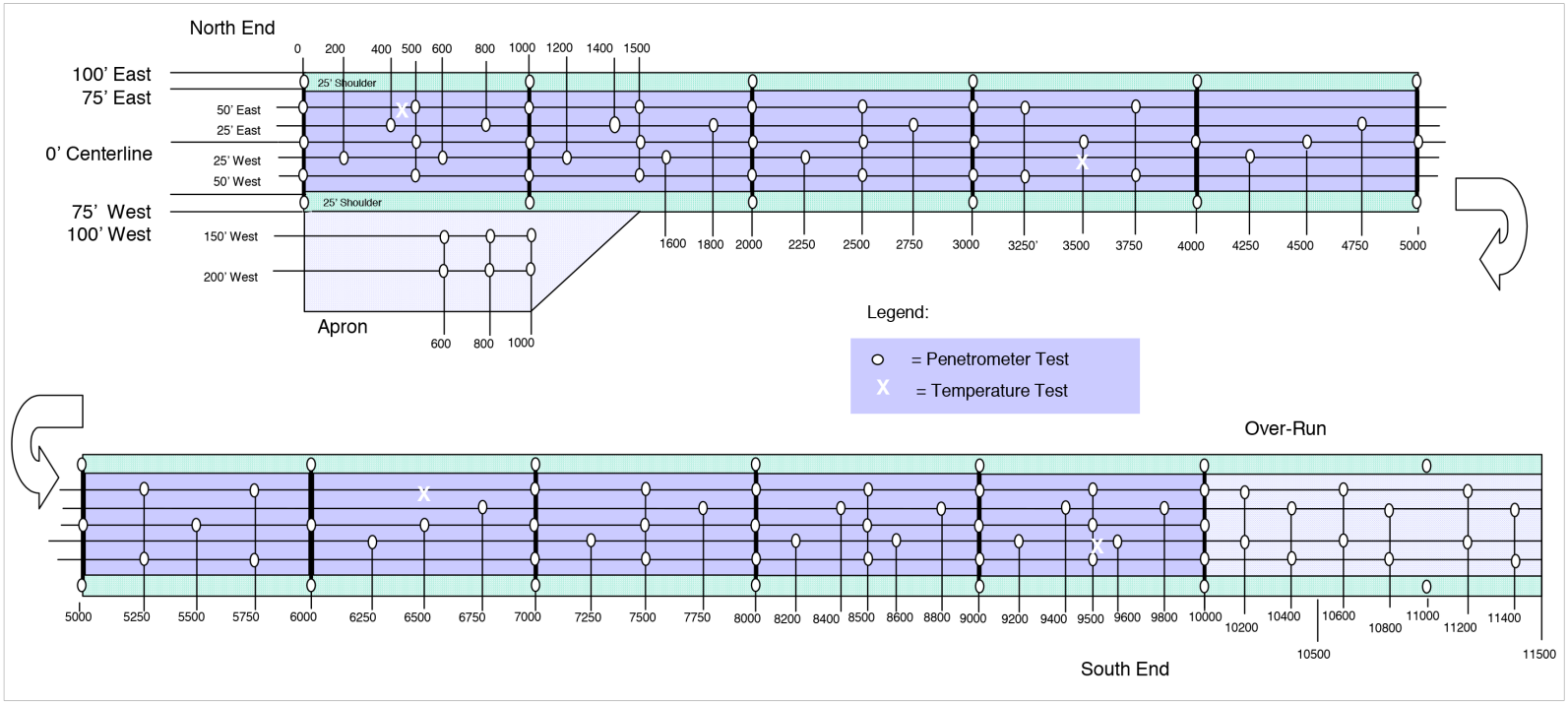

Atch 3
(4 of 5)

Figure 51. Recommended sampling pattern proposed for the Phoenix airstrip.

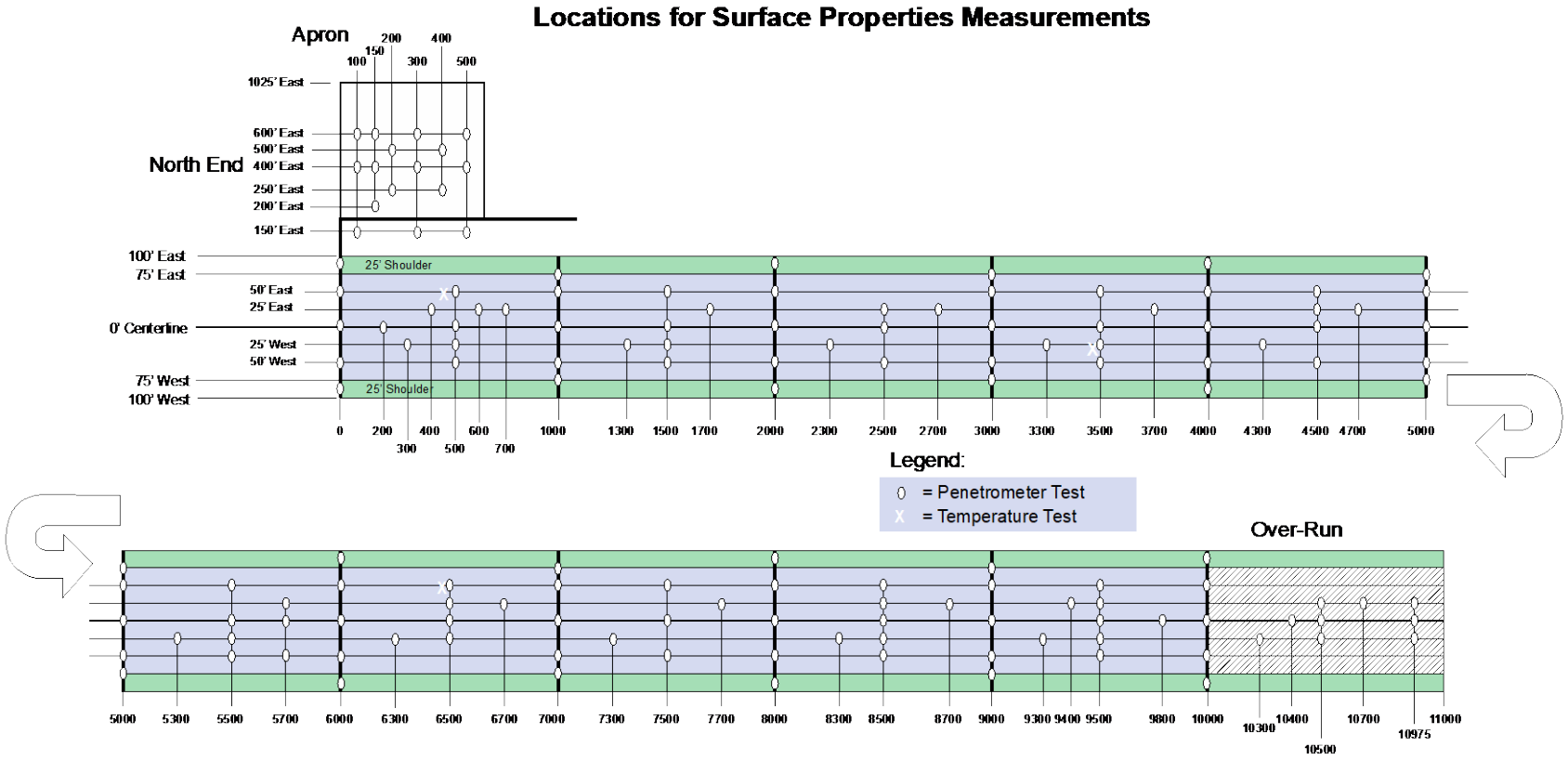

Table 12. Detailed information on strength- and core-measurement locations for the Phoenix Airstrip.

Sample Locations											
Distance from True North Runway Threshold	Distance (ft) East or West of CL	Full Suite		Routine Sample		Distance from True North Runway Threshold	Distance (ft) East or West of CL	Full Suite		Routine Sample	
		RSP	Density	RSP	Density			RSP	Density	RSP	Density
10+975	E 25	*				4+500	E 50	*		*	
10+975	W 25	*				4+500	E 25		*		
10+975	CL			*		4+500	CL	*		*	*
10+700	E 25	*				4+500	W 50	*			
10+500	E 50	*		*	*	4+300	W 25	*			
10+500	CL	*		*		4+000	E 87	*			
10+500	W 50	*				4+000	E 50	*			
10+400	CL		*			4+000	CL	*	*		
10+300	W 25	*				4+000	W 50	*			
10+000	E 87	*				4+000	W 87	*			
10+000	E 50	*				3+700	E 25	*			
10+000	CL	*				3+500	E 50	*			
10+000	W 50	*				3+500	CL	*		*	
10+000	W 87	*				3+500	W 50	*		*	
9+800	CL		*			3+500	W 25		*		
9+500	E 25	*				3+300	W 25	*			
9+500	E 50	*				3+000	E 75	*			
9+500	CL	*				3+000	E 50	*			
9+500	W 50	*		*		3+000	CL	*	*		
9+500	W 25		*			3+000	W 50	*			
9+400	E 25		*			3+000	W 75	*			
9+300	W 25	*				2+700	E 25	*			
9+000	E 75	*				2+500	E 50	*		*	*
9+000	E 50	*				2+500	E 25		*		
9+000	CL	*	*	*		2+500	CL	*		*	
9+000	W 50	*				2+500	W 50	*			
9+000	W 75	*				2+300	W 25	*			
8+700	E 25	*				2+000	E 87	*			
8+500	E 50	*		*	*	2+000	E 50	*			
8+500	E 25		*			2+000	CL	*	*		
8+500	CL	*		*	*	2+000	W 50	*			
8+500	W 50	*				2+000	W 87	*			
8+300	W 25	*				1+700	E 25	*			
8+000	E 87	*				1+500	E 50	*			
8+000	E 50	*				1+500	CL	*			*
8+000	CL	*	*			1+500	W 50	*		*	
8+000	W 50	*				1+500	W 25		*		
8+000	W 87	*				1+300	W 25	*			
7+700	E 25	*				1+000	E 75	*			
7+500	E 50	*				1+000	E 50	*			
7+500	CL	*				1+000	CL	*	*	*	
7+500	W 50	*		*		1+000	W 50	*			
7+500	W 25		*			1+000	W 75	*			
7+300	W 25	*				0+700	E 25	*			
7+000	E 75	*				0+600	E 25		*		
7+000	E 50	*				0+500	E 50	*		*	
7+000	CL	*	*	*		0+500	CL	*			
7+000	W 50	*				0+500	W 50	*			
7+000	W 75	*				0+500	W 25		*		
6+700	E 25	*				0+300	W 25	*			
6+500	E 50	*		*		0+200	CL		*		
6+500	E 25		*			0+025	E 87	*			
6+500	CL	*		*		0+025	E 50	*			
6+500	W 50	*			*	0+025	CL	*		*	
6+300	W 25	*				0+025	W 50	*			
6+000	E 87	*				0+025	W 87	*			
6+000	E 50	*				0+100	E 150	*			
6+000	CL	*	*			0+100	E 400	*			
6+000	W 50	*				0+100	E 600	*			
6+000	W 87	*				0+150	E 200			*	
5+700	E 25	*				0+150	E 400			*	*
5+500	E 50	*				0+150	E 600			*	*
5+500	CL	*		*		0+200	E 500		*		
5+500	W 50	*		*		0+200	E 250		*		
5+500	W 25		*			0+300	E 150	*			
5+300	W 25	*				0+300	E 400	*			
5+000	E 75	*				0+300	E 600	*			
5+000	E 50	*				0+400	E 500		*		
5+000	CL	*	*			0+400	E 250		*		
5+000	W 50	*				0+500	E 150	*			
5+000	W 75	*				0+500	E 400	*			
4+700	E 25	*				0+500	E 600	*			

5 Runway-Strength Certification Procedures

Based on the preceding, we recommend the following procedures apply for verifying the strength of the compacted snow pavement for the Phoenix Airfield, apron, and any other surfaces over which a C-17 will be taxiing or operating. We collectively call all of these surfaces the "runway" in the following procedures as all of these surfaces need to be treated the same. Certification of the runway with respect to flagging, geometric constraints, NAVAID and landing aids, etc., are not discussed here but are addressed in USAF (2015a).

During construction, progressively increase pneumatic-tire cart weight until the runway can support without rutting a total nominal cart weight of 727,000 kg (160,000 lb) (18,200 kg [40,000 lb] per wheel), the maximum weight that the SW cart can apply on the runway. Perform compaction rolling with two carts in offset tandem configuration for 100% coverage. In addition to compacting the top layer, this will also provide compaction and strengthening to the lower layers of the runway. Simulation results presented in Figure 37a from finite element modeling indicate that the weight cart causes compaction to as deep as almost a meter, thereby possibly affecting down to as deep as the base layer of the snow pavement.

Proof the runway by using the weight carts in tandem with alternating tires weighted to the maximum of 18,000 kg (40,000 lb) and a minimum of 6800 kg (15,000 lb). The loading must be either a "Combination" or "Reverse Alternate" as indicated in Figure 38. As previously discussed, either of these patterns is acceptable and should yield the same runway coverage when proofing. Using these load configurations, the proof cart will need to overlap approximately 50% for each pass to get nearly 100% coverage for runway proofing. This will proof the runway with the maximum stresses for a C-17 in so far as is possible as discussed in section 4.1.

We recommend the following criteria for assessing runway condition during proof rolling, as outlined in AFCESA/CES (1997). Rutting shallower than 100 mm (4 in.) in depth is a green condition: low-risk operation. Ruts 100–225 mm (4–9 in.) in depth are an amber severity condition that requires monitoring and repair when possible. Rutting of 225 mm (9 in.) or

deeper requires immediate repair. To be conservative, we recommend that for construction and repair, the rut depth for weight carting and proofing should be no more than 125 mm (5 in.) for operation of a C-17 and that any impression left in the surface between 50 and 125 mm (2 and 5 in.) be repaired before flight operations.

While we view this criteria as acceptable certification procedures for a C-17, other aircraft may require more stringent criteria. Each aircraft that will operate on the Phoenix Airstrip will need to be reviewed to determine acceptable proof-cart design, load requirements, and threshold rut depths for acceptable operations.

Until we have a rigorous set of Fail/No-Fail results for each aircraft type, the RSP limits we have proposed will not be used alone for airstrip certification. However, we recommend documentation of the runway strength with the RSP. The RSP is capable of documenting the strength down to a depth of 400 mm (16 in.). As discussed in section 4.2.3, the target RSP strengths for the top 400 mm (16 in.) of the runway should be at or above the values given in Table 11.

Owing to the very dynamic nature of the Phoenix Airfield material properties (compared to tradition runways), we strongly recommend documenting strength at all 128 locations specified in Table 12 prior to commencing flight operations in the spring and fall of each season. The minimum penetration depth for each strength profile is 400 mm (16 in.) for all of the locations specified in Table 12 and Figure 51. In addition, spot penetrometer measurements may be taken at other locations at the discretion of the certifying engineer on-site.

Following completion of the certification procedures described above, the Phoenix airstrip construction and certification procedures were validated by subjecting the runway surface to typical and extreme aircraft operations on the using a C-17 as described in the next section. We see the validation effort described in section 6 as a one-time event for the runway; following the procedures outlined above is sufficient to annually certify the runway for C-17 operations annually and at the start of any operational period.

6 Runway Strength Validation Plan

As with any piece of important infrastructure, we considered a "verification" event to confirm that it meets design intent prudent to ensure that no surprises interfered with the start of routine operations. This was especially important as this runway's being constructed from snow is extremely uncommon and unconventional.

6.1 Validation test plan background

Validation of the runway with the C-17 would be conducted after the C-17 landed at Pegasus and offloaded the southbound mission's passengers and cargo. The aircraft would then take on fuel to achieve near-maximum gross weight and fly to Phoenix Airfield with only flight crew and perhaps runway engineers on board. Ground (taxi) tests would be followed by one or more takeoff and landing procedures. Airfield Rescue and Fire Fighting support would be on-site throughout the runway validation event.

Upon successful completion of the planned validation test, the runway would be considered cleared for operational use. The C-17 would have the option to return to Pegasus for on-load of northbound cargo and passengers or could embark these at Phoenix Airfield. This decision would be left to McMurdo flight operations personnel and USAF flight managers.

6.2 Validation test plan detail

Table 13 outlines the full set of validation activities conducted, including the aspect of the airfield validated with each step. Shortly prior to the validation test date and during the event, USAF introduced modifications to the original plan, in each case owing to their favorable impression of the runway. Table 13 reflects these modifications (the main change to the original plan was to replace a takeoff abort maneuver with backing up [maneuver 8]). The steps are arranged in order from most benign to most strenuous, from the standpoint of the runway strength. We believed this set of validation tests covers the entire range of runway loading expected during routine operations, except for the duration of parking, which normally would be up to four or five times longer than the planned half hour parking that would occur with the validation test plan (Table 13, step 7). Figure 52 shows the overall arrangement of the airfield; Figures 53–57 depict the movement of the C-17 through the course of the entire validation test.

Runway engineers and the construction crew participated in the entire validation test both in the C-17 cockpit and on the ground. The runway engineers and the aircraft crew were in frequent communication to monitor and gain maximum benefit from the test program. At any point in the testing, any party could call for a slow-down to discuss issues of concern, which would take place face-to-face, between any two steps in the plan when the aircraft was stopped.

Also, part of the validation plan, following departure of the aircraft, strength and stratigraphy profiles would be taken at locations along and immediately adjacent to the wheel tracks. Although we do not expect anything more than shallow tire tread marks, it is possible that more extensive deformations could occur. If more extensive deformation occurs, these locations would be carefully analyzed immediately following aircraft departure to determine if the deformation is the result of inhomogeneous processing of the upper layers or evidence of inadequate bearing strength of the runway.

Any additional feedback from the flight crew during these validation tests would also be solicited and encouraged.

Section 8 provides details of the validation test results.

Table 13. Outline of C-17 validation test steps.

No.	Activity	Purpose	Details	Validation	Desired Input from Flight Crew	Est. Time (minutes)
i	Ground survey	Flight crew familiarization—runway	During routine pre–11 Nov C-17 mission to McMurdo, representatives of 11 Nov flight crew make a ground visit to Phoenix for a briefing about runway structure and a sampling demonstration.	N/A	Questions that may influence confidence or understanding of the competency of the runway	45
ii	Aerial survey	Flight crew familiarization—airspace	During routine pre–11 Nov C-17 mission to McMurdo, representatives of 11 Nov flight crew fly approach to Phoenix to experience visual cues associated with the new runway.	Runway markings; TERPS	Confirmation that markings and visual cues are understandable	30
1	First landing	Typical touch down (relocation of C-17 to Phoenix from Pegasus)	If winds allow, land heading (true) north. No wheel braking; use reverse thrust and coasting to reach taxi speed.	Runway's ability to support C-17 landing loading and comfortable high-speed travel	Runway "feel" at touchdown; impression of roughness at high down to taxi speeds	10 (from takeoff at NZPG to landing at NZFX)
2	Taxi on runway	Track runway at slow speed	Conduct a straight-line taxi at slow speed of 19 km/hr (12 mph) to the north end of the airstrip.	Runway's ability to support slowly moving contact pressure and gross load of C-17	Power level required for maintenance of typical taxi speed	5
3	Taxi and turn on apron	Track apron with turn at slow speed	Perform a gentle turn from the runway into the apron to head (true) east. Execute a typical radius 180° turn using variable thrust assist at the east end of the apron to head the aircraft (true) west.	Apron ability to support C-17 contact and gross load; surface ability to support typical nose-wheel turn	"Feel" of the runway during gradual turn	3
4	"Push" turn	Severe turning load	Perform a sharp radius 90° turn from the apron onto the runway at (true) north end without using variable thrust. Attempt to "skid" nose landing gear.	Pavement's ability to support maximum nose-gear shear loading	"Feel" of the runway during extreme turn	2
5	First takeoff	Typical takeoff	Perform a conventional acceleration and takeoff; conduct a rotation near mid-runway.	Runway's ability to support smooth, comfortable acceleration and rotation loading	Power level required to reach V1;* response of runway to typical rotation	10 (includes takeoff checklist)

No.	Activity	Purpose	Details	Validation	Desired Input from Flight Crew	Est. Time (minutes)
6	Full flaps landing	Severe braking load	After go-around, perform a typical short-field landing with maximum wheel braking effort.	Runway's ability to support severe braking loading	Response of runway to hard braking; directional control of aircraft; estimate of friction rating	10 (includes go-around)
7	Parking	Static loading	While the aircraft brakes cool, keep the aircraft parked in one location on the apron (est. 30 minutes).	Limited deformation response of the pavement	Power level required to start taxi roll	33 (includes 3 min taxi to apron)
8	Backing	Ability to self-back	Perform a typical backing action to observe the power required and the amount of snow dust generated.	Aircraft's ability to roll free of parking divots under its own power	Power level to start roll in reverse; degree of reduced visibility due to lofted snow	15
9	Turnaround	On-runway direction change	Perform a typical turnaround within the width of the airstrip.	Pilot confidence	Ability to comfortably make a 180° turn within the airstrip width	7 (includes taxi back)
10	Short-field takeoff (aircraft return to Pegasus)	Brake hold with significant thrust; hard rotation at V1	Perform a typical short-field takeoff with maximum brake hold during the engine run-up; severe rotation load is applied to the runway.	Pavement's ability to support a significant static brake load; runway's ability to support severe rotation loading	Power level required to reach V1; response of the runway to hard rotation	20 (includes takeoff checklist, fly-back to NZPG and taxi to apron)

* V1 is the point during departure at which the aircraft rotates (nose pitches up) but main landing gear is still on the runway and a high force is exerted on the runway by the main landing gear just before the aircraft becomes airborne.

Figure 52. Phoenix airstrip basic layout.

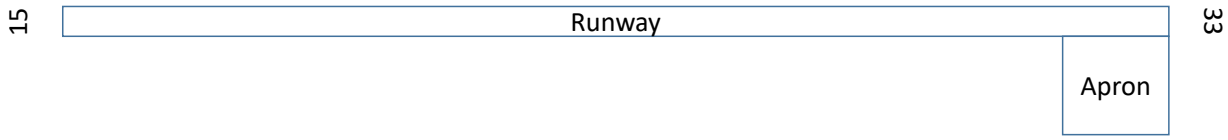

Figure 53. Initial landing (*1*), taxi (*2*), gentle turns (*3*), and stop.

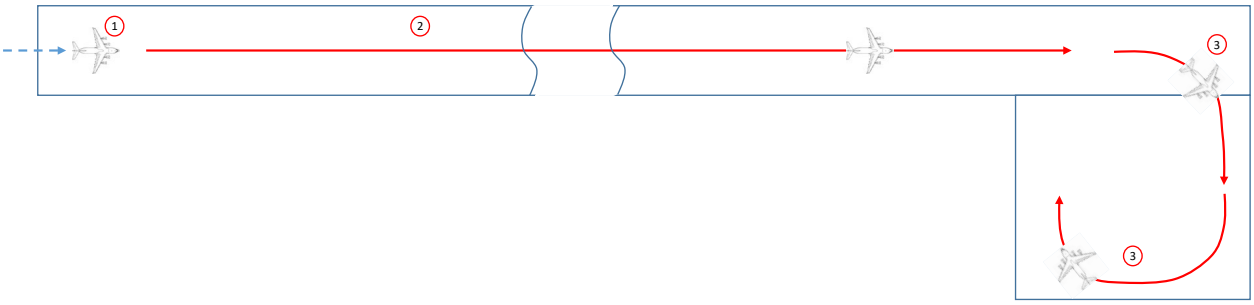

Figure 54. Push turn (*4*) to slide nose-gear tires on snow pavement.

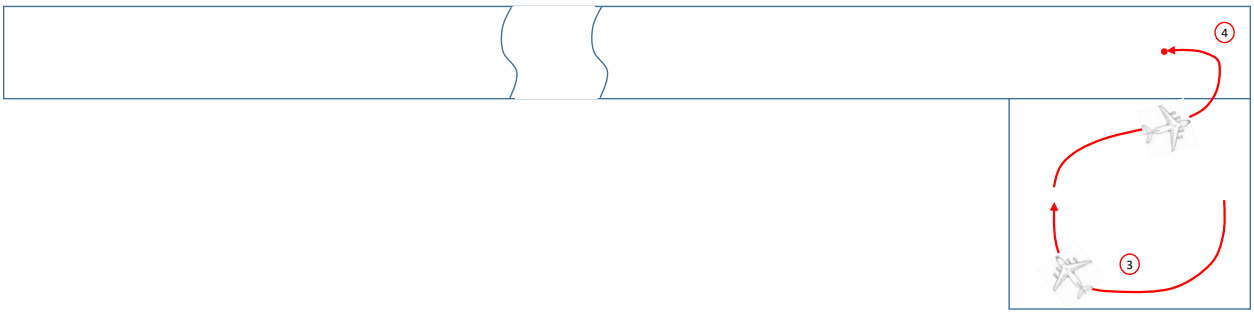

Figure 55. Conventional takeoff (*5*) and "go around."

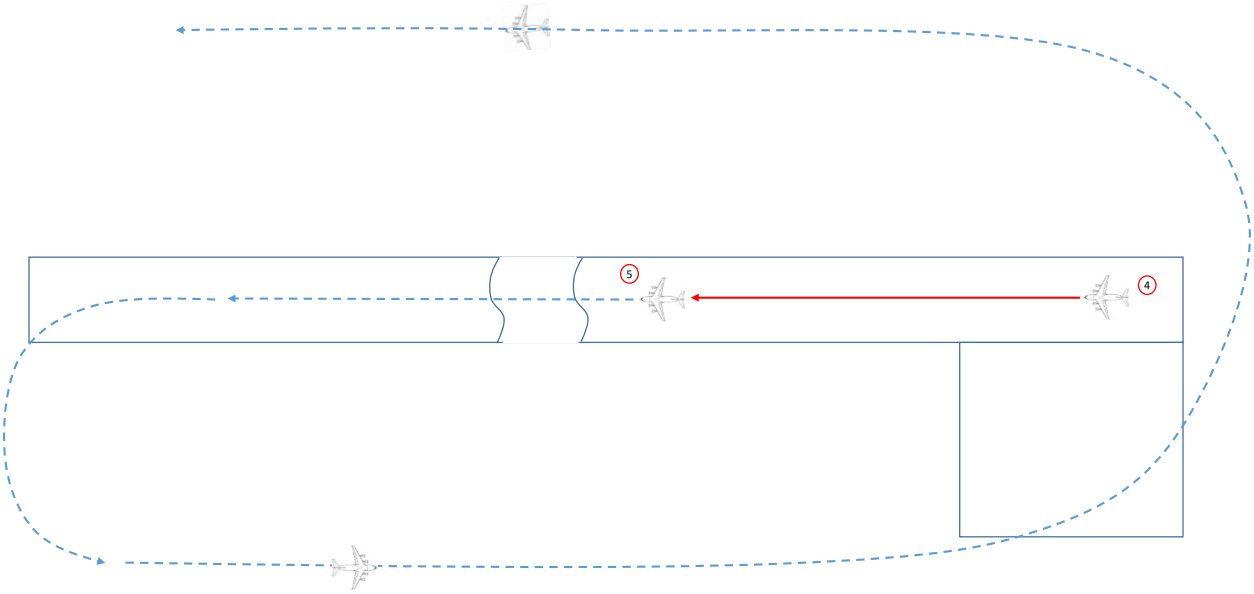

Figure 56. Full flaps (short field) landing (*6*) and taxi to apron, turn to face west, and park (*7*).

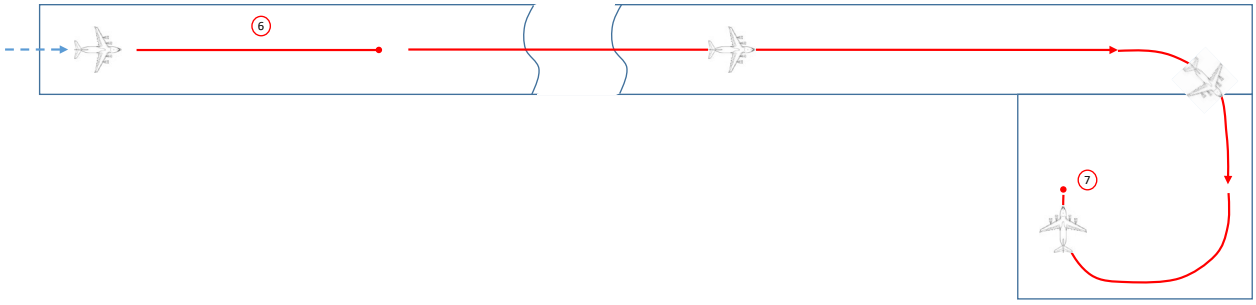

Figure 57. After approximately 30 minutes parking time (*7*), backing (*8*), proceed to runway and perform 180° turn within airstrip width (*9*) and short-field takeoff (*10*).

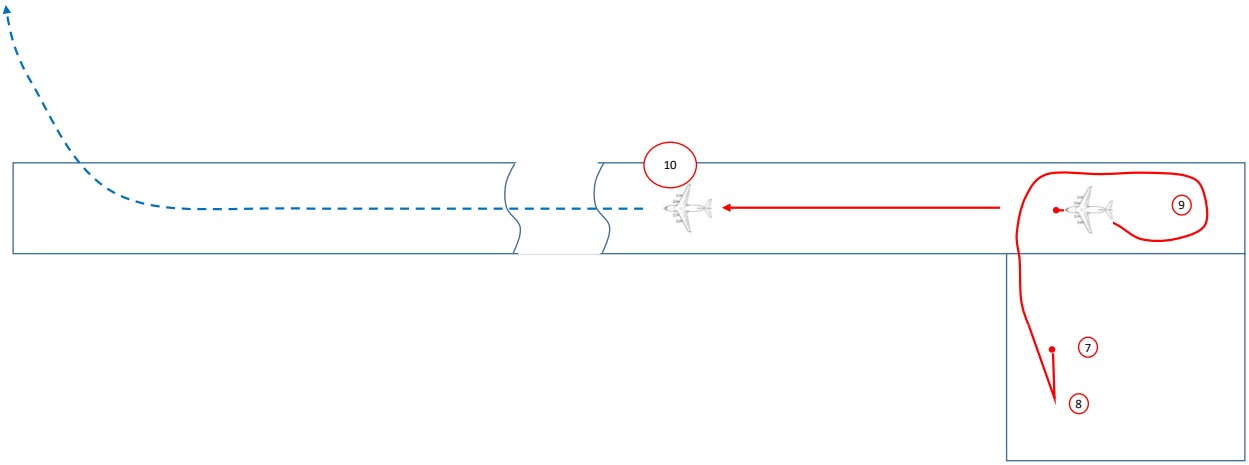

7 Construction and Maintenance

Experience with Antarctic snow compaction for building infrastructure has advanced significantly since 1989 when the Pegasus Airfield project began, in addition to NSF's obtaining new equipment. In particular, the "white ice" snowcap on Pegasus—installed in 2000–2001 to provide a reflective protective cover—proved that a snow layer could be compacted to a density and strength that routinely and reliably support heavy wheeled-aircraft loads. Granted, this was an ideal situation with a very thick, strong glacial ice foundation just below the thin layer of snow being compacted in an environment where seasonal temperatures reached just below the melting point, which facilitates productive bond growth between ice particles.

The original primary apron at the Pegasus Airfield was located on the west side of the airstrip at the north end and, like the runway, was founded on superimposed ice. This apron suffered serious contamination and melting, and all efforts to generate a sustainable pavement failed. During the 2005–2006 austral summer season, a new apron was constructed on the east side of the airstrip, still at the north end. The apron's surface joined the eastern edge of the airstrip, where discontinuous natural snow cover was less than 0.15 m (0.5 ft) thick; yet on the eastern edge of the apron—a mere 130 m (400 ft) away—the apron was founded on a 1 m (3 ft) thick layer of continuous snow. Construction of the new apron entailed temporary removal of all snow to a depth of 0.5 m (1.5 ft) below the original surface and replacement with 15 cm (6 in.) layers of loose snow, which were each compacted to a thickness of 10 cm (4 in.) before the next layer was added. This process proved adequate to create an apron that for over 10 years supported parking, fueling, and cargo operations of the C-17 and other heavy aircraft (e.g., Ilyushin IL-17). Knowing that at least the eastern half of this apron had natural snow beneath the processed pavement also demonstrated the feasibility of constructing an entire airstrip founded on deep natural snow in the McMurdo area.

Further encouragement came from an example in a very different setting. Snow was compacted to levels of strength equal to those created on the Pegasus airstrip on the east apron at NSF's Amundsen-Scott South Pole Station (located at the geographic South Pole) where temperatures never reach above –12°C (–10°F) and snowpack thickness is more than 2750 m (9000 ft). These three experiences led the design team of the new runway to expect

that McMurdo-area snow could be manipulated to reach a thickness-strength combination suitable for supporting the desired aircraft types.

7.1 Plan

Table 5 lays out the pavement design for the runway. The plan was to progressively increase the strength of the snow from the base of the constructed layer by compacting the snow to higher and higher densities with each successive lift. The following sections describe this process.

7.2 Procedures

Aver'yanov et al. (1983) and Russell-Head and Budd (1989) indicate that compaction of the snow is most efficiently accomplished with a lightly loaded pneumatic-tire cart at warm temperatures when the snow is moist, though details of the actual cart weight and configuration were not provided. We interpret this to mean, however, that the cart is loaded enough to allow the snow to support it without excessive rutting occurring (i.e., the cart compresses the snow but does not get bogged down in the snow).

Density by itself is not a terribly reliable indicator of strength in the case of snow. This is because, existing in nature close to its melting point, snow is a strongly metamorphic material with widely varying strength displayed with small changes in temperature in the range between melting and about −10°C (14°F). The primary act of snow metamorphism important to strength is the act of forming and growing bonds between adjacent ice grains. Bonds start forming almost immediately between ice particles upon their coming in contact after deposition and cessation of movement, and this bond formation proceeds most rapidly in fine-grained snow (snow particles 0.2 to 0.5 mm [0.008–0.02 in.] in diameter) (Shapiro et al. 1997; Armstrong 1980).

Left undisturbed for more than a few days under favorable temperature conditions, bonds ("columns" of ice connected at each end to ice particles) add tremendously to the load-bearing capacity of a snow mass while usually changing the snow's measured density imperceptibly. Bonds form most quickly and efficiently at contact points between ice particles. Thus, a dense snow mass having more intergranular contact points (or high coordination number) will most rapidly form bonds and increase in strength. This creates a winning formula for generating a snow pavement: a dense material that by itself is adapted to efficiently support loads along with a

material that can grow of many intergranular bonds that "lock in place" the tightly packed ice-particle matrix.

Snow is typically a two-phase material, a matrix of ice particles surrounded by interconnected space filled with atmospheric air. However, at temperatures above about −5°C (23°F), especially near the snow surface when solar radiation is strong, liquid water can also be included in the matrix. Liquid water is not readily apparent until it reaches a volume fraction of 3%–6%, at which point it can no longer be held by capillary forces as a coating around ice particles (UNESCO 2009). Despite being in very small quantities, this "residual water" is also very valuable in the process of heavy compaction, densification, and strengthening of snow.

Ice particles in the natural glacial snowpack at the Phoenix Airfield site tend to be small (0.5–1 mm [0.02–0.04 in.]), angular, and not overly uniform in size or shape. This fine-grained snow is ideal for forming a strong, dense pavement. At a natural density averaging 400 kg/m^3 (25.0 lb/ft^3) (Figure 4) in the top layers, this snow can typically support foot traffic with little sinking into the surface (sinkage). Based on experience and analysis (section 3), the runway design entailed a layered pavement system with target densities up to 675 kg/m^3 (42.2 lb/ft^3) at the surface (Table 5).

To efficiently and uniformly achieve such high densities in snow, it is necessary to use the following repetitive process:

- Apply loading that breaks the majority of intergranular bonds and creates closer spacing of ice particles.
- Allow time to facilitate growth of new bonds between rearranged ice particles. The duration of this time depends on the environmental conditions (i.e., temperature, humidity, and solar gain).

These steps are repeated over and over until no additional density gains can be achieved or the desired targets are met. The challenge in execution is twofold: determining just the right loading to achieve the first step but not cause mass destruction and displacement of snow ("blow out") and timing the first step so that a minimum of time is needed to allow step two to complete (i.e., understanding daily temperature, solar cycles, and short-term weather patterns and trends are key factors) before the surface is loaded again by construction equipment.

Additionally, it is important to understand that certain environmental conditions combined with many coarse grains mixed in with the snow can create a condition that does not support formation of well-bonded snow. Left alone in these situations, such a snow pavement will "unravel." While the snow's measured density may change little, metamorphic processes can act to sublimate small ice particles and their bonds and deposit their mass on larger particles. At its extreme, this process will produce a nearly unbonded mass of large, uniformly sized particles. Such snow is often called hoar and has extremely low strength, especially in shear. Even with compaction, it is hard to get these large-grained particles to bond together without mixing in fine-grained snow to help encourage bond growth.

To ensure that the processed snow at the Phoenix site did not unravel, compaction activities (dragging and rolling) took place on a schedule that recognized time since last compaction rolling, irrespective of the ability to achieve progress on densification. As environmental conditions favored active metamorphism (strong temperature gradients through the top 0.5 m [1.5 ft] of the pavement system), gaps between successive compaction rolling were shortened to as little as four days. This "maintenance" compaction sought to fractionally repack ice particles in response to any loss of small ice particles and subsequent voids left behind. Notably, while it was rare that any visible sinkage could be seen behind the roller tires when performing maintenance compaction, observers standing alongside of the roller as it passed during such events could hear what sounded like a popcorn popper or pouring milk over popped rice cereal. We took this as evidence that some bonds were being broken as slabs or sections of material were being displaced a very small amount (the "popping" sound) but that the movement of the particles associated with those bonds was very small (no visible rutting).

7.3 Summary of construction activities

Compaction activities during construction of the Phoenix runway took place initially on the natural terrain (pre-compaction densities shown in Figure 59). At the Phoenix site during these first compaction efforts (defined as Lift 1), we focused on turning the top 15–30 cm (6–12 in.) of the existing deep, naturally approximately 450 kg/m^3 (28 lb/ft^3) snow into a homogeneous material with a density greater than 525 kg/m^3 (32.8 lb/ft^3). Following compaction of the natural snow, the first layer of snow above the manipulated natural material was placed by bulldozing snow onto the

runway from adjacent terrain (Lift 2). This was time consuming and imprecise but did allow thickening of the snow pavement to proceed without waiting for the next significant snowfall. Leveling and compaction of this first layer took many equipment passes (compaction with steel-tracked dozers, dragging, and pneumatic tire roller coverage) but did achieve densification to a depth of about 20 cm (8 in.). Additional layers were compacted from naturally falling snow over the course of a year, leading to a thicker, denser, and much more uniform pavement system by the time the first flight arrived to validate the snow runway strength. The runway was evaluated via the certification and validation procedures outlined in sections 5 and 6 and was found adequate to support flight operations.

Figure 58 shows the stratigraphy of the runway in January of 2017 at the end of construction. The top 23 cm (9 in.) is much whiter than the deeper snow owing to this part of the pavement being constructed from new fallen snow that was immediately compacted into the runway. Below that is the pavement that was constructed from old snow that was pushed from the edge of the airstrip onto the runway and then compacted. In addition to being darker in appearance, one can clearly see ice chunks mixed in with the aged snow. In Figure 58, it is not clear where the transition is from Lift 2 (snow pushed from the side of the airstrip unto the runway) and Lift 1 (snow that was compacted in place).

Figure 58. Snow layering in the runway, 20 January 2017.

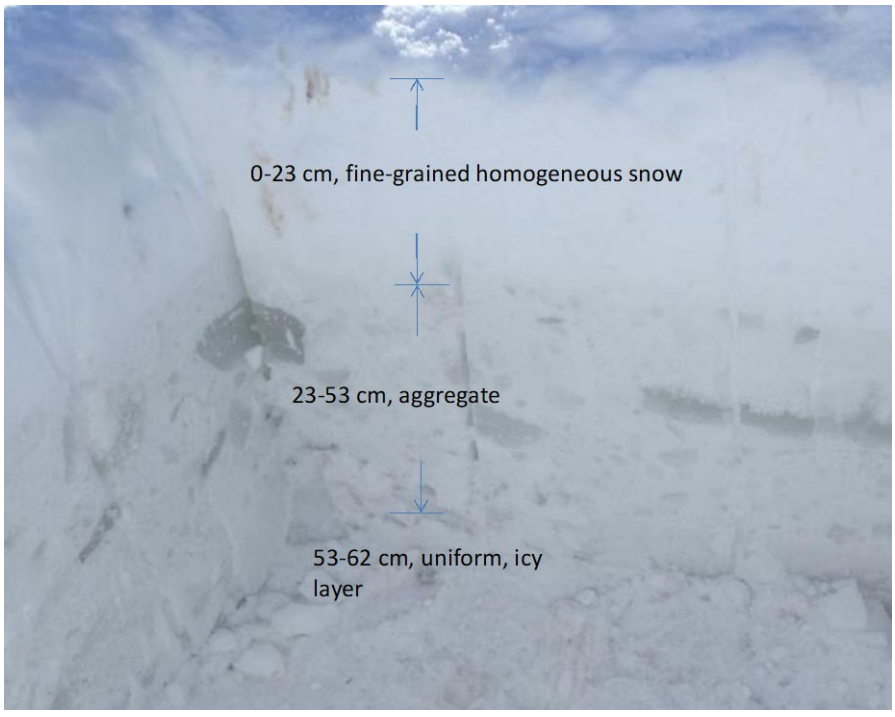

7.3.1 Density evolution

Figure 59 shows the initial conditions of the snow at the Phoenix Airfield. This shows that generally the snow had a uniform density of 350–450 kg/m^3 (22–28 lb/ft^3) with a depth down to about 1 m (39 in.), though there were some locations in the planned airstrip area that had considerably higher localized density. Figure 60 and Figure 61 show how the density increased with depth during the construction process, as well as gaining better uniformity in density spatially along the length and width of the airstrip by the completion of construction (Figure 61, Table 14).

Although our experience suggested that the densities listed in Table 5 were appropriate for a runway supporting heavy wheeled aircraft, the Fail/No-Fail tests described earlier provided an opportunity to validate this assumption. As described, we needed to operate the heavy compaction roller in the town site of the Phoenix Airfield to achieve any pavement compromise.

Figure 59. Vertical density profile for sites along the Phoenix Airstrip before the beginning of pavement-system construction.

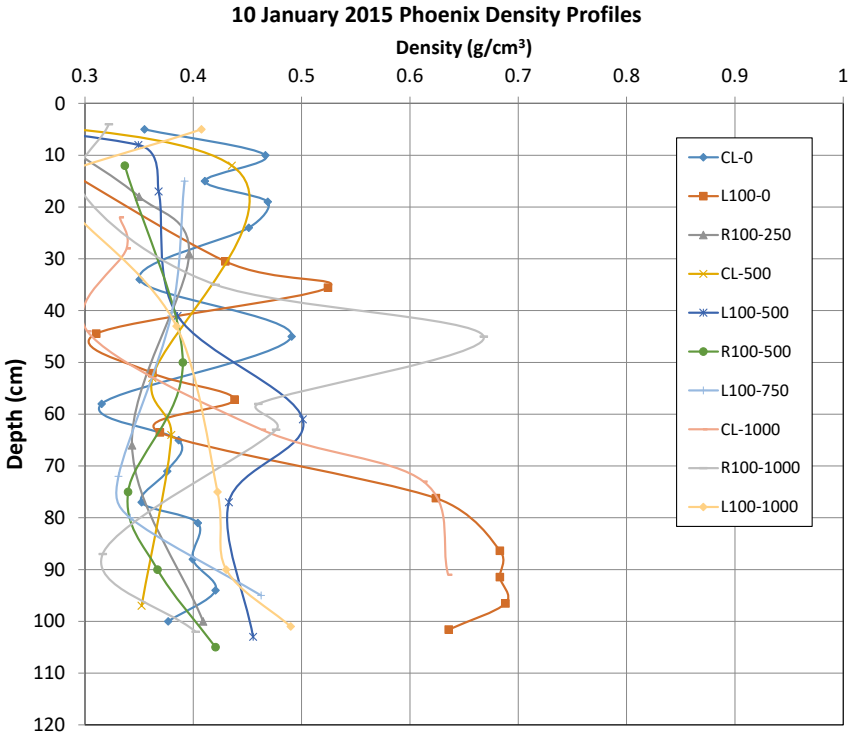

Figure 60. Vertical density profile for sites along the Phoenix Airstrip during the early construction phase after being subjected to sheepsfoot rolling and initial rubber-tire compaction.

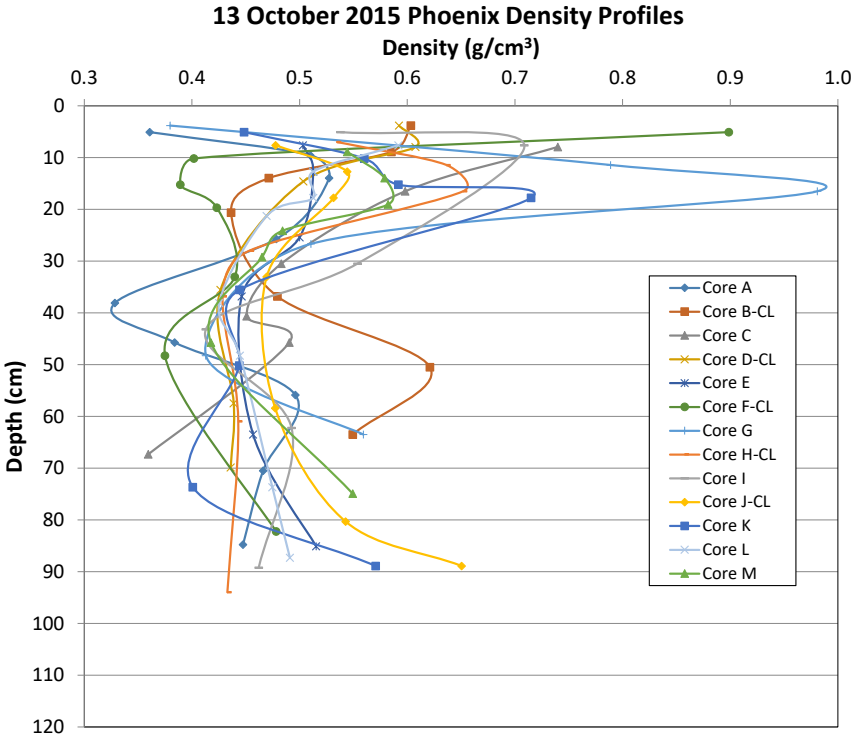

Figure 61. Vertical density profile for sites along the Phoenix Airstrip after the second austral summer of heavy compaction.

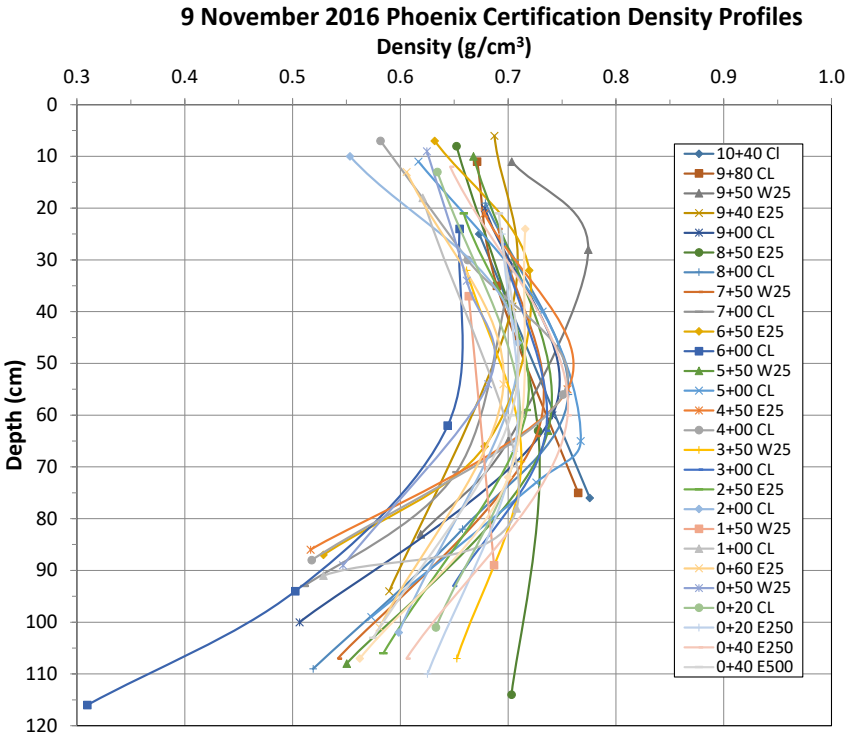

Table 14. Measured density profile in the Phoenix Airfield on 28 November 2016 at the conclusion of the main construction period.

Lift	Layer Thickness, mm (in.)	Depth to Bottom of Layer, mm (in.)	Average Measured Density, kg/m³ (lb/ft³)
3	150 (6)	150 (6)	670 (42)
2	350 (14)	500 (20)	700 (44)
1	200 (8)	700 (28)	640 (40)
Base	400 (16)	1100 (44)	600 (37)
Subgrade	∞	>1100 (44)	Not measured*

* Cores taken extended to a depth of only 1100 mm (43 in.); and therefore, the subgrade density was not measured.

Knowing that the town site had a significantly lesser level of compaction, we expected a clear difference in the vertical density profile there compared to the apron and runway. Figure 62 shows that the target density values we designed for the runway could be achieved and that they were adequate to fully support our heaviest wheeled loads (solid curves). Further, a distinctly lower density profile is present in the town-site pavement system, where surface disturbances and pavement failures took place under the heavy roller (dashed curves).

Figure 62. Comparison of Phoenix pavement density profile on 25 October 2016 in areas on the apron and runway that fully supported a 74,000 kg (163,000 lb) compaction roller and areas in the town site where roller passage left the pavement surface disturbed or failed.

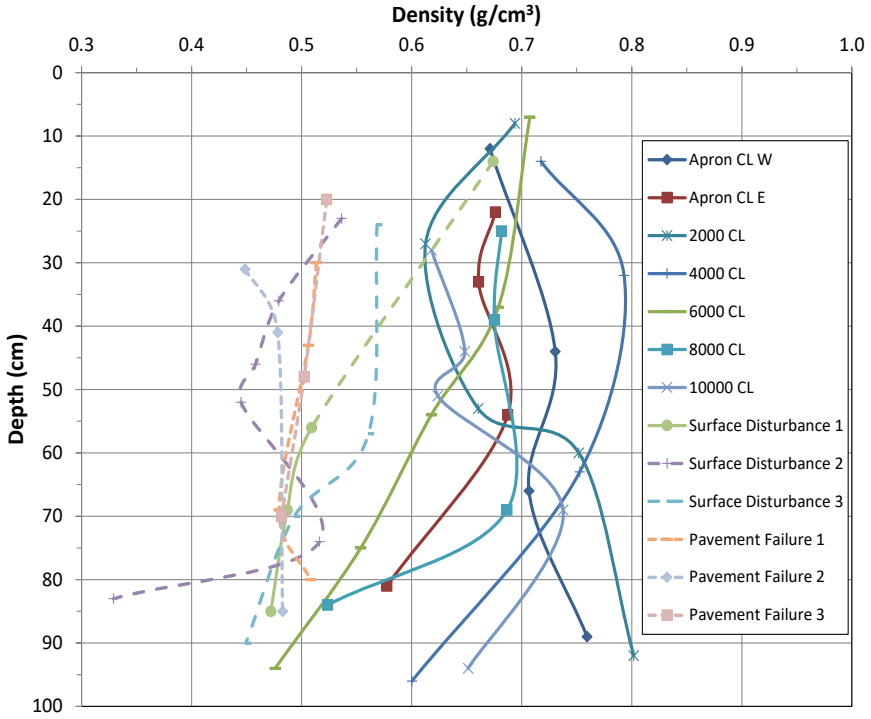

7.3.2 Strength evolution

During initial construction, we were primarily interested in the bulk properties of Lift 1. Thus, we averaged the vertical series of index values at each sample site and compared them spatially with other penetrometer sampling sites. Insights from this data set were used to establish how many construction equipment passes were necessary to

1. achieve the desired levels of uniformity and layer thickness and
2. reach design target strength levels.

Upon achieving the desired strength of Lift 1, Lift 2 was placed mechanically, using bulldozers to move snow from the long-axis edges of the airstrip onto Lift 1. This was aimed at creating as uniform as possible a 200 mm (8 in.) layer of new snow. At this stage, we were exclusively using the RSP to measure strength, and data were still calculated for every 25 mm (1 in.) of penetration; but analysis in this case did not lump the whole lift into one layer. Instead, we divided the lift into an upper and lower horizon with the goal of detecting if the compaction equipment being assigned to the construction task was exerting adequate stress throughout the full thickness of the new layer of snow to achieve a Lift 2 that had a uniform density greater than 525 kg/cm^3 (32.8 lb/ft^3). Analyzing the data in this way allowed us to assess Lift 2 both horizontally and vertically for uniformity.

Subsequent lifts of snow pavement were produced when natural snowfall deposited on the runway surface. In between these events, the pavement system was compacted on an interval determined by a combination of time since last compaction and environmental conditions (temperature and solar gain). Because these lifts were of varying thicknesses (depending on how much snow was naturally deposited) and occurred at unplanned intervals, our focus on layering in the pavement system shifted from being centered on construction lifts to horizons defined by depth below the pavement surface. These layers were established to roughly coincide with what we considered critical stress horizons within the pavement system from the viewpoint of aircraft loading, using the design layering laid out in Figure 30 as an initial guide on layer partitioning.

While continuing to collect blow counts for every 25 mm (1 in.) of penetration, we separated the entire vertical suite of RSP data into three layers for analysis. These layers were defined as 25–125 mm, 125–275 mm, and 275–

400 mm (1–in., 5–11 in., 11–16 in.) and were conceptually related to the pavement, base, and subbase layers in a conventional runway construction profile. Within each layer, the RSP values calculated from each blow set were averaged to give three RSP strength values to characterize the vertical variation in snow-pavement strength at each sample location. Again, the data were used to evaluate the developing pavement system horizontally and vertically for uniformity, variability, and progress toward achievement of target strength levels to inform the construction and maintenance activities. Table 15 provides a summary of the evolution of the runway strength along with the weight of the rubber tire cart used to compact the runway preceding the strength measurements. One can see a decline in runway strength even though the cart weight was increased. The decrease in runway strength was a result of warming snow temperature and new snowfall that was worked into the runway as it was deposited. Still, compaction via the weight carts continued to work the runway and led to a rise in runway strength toward the end of the construction period despite increasing snow temperature.

Table 15. Summary of strength progression (RSP values) through the winter construction period into the spring and just prior to runway validation tests on the runway. The top row of the table notes the weight of the rubber-tired cart used for compaction, and the second row indicates the location where the measurements were taken.

	45 tonnes (100 kips) Cart	64 tonnes (140 kips) Cart	70 tonnes (153 kips) Cart	74 tonnes (163 kips) Cart			
	Runway Only			Runway and Apron	Runway and Apron	Runway CL and ±7.6 m (25 ft) of CL	Runway ±7.6 m (25 ft) of CL
Depth (mm)	22 Jul	3 Oct	14 Oct	20 Oct	29 Oct	31 Oct	2 Nov
25–125	117	117	82	100	82	91	100
125–250	116	165	87	116	108	73	94
250–375	130	108	108	94	101	73	94
375–500	108	144	108	108	73	73	73

7.4 Pavement repair procedures

Aircraft and maintenance equipment operating on the runway may at times damage the pavement system. Various degrees of damage can be anticipated as discussed in section 4; however, we expect that damage associated with construction and maintenance activities will be rare. In either

case, the procedure described next will be used for repair and to bring the pavement system back to a fully operational condition.

Repair should start immediately after damage occurs, including after an aircraft lands and before it takes off in the case of "turn around" missions.

7.4.1 Tracks

When aircraft operations on the runway leave imprints that can be is classified as tracks (25 mm [1 in.] deep or less of tire impressions left in the surface), the runway must be dragged as soon as possible to remove all visual evidence of the aircraft tracks. This is especially important when landing aircraft leave black marks or a melted-refrozen layer during tire spin-up at touch down. At times, evidence of Tracks can be stubborn to remove and may require multiple drag passes or even the use of serrated blades (drag or snow plane).

7.4.2 Surface disturbance

When the impact of aircraft or equipment operations meets the Surface Disturbance definition (rutting of 25–125 mm [1–5 in.] for the C-17), runway repair is required. To start, the entire runway must be surveyed to identify all areas where Surface Disturbances are present. For each impacted area, all loose snow must be removed, leaving a rut whose base is sound pavement-system material. Removal will be performed manually with shovels and bars as required to eliminate all damaged material. All of the material removed from the site will be disposed of well outside the footprint of the runway.

After removing all damaged material, the void must be filled with fresh, loose snow harvested and moved to the void from sources elsewhere on the runway surface or from the natural terrain adjacent to the runway. This can be achieved with a loader or, more efficiently, by a tractor-towed drag or grade box.

The fresh snow can be placed in the void by hand (shovels) or using a drag. The patching material will be tamped by foot and refilled to the existing runway surface or slightly above. The patch will then be track packed by a rubber-track tractor (e.g., Case QuadTrac or Caterpillar Challenger) back and forth in at least two independent directions. If the surface of the resulting patch is below the grade of the runway, another layer of patching

material will be added and the compaction process repeated until the patch is at the level of the surrounding runway surface.

If patching takes place while an aircraft is awaiting takeoff, the flight crew should be encouraged to avoid traveling over the patch although they must be assured that there is no safety issue if they do travel over the patch. If the aircraft passes over the patch and compromises any part of the patch, the damaged portion of the patch will be reexcavated and the patching procedure restarted.

The patch will be left untouched for 24 hours, at which time it will be compacted with a 32,000 kg (70,000 lb) rubber-tire roller (e.g., Ox cart) back and forth in at least two independent directions. After an additional 24 hours (48 hours after the patching process began), the patch will be compacted with a 74,000 kg (163,000 lb) rubber-tire roller (e.g., SW cart) back and forth in at least two independent directions. Upon successfully supporting this load, the patch will be deemed cured and the runway considered fully repaired.

Following either the 32,000 or 74,000 kg (70,000 or 163,000 lb) compaction, if the surface of the patch drops more than 50 mm (2 in.) below the surrounding runway surface, the patch is not completed and requires additional attention. In this situation, fresh snow will be added to the site and compacted in the same fashion as the original patch.

7.4.3 Pavement failure

Patching of Pavement Failures (rutting deeper than 125 mm [5 in.]) will follow the same pattern as for Surface Disturbances. That is, ensure that all failed areas are located and excavated down to sound material; and bring in fresh, loose snow for patching material. However, filling and compaction may take place in layers (or lifts) rather than all at once, as specified below.

If the excavated rut has a maximum depth between 50 and 125 mm (2–5 in.), filling and compaction will be performed exactly as prescribed for a Surface Disturbance. **However, when the runway damage meets the Pavement Failure criteria for a particular aircraft type, it is imperative that that aircraft type not traffic the patch site until it is declared fully repaired and healed.**

For excavated ruts with a maximum depth more than 125 mm (5 in.) but less than 250 mm (10 in.), fresh snow will be initially deposited in the void only to a thickness one-half of the total depth of the excavation. This lift of the patch will be processed as prescribed above for a Surface Disturbance. That is, compaction will take place with the rubber-track tractor, the patch left to heal for 24 hours before being trafficked with the 32,000 kg (70,000 lb) compaction roller, and then after another 24 hours tracked with the 74,000 kg (163,000 lb) roller. Upon this lift reaching fully cured status, a second lift will be placed and processed identically to the first.

For an excavated rut with a depth greater than 250 mm (10 in.), patching will proceed in lifts no greater than 125 mm (5 in.) in thickness for as many lifts as required to bring the area up to the same grade as the surrounding runway surface.

7.4.4 Runway use during patching process

Completed patching of a Surface Disturbance will take no less than 48 hours. During this time, the runway ideally will not receive any aircraft. However, for aircraft for which the original runway damage is classified as a Surface Disturbance, there is no safety issue impinging on operations. For example, a 100 mm (4 in.) damaged area is classified as a Surface Disturbance for the C-17 but is Pavement Failure for an Airbus A-319. Thus, during the repair of such a damaged area, C-17 operations can take place if necessary, but Airbus A-319 missions must not proceed until the patch is fully cured.

For operations that do take place before the patch is fully healed, flight crews should be encouraged to avoid the patched area. The risk if the patched area is trafficked is not to the aircraft but to the patch, which may be damaged, requiring the patching process to restart.

Completed patching of Pavement Failure may take as little as 48 hours for an excavated rut depth less than 125 mm (5 in.). For deeper ruts, completed patch time will be at least 48 hours for each lift required to fill the rut. Ideally the runway should remain closed to aircraft activity until the patch is completed and fully healed. If use of the runway is necessary before the patching process has been completed, there are conditions when it is considered safe to operate aircraft: if the depth to the top of the completed and healed lift from the surrounding runway surface is less than or equal to the specified limit for a Surface Disturbance for a given aircraft type, it is safe

to operate that aircraft type. For such aircraft operations, the depth to the top of the completed lift, or rut depth, and its location must be provided to the USAP airfield manager and be placed in a standard Notice to Airmen (NOTAM). The flight crew should be encouraged to avoid the patch areas but must also be assured that there is no safety issue associated with the remaining rut should they travel over it with their aircraft.

8 Runway Commissioning

Various mechanical tests and surrogate loadings can provide only a sense of how a new piece of infrastructure may behave when first operated as intended. In the case of most infrastructure, initial "loading" can be done in such a way as to "ramp up" from light to heavy/full loading. In the case of a new runway, ideally it would be nice to land an aircraft on a proven, immediately adjacent airfield and taxi over to the new airstrip for low-speed, on-ground testing. This was not possible for the Phoenix Airfield, meaning that a real landing would be the first aircraft contact with the new runway.

As outlined in section 6, we worked with USAF, including site visits by air operations managers and runway certifiers during the final phases of construction and proof testing, to establish confidence that no undue risks were present in landing a C-17 on the new runway. As discussed in section 6, the planned first C-17 operation on the runway was a validation of the runway performance for operation of a C-17 and included a number of maneuvers to verify that the runway performance was adequate to support typical and potential extreme aircraft activities. Table 13 (section 6) lists the sequence of activities.

8.1 Validation with C-17

The first aircraft contact with the runway at Phoenix occurred in the early afternoon of 15 November 2016. As planned (see section 6), a C-17 executing a routine round trip from Christchurch, New Zealand, to the Pegasus airstrip unloaded passengers and cargo and took on a full load of fuel at Pegasus. With only the crew and one CRREL member onboard, the aircraft then took off from Pegasus and landed on runway 33 at Phoenix (Figure 63). After an air-brake-only deceleration, the C-17 entered the apron and parked. Although the aircrew was unconcerned, the CRREL observer was surprised by the degree of runway roughness. Prior to aircraft arrival, runway evaluation visually and in a vehicle traveling near 100 km/hr (60 mph) suggested a smoother surface than what was experienced in the cockpit. Perhaps this should not have been surprising since no special activities during construction (or quantitative measurements) were aimed at runway roughness.

Figure 63. U.S. Air Force C-17 Globemaster III makes first contact with the Phoenix Airfield.

Upon parking after the first landing, the runway construction crew and engineers performed a thorough inspection of the C-17 tracks on the runway, and the flight crew was debriefed while also traveling along the runway to observe its surface. The flight crew indicated complete satisfaction with runway performance and "feel" during landing, taxi, and parking.

The project team's inspection of the runway showed that nearly all of the C-17 tire tracks were just visible when viewed from an appropriate angle relative to the sun (Figure 64 and Figure 65).

We identified two primary areas of interest where the C-17 tracks were not benign. First, as was typical at the Pegasus Airfield, rubber-dust tracks were left on the runway surface during aircraft tire "spin-up" at touch down (Figure 66). Such skid marks are ubiquitous on paved runways, but it is not intuitive that they would be seen on a snow/ice runway. However, adequate friction must be present to cause rubber from aircraft tires erode while the tires transition from zero rotational speed to the landing speed of approximately 130 knots (150 mph). These dark marks on the runway reduce albedo and if not removed can accelerate localized runway melting and reduce runway strength.

Figure 64. Taxi tracks of the C-17 on snow pavement of the runway (*foreground*) and apron (*background*).

Figure 65. Close-up view of C-17 taxi tracks at the north end of the airstrip.

Figure 66. Tracks of eroded rubber from a C-17 landing.

Secondly, several areas showed some degradation of the pavement surface. These took the form of slight "unravelling" of the surface (Figure 67) to outright rutting (Figure 68). Both types of surface disturbances represented a tiny percentage of the area touched by the aircraft tires, and neither was detectable by the aircrew when they occurred. Nonetheless, these areas were of keen interest to the project team since they represent strength levels that perhaps were on the margin of adequate.

The validation event continued as planned with routine turning to maneuver around and off the apron and a tight turn on the runway end to prepare for takeoff. During the later, the front tires were "skidded" on the runway surface (Figure 69) to demonstrate that the pavement strength was adequate for the level of runway surface friction present to avoid having the tires dig in and put unacceptable levels of stress on the nose landing gear.

After aligning for takeoff on runway 15 (heading south), the C-17 executed a typical acceleration and rotation before becoming airborne. Inspection of the runway by the project team revealed a few locations with slight dis-

aggregation (like that seen in Figure 67). We also observed one or two significant ruts along the path of one of the main landing gear in a short section (approximately 3.5 m [12 ft], Figure 70) where the aircraft rotated (the point where the pilot pulled back on the controls to cause lift-off, first by the nose gear followed shortly by the main landing gear).

Figure 67. Area showing slight disaggregation of the surface with the passing of aircraft tires.

Figure 68. One of a handful of areas showing rutting of the runway surface with the passing of aircraft tires.

Figure 69. Tracks of the C-17's nose gear when "skidded" on the snow-pavement surface.

Figure 70. Isolated but deep ruts associated with one tire path of the main landing gear at the point of C-17 rotation at takeoff.

Following takeoff, the C-17 circled the runway and set up for a second landing. This landing was meant to apply maximum tire braking to provide evidence that the snow pavement had both adequate friction to support effective braking and shear strength to resist failure from the heavy longitudinal loading caused by tire braking. As with the first landing, eroded tire rubber tracks were left on the runway where spin-up took place. Close examination showed that spin-up also generates adequate frictional heating to create an approximately 8 mm (0.3 in.) ice layer (Figure 71).

Once spin-up was complete and the tires were traveling at a rotational speed coincident with aircraft's ground speed, the C-17's antilock braking system engaged. This system's impact on the runway could be seen as polished segments along the main landing-gear tire paths (Figure 72). These polished areas also were a results of frictional melting, but the ice layer left behind was less than 3 mm (0.1 in.) thick and commonly not measurable.

Figure 71. Tire rubber and a melt-refreeze ice layer associated with the main landing gear's spin-up during landing.

Figure 72. Segments of the main landing-gear tire tracks showing snow-pavement polishing where the main landing gear's antilock braking system created tire slip and segments where tires were rotating without slip in between antilock braking system pulses.

Eroded rubber tracks and both types of frictional melt-refreeze features represent areas of the runway that will be susceptible to accelerated deterioration if left untreated. Maintenance activities to disaggregate and disperse all of the ice and rubber must be completed as soon as possible after each aircraft mission.

After the second landing, the C-17 taxied onto the apron and parked in a location close to but not on top of its initial parking spot. The aircraft shut down engines and began a deliberated pause in maneuvers so that we could observe the degree of settlement into the snow caused by the aircraft tires during an approximately 40 minute period. As expected, "cups" developed under each tire during the parked period (Figure 73). These depressions are associated mainly with the creep (plastic deformation) response of snow to load. Additionally, the surface of the depressions exhibited a thin melt-refreeze layer (Figure 74) which we attribute to solar heating of the tires during the parking period, leading to localized melting of the snow.

Figure 73. Snow creep depressions under each C-17 tire following approximately 40 minutes of parking time. The black glove in the picture is shown for scale.

Figure 74. Thin melt-refreeze ice layer at the tire-ice interface of the parking depression.

The depressions were observed to be slightly deeper under the main landing gear (Figure 73) than under the nose gear (Figure 75), which is related to the greater tire loading of the main landing gear. The maximum depression we measured was less than 40 mm (1.6 in.). It was also apparent, as expected, that the longer parking time associated with the second landing created deeper depressions that the first, shorter, parking event.

Figure 75. Depressions left in the snow by the nose gear during parking. The black glove in the picture is shown for scale.

At McMurdo-area runways, only the most basic aircraft ground support equipment is present. Aircrews are required to operate in a fashion that is as self-supporting as possible. A key piece of equipment not available in McMurdo is a tug. An aircraft needing to move has to do so under its own power, including backing. Thus, the validation event included the C-17 attempting to back itself up after parking. Of course, the C-17 has more than adequate power to back up on conventional (nondeforming) runways, but understanding that snow creep depressions form under aircraft tires parked on a snow pavement makes backing much more challenging. As seen in Figure 73 through Figure 75, these depressions are molded around each tire, in all directions, making aircraft movement quite effectively blocked even though each depression is not very deep.

After the parking event, the C-17 configured for backing. The flight crew gradually increased reverse thrust in an attempt to roll free of the depressions. After reaching typical reverse thrust levels, the aircraft still had not moved, but snow whirlwinds (similar to a dust devil, a strong, well-formed vertical-axis cylinder of rotating wind) formed in front of the engines on both sides of the aircraft (Figure 76). These whirlwinds alternated randomly between being wide (a 3.5 m [12 ft] diameter) to being very tightly formed (less than 1 m [3 ft] in diameter). The tightly formed whirlwinds "danced" and "snaked" along their vertical axis from the snow surface until they were approximately at the height of the center of the jet engine. There, they sharply bent horizontal and were sucked directly into the engine. To add to the artificial snowstorm, the jet engine exhaust, being deflected toward the front of the aircraft, generated a white-out condition around the cockpit area of the aircraft.

Figure 76. Snow whirlwinds forming in front of the jet engines during high reverse-throttle settings when attempting to back out of parking depressions.

Eventually, at a throttle setting higher than typically associated with backing on a paved runway, the aircraft rolled out of the depressions after which the aircraft rolled easily in reverse with modest throttle settings.

The penultimate validation activity was for the aircraft to execute a U-turn within the width of the runway. This activity was designed to provide aircrews with confidence that they could perform tight turns on the snow pavement and thus not require a cul-de-sac at the ends of the runway. This maneuver (Figure 57, activity 9) was accomplished with no issues.

During its planned final short-field takeoff, two of the C-17's engines shut down shortly after being placed at full throttle settings. After taxiing back to the apron and troubleshooting, the flight crew determined that the engines had ingested so much snow during the backing event that they were still too saturated to perform at full load. By running the engines at moderate throttle settings while parked for a few minutes, the flight crew deemed them to be dry and fully functional. The final takeoff took place without incident (Figure 77), and the aircraft returned to the Pegasus Airfield for cargo and passenger upload and the return flight to Christchurch.

Figure 77. C-17 takeoff from Phoenix Airfield after successful completion of the validation test plan.

8.2 Runway observations during 2017 operations

As discussed in section 7.3, the runway continued to be groomed and compacted with the 74,000 kg (163,000 lb) weight cart until 13 December 2016, when the increasing temperatures weakened the runway to the point

that the full weight-cart load caused significant rutting in the runway. The weight in the cart was reduced to a value that the runway would support without rutting: 45,300 kg (99,700 lb). The weight then was progressively increased as the runway would support it to return to the full load of 74,000 kg (163,000 lb) on 22 January 2017. The compaction roll with the fully loaded weight cart was completed on the morning of the 23rd, with compaction proceeding around the clock. During the compaction rolling, minor surface disturbances were noted at four locations at or near the runway centerline along the length of the runway wherein one or three tires caused minor rutting (rut depth of 75 mm [3 in.] or less) in the runway (Table 16). There were three other surface disturbances 30 m (100 ft) or more from the runway centerline; Table 16 also summarizes the characteristics of these.

Table 16. Summary of surface disturbances to the runway during compaction with the 74,000 kg (163,000 lb) weight cart during 22–23 January 2017 (J. Green, Antarctic Support Contract, email communication, 23 January 2017).

Location along runway 33	Number of ruts	Depth, mm (in.)	Maximum rut length, m (ft)
2200 m (7100 ft), 12–15 m (40–48 ft) east of centerline	3	75 (3)	3.7 (12)
2100 m (7000 ft), on centerline	1	<50 (2)	2.4 (8)
1520 m (5000 ft), on centerline	2	<50 (2)	1.2 (4)
1510 m (4950 ft), on centerline	1	<50 (2)	Not specified
838 m (2750 ft), 35.4 m (116 ft) east of centerline	1	<25 (1)	Not specified
460 m (1500 ft), 35.1 m (115 ft) west of centerline	1	<25 (1)	Not specified
107 m (0350 ft), 55.5 m (182 ft) west of centerline	2	50 (2)	1.5–1.8 (5–6)

The length of these ruts was typically less than 2.4 m (8 ft) long. The most severe rut was 3.7 m (12 ft) long and about 75 mm (3 in.) deep (Figure 78a). This level of rutting is a minor surface disturbance and, as discussed in section 4.1, is classified as “low risk” (AFCESA/CES 1997) and therefore within the operating parameters of the C-17. These ruts were repaired following the protocol described in section 7.4; Figure 78b shows the surface

after repair of the ruts at the 2200 m (7100 ft) distance from the north end of the runway.

Figure 78. (*a*) Rutting caused by the fully loaded (74 tonnes [163 kips]) weight cart during runway compaction on 22–23 January 2017 on the Phoenix Airfield at the 2200 m (7100 ft) distance mark, 12–15 m (40–48 ft) west of centerline. (b) The same area following repairs. (Photos by Jonathan Green, Antarctic Support Contract.)

a. Before repair b. After repair

Six cores were taken along the length of the runway (from 2900 m [9500 ft] to 460 m [1500 ft] distance from the north end of the runway and an additional core in the apron) on 24 January 2017 to observe the stratigraphy and the snow density variation with depth (Figure 79). These showed that, in general, the density of the runway had changed little since late November except that, at a depth of approximately 150–500 mm (6–20 in.), the average density had increased from about 700 kg/m^3 (44 lb/ft^3) to about 750 kg/m^3 (74 lb/ft^3). Of particular note is in the vicinity near the surface disturbances 2200 m (7100 ft) and 1500m (5000 ft) from the north end of the runway, the cores showed that the snow was more granular at a depth of 180–290 mm (7–11.5 in.); and they broke in two places in that depth range, as highlighted in Figure 79, rather than a single break in that range. This is approximately the horizon between the second and final lift in the runway as shown in Figure 58. The consistency of all of the cores breaking at about this depth seems to indicate that there is generally weak bonding at the interface between these two lifts.

The reason for the extra breaks in the regions indicated in Figure 79 may indicate that the thickness of the weak layer is greater in those regions than elsewhere in the runway. As discussed in section 7.3, Lift 2 was the last lift that was formed by dozing adjacent snow onto the runway and contains many ice aggregates and is darker while the final lift was formed

by compacting naturally fallen snow as it arrived on the runway surface and is whiter and more-uniform compacted snow. It is possible that at the interface between these two lifts, a combination of temperature gradient metamorphism and lower-density snow at the bottom of the final lift created a hoar-like layer and resulted in a poorly bonded interface between the two layers in some locations while in most of the runway the interfacial weak layer was very thin (on the order of a couple of millimeters or less).

Figure 79. Cores taken from the runway on 24 January 2017. The locations are indicated to the right of each core.

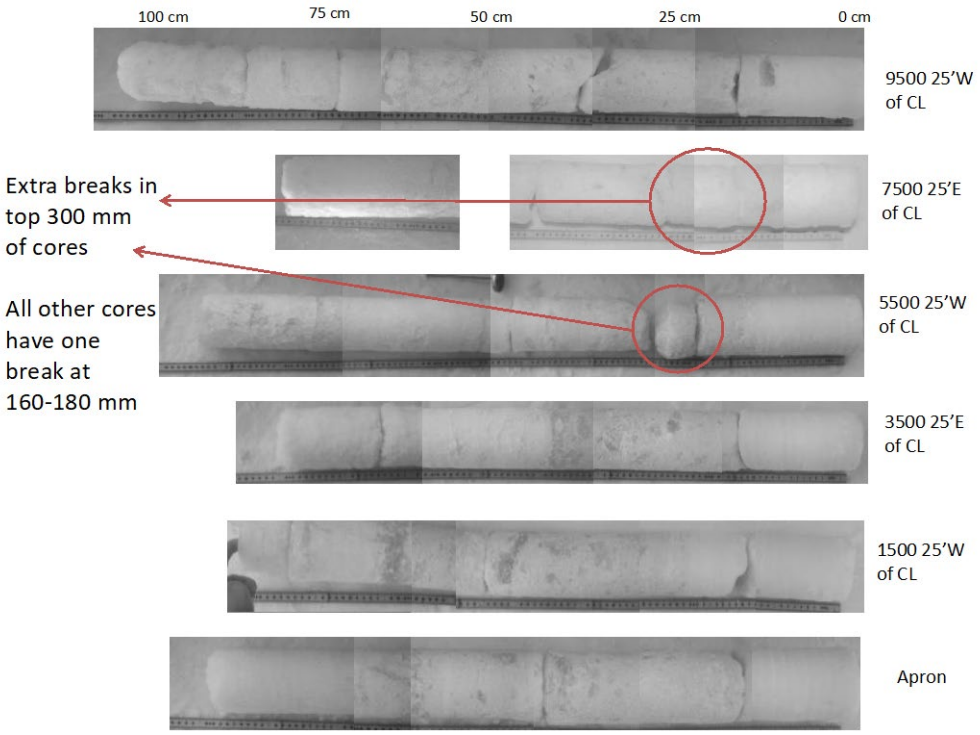

On 25 January 2017, we documented the strength of the runway by using the RSP following the pattern given in Figure 51 (121 sampling points). Table 17 summarizes the strength for the upper 400 mm (16 in.) of the runway. The measured strength for the top and lower layer are above the recommended value while the strength for the middle layer is below the recommended value for a C-17. Still, following the runway certification requirements outlined in section 5 and owing to the minimal surface damage by the fully loaded weight cart, the runway was cleared for C-17 flight operations.

Table 17. Comparison of runway strength measured on 25 January 2017 to the recommended values for the C-17.

Depth, mm	RSP Index, kg	C-17 Recommended RSP
25–125	82	60
125–250	62	73
250–400	73	55

Operations of the Phoenix airstrip commenced on 27 January 2017 with arrival of a C-17 carrying cargo and passengers. Table 18 details that flight the other first five flights. Though the plane landed and departed without incident, minor surface disturbances occurred on the runway as summarized in Table 19. These were repaired following the procedures outlined in section 7.4.

The subsequent three flights also proceeded without incident, only with minor surface disturbances as noted in Table 19. These were also repaired as per protocol. The extent of runway damage lessened with each passing flight until on 9 February 2017 there were no surface disturbances experienced. This held true for the remainder of the fall flight season. A total of 14 flights were serviced at the Phoenix Airfield during the first operational period from 27 January through 25 February, including one Airbus A-319 mission; the remaining missions were all flown by C-17s.

Table 18. Summary of the first five operational flights on the Phoenix Airfield.

Date	Arrival/Departure Time	Arrival/Departure Runway	Gross weight, kg (lb)	Touchdown, m (ft), from North End of Runway
27 Jan 2017	1950/2200	33/33	215,000 (473,000)	460 (1500)
30 Jan 2017	1415/1437	33/33	217,000 (477,000)	700 (2300)
1 Feb 2017	1319/1500	33/33	207,000 (455,000)	790 (2600)
3 Feb 2017	1333/1745	33/33	204,000 (448,000)	790 (2600)
9 Feb 2017	1351*	15/33	203,000 (446,500)	2880 (9450)

*Departure time not noted but approximately 2 hr later

Table 19. Summary of surface disturbances on the Phoenix Airfield.

Date	Temp	# of Disturbances	Location on Runway 33	Length/Width, m (ft)	Depth, mm (in.)
27 Jan 2017	−6°C	4	CL: 1830 m (6000 ft); CL: 1770 m (5800 ft); CL: 1500 m (4900 ft); 1540 m (5050 ft), 4.6 m (15 ft) left of CL	1.2/0.3 (4/1) 1.2/0.3 (4/1) 1.2/0.3 (4/1) 6.1/0.3 (20/1)	101.6–127 (4–5)
30 Jan 2017	−3°C	2	980 m (3200 ft), 7.6 m (25 ft) left of CL; CL: 1550 m (5100 ft)	3.7/0.3 (12/1) 9.1/0.3 (30/1)	177.8 (7) 101.6 (4)
1 Feb 2017	−11°C	1	1510 m (4950 ft), 7.6 m (25 ft) left of CL	3.1/0.3 (10/1)	101.6 (4)
3 Feb 2017	−12°C	1	CL: 1550 m (5100 ft)	6.4/0.3 (21/1)	50.8–101.6 (2–4)
9 Feb 2017	−7°C	None			

The recurring location where surface disturbances occurred through the first four operational flights was in the region around 1500 m (5000 ft) from the north end of the runway, one of the areas that exhibited a double break in the cores at a depth of 180–290 mm (7–12 in.). It seems that this weak layer caused some minor surface disturbances during the early flights. With successive cleaning out of the loosely bonded material and replacement with fresh fine-grained material during each repair, we saw progressive improvement in the runway until on 9 February there was no visible damage during flight operations. Another important factor that may have helped to eliminate runway damage on the 9th was that there were six days between flights, owing to a weather-related flight cancelation, that allowed more time for the snow in the repaired areas to sinter and gain strength, though it is clear even with the flight operations tempo that required 48 hr between flights (30 January–3 February) that there was a steady improvement in the runway performance (Table 19).

Following the first operational season at Phoenix Airfield, the project team compiled lessons learned during these first 2 months of operation. These are issues that either were unanticipated or did not evolve as expected and that require fixes to ensure efficient and reliable capitalization on this new piece of infrastructure. The listed issues will likely play a major role in defining future work on the Phoenix Runway:

1. The magnitude and duration of high temperatures and the existing USAP SW compaction rollers as deployed prohibit construction of a suitably robust deep-snow runway that can support C-17 operations during mid-November to mid-February. During this time, operation of the C-17 was

shown to be possible, albeit with unpredicted and random rutting associated with both nose and main landing gear. As an aircraft designed for operation in the presence of some rutting, this was not viewed as a safety problem. However, operations with rutting requires continual runway repair and healing and is not the preferred acceptable standard operating procedure. The SW rollers as deployed have shown that they can generate an acceptable deep snow runway for routine C-17 operations between late February and early November each year at the Phoenix site.

2. The existing SW rollers as currently deployed are not an adequate proof tool for C-17, Airbus A-319, P3, or Boeing 757 airframes. While some of the SW roller's runway loading characteristics meet or exceed landing gear on these aircraft, the SW roller does not provide an appropriate surrogate for the overall loading of these aircraft. Thus, the performance of the SW rollers cannot be directly applied to infer aircraft performance.

3. The RSP used for this project provides an indication of runway pavement system strength, but the RSP tool is insufficient for establishing precise aircraft operation limits for a new aircraft type. After observing RSP values occasionally showing an inverse relationship with runway rutting by the C-17, we conclude that the RSP tool does not adequately capture the overall strength of the pavement system in response to aircraft loading, as the RSP and aircraft loading conditions are vastly different. However, with repeated use, an RSP database can be correlated satisfactorily with compaction roller and specific aircraft-type pavement performance so that operational limits for that aircraft type can be safely stated.

4. One deficiency of the RSP tool is the inability to directly correlate its output values with any standard materials-engineering properties. However, we have demonstrated in this study that the RSP values obtained by conversion of runway stress via BAKFAA to RSP and CBR (e.g., Table 9 and Figure 32–Figure 34) provide conservative, though not excessively so, initial runway-strength limits. Validation of these RSP values via direct measurement as described in section 4.2.3 showed that they can be further refined to provide operational strength values that are still conservative but not overly so.

5. The conclusions described in items (2) and (3) above combine to imply that there is currently not yet a technique for clearly defining the Phoenix runway-strength limits required to adequately support C-17, Airbus A-319,

P3, or Boeing 757 airframes without the possibility of surface rutting. However, experience has shown that the SW rollers, operated in a tandem, offset configuration, each ballasted at 74,000 kg (163,000 lb), provide an adequate go/no-go determination for C-17 operations. This can be stated for the C-17 but not for the other aircraft types because it is known that the C-17 can withstand operating in the presence of limited pavement rutting.

6. The BAKFAA model engaged in this project appears to reasonably represent the vertical distribution of loading from pneumatic tires and other equipment operating on a runway pavement system like that present at Phoenix (e.g., SW cart tires and sheepsfoot rollers and aircraft tires). Applicability of the model to the Phoenix runway is currently limited by our ability to measure directly or infer from other measurements the required pavement-system stiffness parameters essential for accurately modeling the runway pavement structure.

7. The BAKFAA model's limitations (see item 6 above) do not allow it to be used directly to generate reliable strength limit criteria for the Phoenix runway for any aircraft type without validation data.

8. The combined conclusions of items (5) and (7) severely constrain our ability to unequivocally certify the Phoenix runway for operation of various types of aircraft during the warmest portion of the operating season. Based on on-site experience, including observations of SW roller trafficking, a large set of RSP values associated with fully performing and rutted pavement sections, and the comparison of aircraft loadings from the BAKFAA model, we established limit criteria for the Airbus A-319 prior to operation of the airfield. Following successful performance by the A-319 (no rutting), and the SW roller performance and RSP values measured in association with those missions, we have adjusted those limit criteria upward to reflect what is now known to be acceptable strength levels. However, the points in item (5) above still apply, and further revision of the A-319 limit criteria are likely to result.

9. A major factor influencing snow-pavement strength is temperature. While we assumed that RSP measurements would automatically integrate the effect of snow temperature, a potential explanation of the "inverse" relationship noted in item (3) above may be related to the shape of the temperature profile with depth in the pavement system or the transition of the snow from ductile to brittle behavior as the snow gets colder. Temperature

measurements along a vertical profile to at least 400 mm (16 in.) (where pavement temperature has been seen to be constant) at one or more places in the pavement material is necessary frequently or continuously, at least from October through March each year.

10. Poorly bonded hoar-like layers have been observed in the Phoenix pavement system. These hoar-like layers are very thin and are not like hoar layers found in natural snow although their dynamics of formation are the same. Specifically, hoar layers form as a result of snow-temperature-gradient-driven vapor flow. Owing to the very high density of the Phoenix pavement system, snow temperature gradients are higher than supportable in natural snow (which would normally enhance hoar-layer development). However, this same high density (low permeability) severely restricts vapor flow (stunting hoar-layer development).

11. Hoar-like layer formation is ideally avoided altogether in a runway pavement system but, being environmentally driven, is difficult to prohibit. The process of adding layers of pavement to the Phoenix runway as new snow arrives must achieve as seamless a transition as possible with the previous layers to limit density and grain size unconformities that tend to be magnets for hoar development.

Despite encountering these unanticipated issues, the runway pavement performed very well during January–February 2017, and none of the issues encountered are viewed as insurmountable. Future work has been outlined (section 10) to begin to address these lessons learned.

9 Maintaining Runway Health

All infrastructure is prone to deterioration associated with use and environmental exposure. And, while the Phoenix Airfield, like Pegasus before it, was designed and constructed to the maximum extent possible to be in harmony with the natural environment in which it exists, nature's forces nonetheless will act to revert the landscape back to its original state. Of course, ground vehicle and aircraft traffic also introduce factors that are foreign to the site. In this section, we identify many of the issues that we believe will be important to watch and manage to maximize the lifespan of the Phoenix facility.

Being early days in our experience with the Phoenix Airfield, some of the factors we identify may be more or less impactful than we anticipate at this time. As the site develops, both in its use as an airfield and in the operations and maintenance practices, and as long-term environmental trends are made manifest, the importance of each of these factors, and perhaps new factors, will become clearer.

9.1 Snow accumulation

At this time, we consider "excessive" buildup of snow to be potentially the most significant issue affecting availability of the Phoenix Airfield for flight operations. Recent data (see section 2.5) suggest that the site receives an annual accumulation of about 300–450 mm (12–18 in.) of 400 kg/m^3 (25 lb/ft^3) density snow. However, these observations took place when there were no structures or surface disturbances caused by human activity. Such changes in site conditions inevitably increase snow accumulation by creating obstacles that cause snow drift formation. Drifted snow depths are associated with the geometry and size of the obstacle and thus can be very nonuniform across the area and can be meters in magnitude near buildings and parked equipment or as low as zero on flat terrain. Drifted snow can pose a huge maintenance requirement.

The largest and most important portion of the Phoenix site is the runway. Fortunately, it should also be the easiest to manage for minimal snow drifting. The key factors are keeping the operating surface at or slightly above the level of the surrounding terrain, not allowing runway maintenance activities to generate any berms along the flanks of the airstrip, and tapering of the grade from the airstrip edge to the surrounding terrain to a

1:6 to 1:12 (vertical:horizontal) slope. Additionally, although seemingly insignificant in size, removal of all runway markers and NAVAIDS during time periods when the runway will not be in use greatly helps in keeping snow drifting from occurring on or immediately adjacent to the runway.

Snow drifts that do occur on the runway during wind and snow events must be broken up and evenly distributed over the entire runway surface as soon as practical after a storm. (In the event of a protracted storm, maintenance activity to ameliorate snow drifting should be accomplished during the storm if conditions allow and it is safe to do so.)

Snow accumulation on the runway, whether from drifting or direct deposition from falling snow, must be processed as soon as possible. The importance of this cannot be overstated. The design of the Phoenix Airfield requires that any new layers of snow become compacted as quickly as possible and integrated into the underlying layers so as to preserve a robust runway base. Knowing that the site will continue to accumulate material on the top surface, it is critical that no weak layers be "buried" as this will represent a serious bearing capacity flaw for supporting aircraft. This happens when a newly deposited snow layer becomes too thick (more than about 20 cm [8 in.]) to compact uniformly such that the top surface is compacted by maintenance operations but the deepest section of the new snow is not compacted significantly. Once present, a buried weak layer may cause the runway to be unavailable for an extended period until adequate new snow is built up and processed so as to bury the weak layer to a depth where it no longer limits aircraft loads.

Avoiding snow drifting on the apron and in the Phoenix town site, while not quite as critical, will be more challenging since concentrated vertical infrastructure (buildings, towers, etc.) exist on and around these areas. All of this infrastructure is vital to runway operations, so an operational airstrip may not be usable if the apron and town-site facility are compromised by drift snow.

Knowing prevailing and storm winds (section 3.4) is valuable in designing the placement and orientation of structures to limit snowdrift potential. Considerable study of building layout to limit snowdrift potential has been reported on and should be practiced at the Phoenix site (Haehnel and Weatherly 2014). Likewise, removing deposited snow to the downwind side of the apron and town site and keeping the windward side of these

spoil piles at a slope of less than 1:6 helps greatly to not exacerbate future snow drifting potential (Finney 1934).

9.2 Foreign contaminants

We have considerable first-hand experience with contaminants deposited on the snow impacting airfield facilities. Two categories of contaminants can be identified: foreign and natural. The first type, foreign contaminants, are materials introduced to the site by human activities and equipment/facilities. This includes but is not necessarily limited to the following:

- Sand and gravel dropped from the underside of ground vehicles after operating on the dirt roads on Ross Island
- Petroleum, oils, and lubricants dripping from leaks, system failures, or unclean areas of ground vehicles, aircraft, or facilities (including on-site fuel stores and glycol-based heating systems)
- Eroded rubber from tires of aircraft (Figure 66 and Figure 71), including skid marks and small chunks of rubber
- Exhaust soot from ground vehicles and especially certain aircraft types
- Frozen melt areas caused by stationary heat sources (running aircraft or ground vehicles or solar-induced warm microclimates adjacent to equipment or facilities)
- Litter

On concrete or dirt runways, most of these foreign contaminants would not immediately threaten an airport; however, they can compromise an air facility constructed entirely of snow. Any of the foreign contaminants listed above can bring about short- or long-term cessation in the availability of the runway and can may require significant maintenance.

Vigilance in avoiding foreign contamination of the Phoenix site must be practiced by ensuring only properly maintained equipment and facilities are allowed on site; daily inspection of the runway, apron, and town-site surfaces needs to take place to look for any signs of contaminants or deterioration. Operators working anywhere on the site must constantly be on the lookout for signs of contamination and must continuously monitor the integrity of their equipment. Anything identified must be immediately addressed. That means if a piece of equipment is depositing contaminants, remove it from the runway or apron (do not drive back to the town site on the

runway) or shut it down immediately if that is necessary to preserve the vehicle or will generate less overall contamination to operational surfaces. Likewise, discovery of a contaminated area must be reported to the Phoenix site manager and clean-up and remediation started expeditiously. Further, aircraft that generate excessive soot (e.g., LC-130) should have access to the snow runway only for emergency operations when the Williams skiway is not available to land on due to hazardous conditions (e.g., low visibility).

9.3 Natural contaminants

Foreign contaminants tend to occur in isolated, relatively small areas compared to natural contaminants. Natural contaminants appear to be more prevalent on the MIS over the past ten years. As discussed in section 2.6, wind-blown mineral dust from the south is known to spread over large portions of the snow surface (Figure 12, section 2.6). When siting the Phoenix airstrip, we made an effort to locate it in an area that, from satellite imagery and helicopter surveys, showed less deposit of natural contamination. Still, a potential remains for invasion of mineral dust from strong southerly winds.

Recent and on-going observations of the organic material that appears to be symbiotic with mineral dust deposits on the MIS suggest that it becomes active and propagates rapidly, forming dark mats or colonies (top of Figure 80) in the peak of the austral summer, owing to melt water generated initially by solar heating of the mineral particle and later by heating of the dark organic matter itself. This understanding of the likely propagation process led us to experiment with interruption of the growth cycle through grooming (dragging or planing) of the runway surfaces as soon as a mineral deposit was apparent or organic growth was detected on any operating surface of the runway. This action spread out any dark material—inorganic or organic—that was concentrated on the surface and thereby interrupted the warming and water-generation cycle and stunted or prohibited organic growth. This proved successful but clearly requires immediate action by the runway maintenance crew. This maintenance activity needs to be instigated early and repeated as soon as reactivation of growth appears and until a fresh snow cover or dropping temperatures no longer allow water formation.

Figure 80. Mineral and organic-matter deposits with sponge spicules deposited on the surface of the McMurdo Ice Shelf (*top*); sponge spicules photographed on the sleeve of a site worker (*bottom*) for contrast/visibility.

Our observations have confirmed that planing or dragging of operating surfaces, when done early and as often as necessary, does prohibit snow-pavement damage from mineral dust and its associated organisms. Further, we have witnessed complete shutdown of the organic regeneration process upon burial to a depth of as little as 3 cm (1 in.).

Other natural contaminants have been observed on the MIS, specifically sponge spicules. Speculation still exists on how these slender, fragile "hairs" (Figure 80) get deposited on the ice shelf; but as they are clear in color, we have seen no evidence that they present a hazard to creating and sustaining a snow runway facility.

9.4 Quality maintenance

Wear and tear are unavoidable consequences of infrastructure use. Compared to conventional runways, the Phoenix facility will likely experience far greater deterioration owing to its more ephemeral construction material and the strong impact of the environment (i.e., temperature and solar gain) on that material's strength. However, this runway is much more easily and quickly repaired compared to a conventional paved runway.

Availability of the runway during the air operations season will rely heavily on knowledgeable and timely repairs of any ruts from aircraft landing gear, iced and rubber streaked tracks from aircraft braking, and contaminants of all kinds. Long-term season-to-season availability will be achieved by ensuring that no weak layers or localized areas have inadequate strength levels before they become buried too deeply to be affected by compaction rolling. It is vital that new snow be processed as quickly as possible and during the time periods when environmental conditions are most favorable (as discussed in section 9.1). Likewise, any areas patched due to wheel rutting, construction and maintenance mishaps, or excavations for contamination removal must be brought back to the strength of the rest of the runway and apron as soon as practical (see section 7.4).

9.5 Glacial movement

It is now well understood that the primary cause of the demise of the Pegasus airstrip was movement away from a portion of the MIS with thin but permanent snow cover, the west edge of the net accumulation zone, into the net ablation zone, a region with ubiquitous exposed glacial ice and melt-refreeze. Phoenix Airfield is also located on the MIS but is 5 km (3 miles) east (and "up ice") from the edge of the ablation zone in an area that has considerable snow accumulation and cover as discussed in section 9.1.

Nonetheless, in its current position, the Phoenix airstrip is moving west (in the direction of the ablation zone) at a rate of approximately 44 m/yr (145 ft/yr). If the rate of movement of the MIS remains constant and the

edge of the ablation zone remains more or less stationary, the Phoenix airstrip would occupy the current position of the Pegasus airstrip in approximately 109 years (in 2126) making it extremely unlikely that movement into the ablation zone will cause the new runway's demise.

Survey data show that the north and south ends of the airstrip are moving westward at different rates, introducing a rotation in alignment amounting to about 1.5 minutes (0.025°) clockwise annually. This small amount of rotation would require 40 years to make a 1° change in runway orientation, a trivial change with respect to wind direction and airspace design.

Additionally, the survey data indicate that movement on each end of the runway is in slightly diverging directions, creating an approximately 1 m (3 ft) extension annually. Ice and snow are usually not thought to be very tolerant of tensile forces. However, on a floating ice shelf in an accumulation area, slow plastic stretching, creep relaxation, and continual addition of new material on the surface appears to result in a slight thinning of the ice shelf in the direction of its motion in the area between Williams Field and Pegasus rather than crevassing. Other than the rift identified in section 2.1 (and shown in Figure 4), no crevasses have been discovered on the MIS from a point well east of Williams Field up to the edge of the ablation zone. Thus, the apparent stretching of the glacial ice in the area of the Phoenix Airfield does not seem to create strains that pose a threat to the runway's integrity.

9.6 Climate change

Weather records for the McMurdo area have been kept with increasing sophistication since about 1955. For example, temperature records can be accessed from the University of Wisconsin's Antarctic Meteorological Research Center (https://amrc.ssec.wisc.edu/). Analysis of temperature and other associative environmental factors is occurring continuously (e.g., see research results from the McMurdo Dry Valleys Long Term Ecological Research project [LTER] at https://www.mcmlter.org/).

Unlike for the Antarctic Peninsula where wide agreement and evidence indicate a strong warming climatic temperature trend, there is not yet a definitive trend identified for the MIS. However, overall global evidence suggests that, at some point in the future, the Phoenix Airfield area will likely experience increased temperatures throughout the typical annual seasonal cycles. Such a change is unlikely to be obvious on an annual scale but

could well impact McMurdo-area operations on a decadal time frame. Planning or preparing for such a change impacting the Phoenix Airfield is challenging and perhaps futile. Many vital aspects of the operational and logistics support of McMurdo will be strongly negatively affected should local climate change as much as is being seen in the Antarctic Peninsula.

Resisting the effects of an annually trending increase in temperature and perhaps solar gain is possible for the short term. The most important controlling factor is albedo (reflectivity). We know and understand that at a site like Phoenix, serious damage can occur to snow and ice infrastructure when high albedo is not maintained during the peak eight or so weeks of the summer. Natural and foreign contaminants (sections 9.2 and 9.3) can significantly reduce albedo, and we have discussed means for mitigating their impacts. More subtle is the effect of melt water and refreezing of dispersed and, especially, concentrated melt water. A small area of water (as may be associated with a contaminated area left unmaintained) has an albedo of about 0.1 (90% of solar energy absorbed); frozen water has an albedo of about 0.5, and fresh snow reflects greater than 80% (albedo 0.8) of incoming solar radiation.

With intelligent and diligent maintenance, even if the adjacent terrain deteriorates, keeping the airfield site and access roads highly reflective may allow air operations to continue unaffected. Recovery of albedo (to levels greater than 0.7) and surface permeability is mandatory as soon as possible after the melt deterioration of an area so as to ensure both resistance to further solar energy absorption and its damage and to maximize the ability of cold air from depth to conduct and perhaps convect upward and cool the near-surface snowpack.

10 Summary and Recommendations

Following a review of potential sites to locate a new airfield to replace the failing Pegasus Airfield, the project team determined that the best compromise was to place the airfield at approximately Mile Post 11 along the Pegasus access road. Unlike Pegasus, which was founded on glacial ice, this new location would require construction of a runway on snow. Capitalizing on the experience of other countries' building snow runways and recent success in the USAP building high-strength snow foundations, construction of the new Phoenix Airfield commenced in October of 2015. Using a combination of numerical computation methods and field experience, we proposed feasible design and construction methods for constructing a runway out of snow that would support a wheeled aircraft as heavy as a C-17 Globemaster III, the main aircraft needing this new runway.

Following compaction of the existing snow cover with a sheepsfoot roller and rubber-tired weight carts, the construction proceeded in lifts with the objective to provide final compacted lifts that were about 75 mm (3 in.) thick. The first of these lifts was constructed by pushing snow adjacent to the runway onto the compacted base layer and then compacting them again with a sheepsfoot roller and rubber-tired weight cart. The load in the weight cart was progressively increased as the runway was able to support the load without rutting of the runway. Following completion of the first lift, subsequent lifts took advantage of naturally falling snow to deposit snow on the runway, which was compacted as soon as it was deposited. In this way, the runway is constantly under construction, as every snowfall is incorporated into the surface of the evolving pavement structure. Completion of the compaction process for an additional layer of snow occurs when the surface can support a fully loaded weight cart (73,000 kg [160,000 lb]) without rutting the runway. The compaction process needs to occur immediately after a snowfall to prevent the fresh snow from becoming too deep before it can be uniformly compacted, thus preventing a hard compacted surface over a softer poorly compacted snow layer; such an "egg shell" condition would not support the weight of a C-17 and would promote hoar formation that would further weaken the pavement structure.

Following construction, the runway was proofed with a fully loaded weight cart to confirm that there were no weak spots in the runway. The runway strength was verified by landing a fully loaded C-17 on the runway. In addition to landing, several maneuvers were carried out on the runway to

test the strength of the runway under normal and extreme loading conditions (e.g., 180° turns in the runway and short-field takeoff) to confirm that the runway would stand up to the rigors of flight operations. After successful completion of these validation tests in November of 2016, the Phoenix Airfield was certified for operations.

Owing to warming weather, the runway was not operated from mid-November 2016 until the end of January 2017. During this time, runway maintenance continued with the weight cart being used twice a week to compact the runway. As the runway warmed during the summer, the load in the weight cart was reduced to a level that the runway would support without rutting. As the runway began to cool, the load in the weight cart was progressively increased until the runway could support the fully loaded weight cart without producing ruts in the runway. Once the runway was able to support the fully loaded (73,000 kg [160,000 lb]) weight cart, the runway was cleared to resume operations.

The first operational flight on the Phoenix Airfield occurred on 27 January 2017. The mission was carried out successfully with minor rutting that was well within the operations limits for the C-17. Flight operations continued for another month on the airfield to support transport of personnel and cargo prior to station close.

Maintaining runway health going forward requires management of some key issues, including working new snow accumulations into the pavement structure as quickly as possible by compaction and ensuring that weak layers do not have a chance to form in the pavement structure. Furthermore, management of foreign and natural surface contaminants is crucial to keep the albedo of the surface high to prevent melting and weakening of the pavement structure.

To improve runway reliability and to streamline operations at the Phoenix runway we recommended the following items be addressed in future efforts:

1. Design and construct a new proof cart that can be tailored for each aircraft that will be operated on the runway, not just the C-17.
2. Vet and apply new strength assessment methods that can be easily related to the engineering properties of the snow and computational stress analysis methods such as BAKFAA. This will allow operators to directly relate

runway stress analysis for new aircraft to the measured runway strength and determine when the runway can support operations for specific aircraft.

3. Identify parameters to monitor (e.g., temperature, strength, and albedo) and develop a monitoring plan to assess runway health, and use this data to determine criteria for opening and closing the airfield for specific aircraft types. Along with this plan, develop a forecast model to predict when operational windows are closing and opening for mission-planning purposes.
4. Develop methods to understand how and when hoar-like layers can form in the runway and methods to predict, detect, and mitigate any hoar-like layer formation before it can compromise runway operation.
5. Determine the limits to runway life expectancy to better manage potential threats and determine for long term planning when a replacement runway will need to be reestablished at a new location.

Addressing these issues will provide fully capable operations and assessment of the Phoenix Airfield for the foreseeable future.

References

Abele, G. 1963. *A Correlation of Unconfined Compressive Strength and Ram Hardness of Processed Snow*. Technical Report 85. Hanover, NH: U.S. Army Cold Regions Research and Engineering Laboratory.

———. 1990. *Snow Roads and Runways*. CRREL Monograph 90-3. Hanover, NH: U.S. Army Cold Regions Research and Engineering Laboratory.

Abele, G., R. O. Ramseier, and A. F. Wuori. 1968. *Design Criteria for Snow Runways*. Technical Report 212. Hanover, NH: U.S. Army Cold Regions Research and Engineering Laboratory.

AFCESA/CES (Air Force Civil Engineer Support Agency and Civil Engineering Support Directorate). 1997. *Criteria and Guidance for C-17 Contingency and Training Operations on Semi-Prepared Airfields*. ETL 97-9. Tyndall Air Force Base, FL: AFCESA/CES.

Armstrong, R. L. 1980. An Analysis of Compressive Strain in Adjacent Temperature-Gradient and Equi-Temperature Layers in a Natural Snow Cover. *Journal of Glaciology* 26 (94): 283–289.

ASTM International. 2015. *Standard Test Method for Use of the Dynamic Cone Penetrometer in Shallow Pavement Applications*. D6951/D6951M-09. West Conshohocken, PA: ASTM International.

Aver'yanov, V. G., V. D. Klokov, G. Y. Klyuchnikov, Y. S. Korotkevich, and V. N. Petrov. 1983. Construction of Snow Airstrips for Wheeled Aircraft in the Antarctic. *Polar Geography and Geology* 9 (1): 37–41.

Blaisdell, G. L., V. Klokov, and D. Diemand. 1995. Compacted Snow Runway Technology on the Ross Ice Shelf near McMurdo, Antarctica. In *Contributions to Antarctic Research IV*, ed. D. H. Elliot and G. L. Blaisdell. Washington, DC: American Geophysical Union. doi:10.1002/9781118668207.ch9.

Blaisdell, G. L., R. M. Lang, G. Crist, K. Kurtti, R. J. Harbin, and D. Flora. 1998. *Construction, Maintenance, and Operation of a Glacial Runway, McMurdo Station, Antarctica*. CRREL Monograph 98-1. Hanover, NH: U.S. Army Cold Regions Research and Engineering Laboratory.

Daly, S. F, R. B. Haehnel, and C. Hiemstra. 2015. *Vertical Temperature Simulation of Pegasus Runway, McMurdo Station Antarctica*. ERDC/CRREL TR-15-2. Hanover, NH: U.S. Army Engineer Research and Development Center.

DOD (Department of Defense). 2001. *Pavement Design for Airfields*. UFC 3-260-02. Washington, DC: U.S. Department of Defense.

FAA (Federal Aviation Administration). 2016. *Airport Pavement Design and Evaluation*. AC 150/5320-6F. Washington, DC: Federal Aviation Administration. https://www.faa.gov/documentLibrary/media/Advisory_Circular/150-5320-6F.pdf.

Finney, E. A. 1934. *Snow Control on the Highway*. Bulletin 57. East Lansing, MI: Michigan Engineering Experiment Station.

FlightAware. 2019. ILS or LOC RWY 1L. Airport Resources. Houston, TX: FlightAware. https://flightaware.com/resources/airport/LAS/IAP/ILS+OR+LOC+RWY+01L/pdf.

Haehnel, R.B. 2017. *A Creep Model for High Density Snow*. ERDC/CRREL TR-17-7. Hanover, NH: U.S. Army Engineer Research and Development Center.

Haehnel, R. B., and J. Weatherly. 2014. *Antarctica Camps Snow Drift Management Guide*. ERDC/CRREL TR-14-21. Hanover, NH: U.S. Army Engineer Research and Development Center.

Haehnel, R, M. A. Knuth, T. Melendy, C. Hiemstra, and R. Davis. 2014. *Design and Implementation of a Consolidated Airfield at McMurdo, Antarctica*. ERDC/CRREL TR-14-22. Hanover, NH: U.S. Army Engineer Research and Development Center.

Hawkes, I., and M. Mellor. 1972. Deformation and Fracture of Ice Under Uniaxial Stress. *Journal of Glaciology* 11 (61): 103–131.

Hayhoe, G. F. 2002. LEAF—A New Layered Elastic Computational Program for FAA Pavement Design and Evaluation Procedures. In *Proceedings, 2002 FAA Airport Technology Transfer Conference*, 2 May.

Herrick, J., and T. Jones. 2002. A Dynamic Cone Penetrometer for Measuring Soil Penetration Resistance. *Soil Science Society of America Journal* 66:1320–1324.

Klokov, V., and D. Diemand. 1995. Glaciology of the McMurdo Ice Shelf in the Area of Air Operations. In *Contributions to Antarctic Research IV*, ed. D. H. Elliot and G. L. Blaisdell, 175–195. Washington, DC: American Geophysical Union.

Manning, K., and J. Powers. 2011. *AMPS Weather Conditions at Potential Alternate Pegasus Sites*. Boulder, CO: National Center for Atmospheric Research.

Masterson, D. M, W. P. Graham, S. J. Jones, and G. R. Childs. 1997. A Comparison of the Uniaxial and Borehole Jack Tests at Fort Providence Ice Crossing, 1995. *Canadian Geotechnical Journal* 34:471–475.

Mellor, M. 1988. *Hard Surface Runways in Antarctica*. CRREL Special Report 88-13. Hanover, NH: U.S. Army Cold Regions Research and Engineering Laboratory.

———. 1993. *Note on Antarctic Aviation*. CRREL Report 93-14. Hanover, NH: U.S. Army Cold Regions Research and Engineering Laboratory.

Mosher, E. H., and G. E. Sherwood. 1967. Load Carrying Capacity of Depth-Processed Snow on Deep Snow Fields. In *Proceedings, Physics of Snow and Ice*, Hokkaido, Japan, 1 (2): 993–1005

NSF (National Science Foundation). 2015a. Alpha Site Construction. Internal presentation for the Antarctic Support Contract and National Science Foundation. Arlington, VA: National Science Foundation.

———. 2015b. *McMurdo Station Master Plan 2.1, December 16*. Arlington, VA: National Science Foundation. https://www.usap.gov/news/documents/McMurdoMasterPlan_2.1.pdf.

———. 2016. *A New Runway for McMurdo Station is Named*. 7 April. Arlington, VA: National Science Foundation, Division of Polar Programs. http://www.usap.gov/News/contentHandler.cfm?id=4212.

Palt, K. 2017. Antonow / Antonov An-72 / An-74. Glugzeuginfo.net. http://www.flugzeuginfo.net/acdata_php/acdata_an74_en.php.

Parker, F., W. R. Barker, R. C. Gunkel, and E. C. Odom. 1979. D*evelopment of a Structural Design Procedure for Rigid Airport Pavement*. Technical Report GL-79-4. Vicksburg, MS: U.S. Army Waterways Experiment Station.

Russell-Head, D. S., and W. F. Budd. 1989. *Compacted-Snow Runways: Guildlines for their Design and Construction in Antarctica*. Special Report 89-10. Hanover, NH: U.S. Army Cold Regions Research and Engineering Laboratory.

Shapiro, L. H., J. B. Johnson, M. Sturm, and G. L. Blaisdell. 1997. *Snow Mechanics: Review of the State of Knowledge and Applications*. CRREL Report 97-3. Hanover, NH: U.S. Army Cold Regions Research and Engineering Laboratory.

Smith, R. A, A. Ellies, and R. Horn. 2000. Modified Boussinesq's Equations for Nonuniform Tire Loading. *Journal of Terramechanics* 37 (4):207–222.

Sopher, A., and S. Shoop. 2017. Stress Analysis of the Phoenix Compacted Snow Runway to Support Wheeled Aircraft. In *Proceedings, ASCE Congress on Technical Advancement*, 10–13 September, Duluth, MN.

UNESCO (United Nations Educational, Scientific and Cultural Organization). 2009. *The International Classification for Seasonal Snow on the Ground*. International Hydrology Programme VII, Technical Documents in Hydrology no. 83. Paris: United Nations Educational, Scientific and Cultural Organization, International Hydrological Programme.

USACE (U.S. Army Corps of Engineers). 2001. *Airfield Pavement Evaluation*. UFC 3-260-03. Washington, DC: U.S. Army Corps of Engineers (Preparing Activity), Naval Facilities Engineering Command, and Air Force Civil Engineer Support Agency.

———. 2010. *User Manual, Version PCASE 2.09*. Omaha, NE: U.S. Army Corps of Engineers, Transportation Systems Center.

USAF (U.S. Air Force). 2002a. *Design, Construction, Maintenance, and Evaluation of the Pegasus Glacial Ice Runway for Heavy Wheeled Aircraft Operations*. ETL 02-16. Tyndall Air Force Base, FL: U.S. Air Force.

———. 2002b. *Airfield Pavement Evaluation Standards and Procedures*. ETL 02-19. Tyndall Air Force Base, FL: AFCESA/CES.

———. 2015a. *Air Force Design, Construction, Maintenance, and Evaluation of Snow and Ice Airfields in Antarctica*. FC 3-260-06F. U.S. Air Force.

———. 2015b. *General Vehicle Manual, USAF Series C-17A Aircraft*. TO 1C-17A-2-00GV-00-1. U.S. Air Force.

U.S. Geological Survey. 1970. *Ross Island Antarctica ST 57-60/6*(162°E–170°E)*. Washington, DC: U.S. Geological Survey.

Wong, J., and G. Irwin. 1992. Measurement and Characterization of the Pressure-Sinkage Data for Snow Obtained Using a Rammsonde. *Journal of Terramechanics* 29 (2): 265–280.

Appendix A: Determination of Elastic Modulus of Snow for the Molodezhnaya Runway

Mellor (1993) provides the design strength profile for the Molodezhnaya runway. However, to estimate the stress distribution created by landing gear on the runway surface, this strength data needs to be related to the stiffness of the snow. Considering the rapid loading applied by the landing gear of a landing or departing aircraft on the runway, the elastic modulus, *Y*, may be considered as a reasonably accurate stiffness measure for determining the stresses in the runway from the applied loads. That is, the strain rate is high enough that the snow in the runway predominately behaves as an elastic material; there is not enough time for the snow to undergo viscoelastic deformation. The *Y* for each snow layer can then be used in software such as BAKFAA 2.0 to compute the stress profile based on a given landing-gear load.

We are not aware of any published data or correlations that translate directly from uniaxial compressive strength, σ_c, to the *Y* of snow. However, there is data that correlates σ_c to snow density (Abele 1990). Then using Table 4, we can determine *Y* for the snow layer.

Abele (1990) presents data that correlates σ_c to snow density for undisturbed and processed snow that has been allowed to sinter for 2 weeks following milling. This has been reproduced here in Figure A-1. We note that the bounds in the data for the undisturbed snow show that it exhibits a higher strength than processed snow. This seems counterintuitive; however, snow that is undisturbed and is allowed to reach a higher density through natural processes of melting, refreezing, vapor transfer, and deposition or compaction by overburden snow experiences a much longer sinter time than the 2 weeks experienced for the processed snow and therefore is able to reach a higher strength. We expect that the processed snow given a longer time to rest and sinter would also be able to achieve the same strengths as the undisturbed snow. Note how the upper bound for the processed snow lays almost exactly on the lower bound for the undisturbed snow. This suggests that the trends exhibited for natural transformation of undisturbed snow and sintering of processed snow are the same and that given more time to sinter, the processed snow would achieve the same strengths as the natural snow. Based on this reasoning, we will assume that the strength limits for the undisturbed snow are a reasonable

bound on the performance of snow provided it is given time to reach full strength. Therefore, we use that data to determine a correlation between snow strength and density. A curve fit to these bounding lines is

$$\sigma_c(\text{MPa}) = \begin{bmatrix} -64.61\rho^3 + 119.9\rho^2 - 61.56\rho + 9.973: \text{Upper bound} \\ -51.66\rho^3 + 99.59\rho^2 - 57.71\rho + 8.569: \text{Lower bound} \end{bmatrix}. \quad (13)$$

These were then used together with Table 4 to determine a variation of Y with depth from the snow strength profile given in Abele (1990).

Figure A-1. Comparison of the snow strength for undisturbed snow (*blue line*) to processed snow (*thin red line*). The two lines for each indicate the upper and lower bounds in the charts presented in Abele (1990).

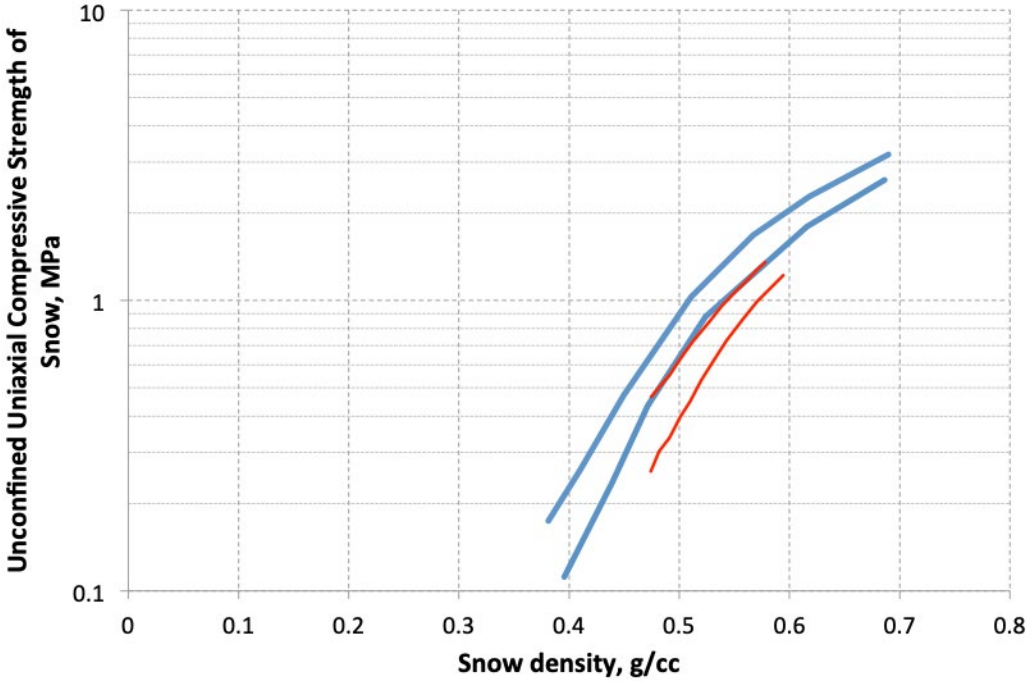

Appendix B: Landing-Gear Configuration for Soviet Aircraft

Ilyushin Il-18D: Dual tandem or twin tandem. Each tire is 930 × 305 mm (3.05 ft dia. × 12 in. width) (Mellor 1993). Effective contact radius = 16.4 cm (6.5 in.).

Antonov An-74: Tandem (or single tandem). Each tire is 1050 × 400 mm (3.44 ft dia. × 15.7 in. width) (Mellor 1993). The standard tire pressure is 790 kPa (114 psi) but can be reduced to as low as 490 kPa (71 psi) (Mellor 1993). Effective contact radius = 18.5 cm (7.2 in.) 790 kPa (114 psi) to 23 cm (9.2 in.) 490 kPa (71 psi).

REPORT DOCUMENTATION PAGE

Form Approved
OMB No. 0704-0188

1. REPORT DATE *(DD-MM-YYYY)*	**2. REPORT TYPE**	**3. DATES COVERED** *(From - To)*
May 2019	Technical Report/Final	

4. TITLE AND SUBTITLE

A Snow Runway for Supporting Wheeled Aircraft: Phoenix Airfield, McMurdo, Antarctica

5a. CONTRACT NUMBER

5b. GRANT NUMBER

5c. PROGRAM ELEMENT NUMBER

6. AUTHOR(S)

Robert B. Haehnel, George L. Blaisdell, Terry Melendy, Sally Shoop, and Zoe Courville

5d. PROJECT NUMBER

5e. TASK NUMBER
EP-ANT-15-1

5f. WORK UNIT NUMBER

7. PERFORMING ORGANIZATION NAME(S) AND ADDRESS(ES)

U.S. Army Engineer Research and Development Center (ERDC)
Cold Regions Research and Engineering Laboratory (CRREL)
72 Lyme Road
Hanover, NH 03755-1290

8. PERFORMING ORGANIZATION REPORT NUMBER

ERDC/CRREL TR-19-4

9. SPONSORING / MONITORING AGENCY NAME(S) AND ADDRESS(ES)
National Science Foundation, Office of Polar Programs
2415 Eisenhower Avenue
Alexandria, VA 22314

10. SPONSOR/MONITOR'S ACRONYM(S)
NSF

11. SPONSOR/MONITOR'S REPORT NUMBER(S)

12. DISTRIBUTION / AVAILABILITY STATEMENT
Approved for public release; distribution is unlimited.

13. SUPPLEMENTARY NOTES

Engineering for Polar Operations, Logistics, and Research (EPOLAR)

14. ABSTRACT

Historically, there has been a system of as many as three airfields operated at McMurdo, Antarctica, to transport cargo and personnel to and from the continent via ski-equipped and wheeled aircraft. Owing to the runways' being founded on snow and ice, there is a constant need to adapt the airfield system to accommodate changing environmental conditions while still meeting program needs. This report provides an overview of the implementation of a new airfield to support landing wheeled aircraft that replaces the Pegasus Airfield that was founded on the superimposed glacial ice layer on the McMurdo Ice Shelf in the McMurdo Sound.

The new airfield is located approximately 5 km (3 miles) east and up shelf from the former Pegasus Airfield and is the first runway constructed on compacted snow that supports a wheeled aircraft as large as a C-17. Herein we document the design, construction, and commissioning of the new airfield. Also provided in this report are recommendations for maintenance and monitoring to prolong the life of the airfield and to determine when operations need to be suspended due to warm weather.

15. SUBJECT TERMS
EPOLAR, McMurdo Station (Antarctica), McMurdo Ice Shelf (Antarctica), NSF, Runways (Aeronautics)--Design and construction, Runways (Aeronautics)--Snow and ice control, Snow pavement, Snow runways

16. SECURITY CLASSIFICATION OF:			**17. LIMITATION OF ABSTRACT**	**18. NUMBER OF PAGES**	**19a. NAME OF RESPONSIBLE PERSON**
a. REPORT	**b. ABSTRACT**	**c. THIS PAGE**			**19b. TELEPHONE NUMBER** *(include area code)*
Unclassified	Unclassified	Unclassified	SAR	175	